A National Safety System for the Netherlands

Design Synthesis Exercise - AE3200

Final Report

July 4, 2017

Project Group 13

Faculty of Aerospace Engineering

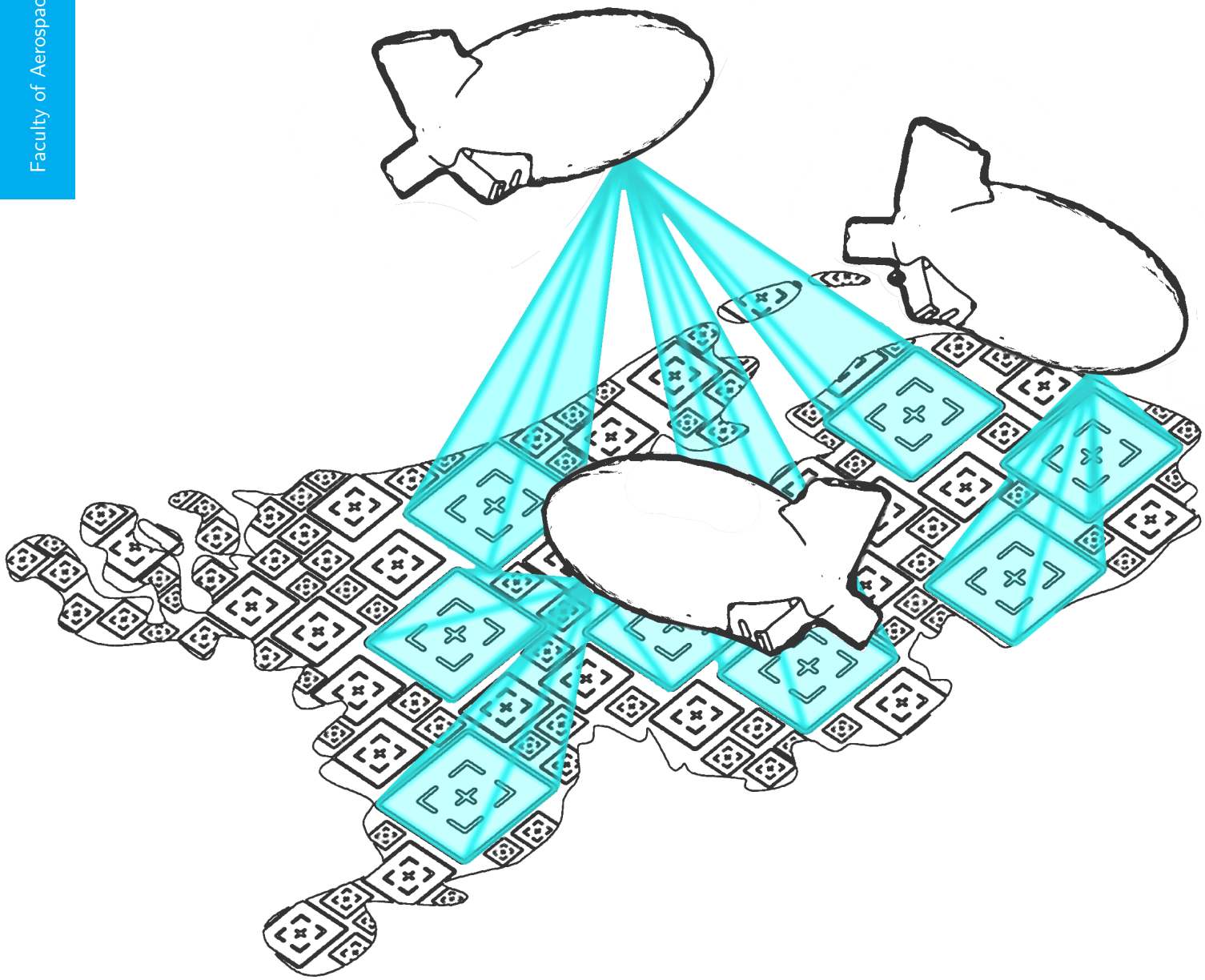

TU Delft Delft University of Technology

Challenge the future

A National Safety System for the Netherlands

Design Synthesis Exercise - AE3200

Final Report

July 4, 2017

by

Project Group 13

In partial fulfilment of the requirements for the degree of

Bachelor of Science
in Aerospace Engineering
at Delft University of Technology

Project duration: April 24, 2017 - July 7, 2017

Authors:	F.M. Knyszewski	(4363639)
	J.J. Lubberding	(4291867)
	A. Malkaoui	(4352688)
	R.J. Meesen	(4136349)
	C.M. Niemeijer	(4345665)
	B.G. van Noort	(4363973)
	M. Rozemeijer	(4207130)
	R. Sprenkels	(4351584)
	J.M. de Zoete	(4350685)
Tutor:	dr. ir. J.M. (Hans) Kuiper,	TU Delft
Coach:	dr. ir. J. Ellerbroek,	TU Delft
Coach:	ir. T. Hartuç,	TU Delft

TU Delft

Preface

This report is the fourth and final report from the 13th Design Synthesis Exercise group consisting of 9 Aerospace Engineering students. A total of 1440 man hours were put into this report over a period of four weeks.

This report follows from the 3rd report and will contain the final system design. The payload size, airship characteristics, and general system operations are all discussed in this report. The goal was to work out the chosen design concept from the Mid-term report in detail, and provide the Ministry of Security and Justice with a solution to their problem. In order to ensure an accurate interpretation of the data that has been generated, and is present in this report, we recommend readers to use a coloured version of the report. Whether it be online, or colour-printed.

Finally, we would like to thank our tutor dr. ir. J.M. (Hans) Kuiper and our coaches dr. ir. J. Ellerbroek and ir. T. Hartuç whom assisted us in designing the National Safety System and making the right choices, both on technical and management level. Also, we would like to thank dr. S. Speretta and ir. J. Bouwmeester for their help on the communications and the attitude determination and control system.

Delft,
July 4, 2017

F.M. Knyszewski
J.J. Lubberding
A. Malkaoui
R.J. Meesen
C.M. Niemeijer
B.G. van Noort
M. Rozemeijer
R. Sprenkels
J.M. de Zoete

Contents

Summary

In the Netherlands, the ministry of Security and Justice (VenJ) has the task to ensure the safety of civilians of the Netherlands by enforcing the legal order. The ministry of VenJ wants to solve issues faster and more efficiently by using satellite technology to contribute to a safer and more just Netherlands. The ministry of VenJ asked the Delft University of Technology to perform a feasibility study and design a National Safety System (NSS). Therefore, the mission need statement of this project is to ensure the safety and security of the Netherlands by preforming the use of: an identification and tracking system (ITS) to track specific objects marked by the Ministryl. A fire and smoke detection system that uses earth observation techniques and is able to perform chemical analysis of gas and smoke clouds. Chemical analysis of the smoke clouds is performed in order to identify the presence of toxic substances. This allows populated areas to be evacuated in case the toxic clouds reach these areas. For target tracking the ministry currently uses beacons that emit radio waves to track or follow targets. This requires a lot of manpower and is easily detected, therefore a more efficient way of ensuring the safety of the citizens of the Netherlands has to be designed.

In order to detect fires, monitor and predict the movement of smoke and gas, imaging is done at a number of specific wavelengths. The wavelengths around 3.9 and 10.8 μm are used for primary fire detection and the wavelengths 0.47, 0.64, 0.86 and 2.26 μm enable the system to visualise additional features that might be of interest. The chemical analysis of smoke and gas clouds is based on recreating spectra and thus benefits from having data from a larger number of spectral bands.

For the identification and tracking of targets, the targets will be coated either with panchromatic paint or paint containing quantum dots. The quantum dots detection method relies on absorbing incoming radiation and re-emitting it in another wavelength, such that a peak at this particular wavelength can be detected. The panchromatic paint is used as a coating for another detection method. It relies on the fact that two paints have the same perceived colour, but a different electromagnetic spectrum. A panchromatic coating can be detected by imaging in the visible part of the electromagnetic spectrum and by measuring the difference in the electromagnetic spectrum. Quantum dots can be detected by imaging in the near and shortwave infrared part of the spectrum. There is a difference in bandwidth for the two methods. For panchromatic coating, a bandwidth of 5 nm is necessary and for the quantum dot paint a bandwidth of 10 nm is sufficient.

A proper payload design is absolutely crucial for the success of the NSS operations due to the nature of the detection methods. Since Earth observation techniques are being used, the payload mainly consists of cameras. These cameras will be flown aboard a network of airships, which was concluded to be the most efficient way of executing the tasks of the NSS from the Mid-term report. Each airship has four different types of imagers; their specifications are tabulated in Table 0.1.

One imager, the AMS Wildfire, will be used for the detection of fire, smoke-, and gas clouds. This will be done by imaging at different wavelengths that range from visible light to thermal infrared. Chemical analysis will be done with a hyper-spectral camera (Hyperion) whenever a smoke cloud is detected. Hyperion is also used for target tracking purposes. During measurement, the camera outputs large strings of spatial-spectral data, which will be analysed and the types of substances in the cloud can be determined using the spectrum.

The main challenge is to identify and track the targets, this is because a different detection technique is required to do this. The hyper-spectral camera will identify a vehicle based on the difference between these electromagnetic spectra. Four colour imagers (CI) will be used to sweep the field of view (FOV) of the airship for potential targets, which is a circle with a radius of 34 km. The hyper-spectral camera will then determine if the potential targets are the ones being tracked by

the system. This approach was chosen, as scanning the entire FOV by means of the hyper-spectral camera would take too long, because of the small swath width and the large amount of data generated by the camera. Moreover, this approach is taken to reduce the risks associated with having a heavy payload with high manoeuvrability (mechanical wear off for example). A final infrared camera (IRIS) will be used to track vehicles after sunset. The infrared imager will allow only for limited night-time operations, as it will not be able to identify the marker of a vehicle and must be operated manually.

Table 0.1: Payload summary

	AMS Wildfire	**CI**	**Hyperion**	**IRIS**
FOV [arcmin]	5154 x 8.6	433 x 329	36.5 x 0.15	99 x 79
Swath width [m]	37250 x 50	2534 x 1921	213 x 0.9	576 x 461
Mass [kg]	57	3 ± 1	49	35 ± 6
Power [W]	140 (approximated)	3	51	0.75
Size [cm^3]	38 x 38 x 38	13 x 13 x 22	20 x 75 x 66	34 x 34 x 66
Bits/pixel	8	12	12	14
Pixels	716 x 1	7920 x 6004	250 x 1	1280 x 1024
No. Bands	16	3	220	1
GSD [m]	50	0.32	0.85	0.45
Spectral Range [nm]	420 - 11260	400 - 700	400 - 2500	3700 - 4800
SNR	-	74 - 149	> 65	60 - 121

The Thales Stratobus will be used for the NSS. Figure 0.1 is a representation of what the airship will look like. The Stratobus has a payload of 250 kg with a power generation of 5 kW. A dedicated Attitude Determination and Control System (ADCS) will provide stabilisation for the four colour imagers, the Hyperion and the IRIS imager. The main challenge is to limit the total weight of these stabilisers to 70 kg, as the first design iteration yielded a mass of 92 kg. On the Stratobus, an electric propulsion system is already present. It is capable of propelling the airship at a speed of 20 m/s, so the airship itself does not have to be designed. The lift is generated by the gasses inside the airship and different gasses can be used to fulfil this task. However, there is only one obvious option: hydrogen. Overall, it will be cheaper than any of the other gasses as well as more efficient and environment friendly. Hydrogen can be used on board to generate energy and use as the lifting gas. For the navigation of the airship, it is best to use GNSS receivers, because they are highly accurate, in the order of 0.01 m. The airship will generate a large amount of data during operations, for the airship has a total of 7 cameras on board, all of which will be imaging constantly. The data should therefore be processed on board. To do this properly, each airship will have 12 processors on board together with 10 storage units, which are capable of storing 12 TB of data each. This is important in case of communication problems, because the gathered data can be stored on board and sent once the problems are resolved. The data will be processed, compressed, and encrypted before it is sent down because the information may end up in the wrong hands. For the communication subsystem, an Signal-to-noise ration (SNR)of 23.4 dB is used with a transmitter antenna diameter of 0.05 m and a receiver antenna diameter of 0.5 m. The required SNR is 7.7 dB, so 23.4 dB is quite high for a SNR, it is even possible to take a cheaper modulation technique which requires a larger SNR. It is most probable that the airship is going to need a heating system inside the payload bay, as most optical elements (like sensors) operate at a temperature between -40 °to 71 °C. Heaters and coolers are already integrated in many flying objects, mostly spacecraft. Since thermal control has been applied to so many aerospace systems, it can be implemented on the airship as well.

To meet the requirement of full coverage of the Netherlands, 15 active airships will be needed. One extra airship is always on the ground such that the maintenance can be circulated amongst airships, with the added benefit that it can be deployed in case one of the other airships is lost. The airships will communicate with 2 different ground stations, one located in Flevoland and one located near Tilburg. These ground stations will have multiple antennas, each pointing to a dedicated airship. The ground stations shall be highly secured to prevent individuals from dismantling activities of the NSS. The airships have to land once a year for maintenance, therefore a ground base will be located in the centre of the Netherlands, such that it is easily accessible for all airships.

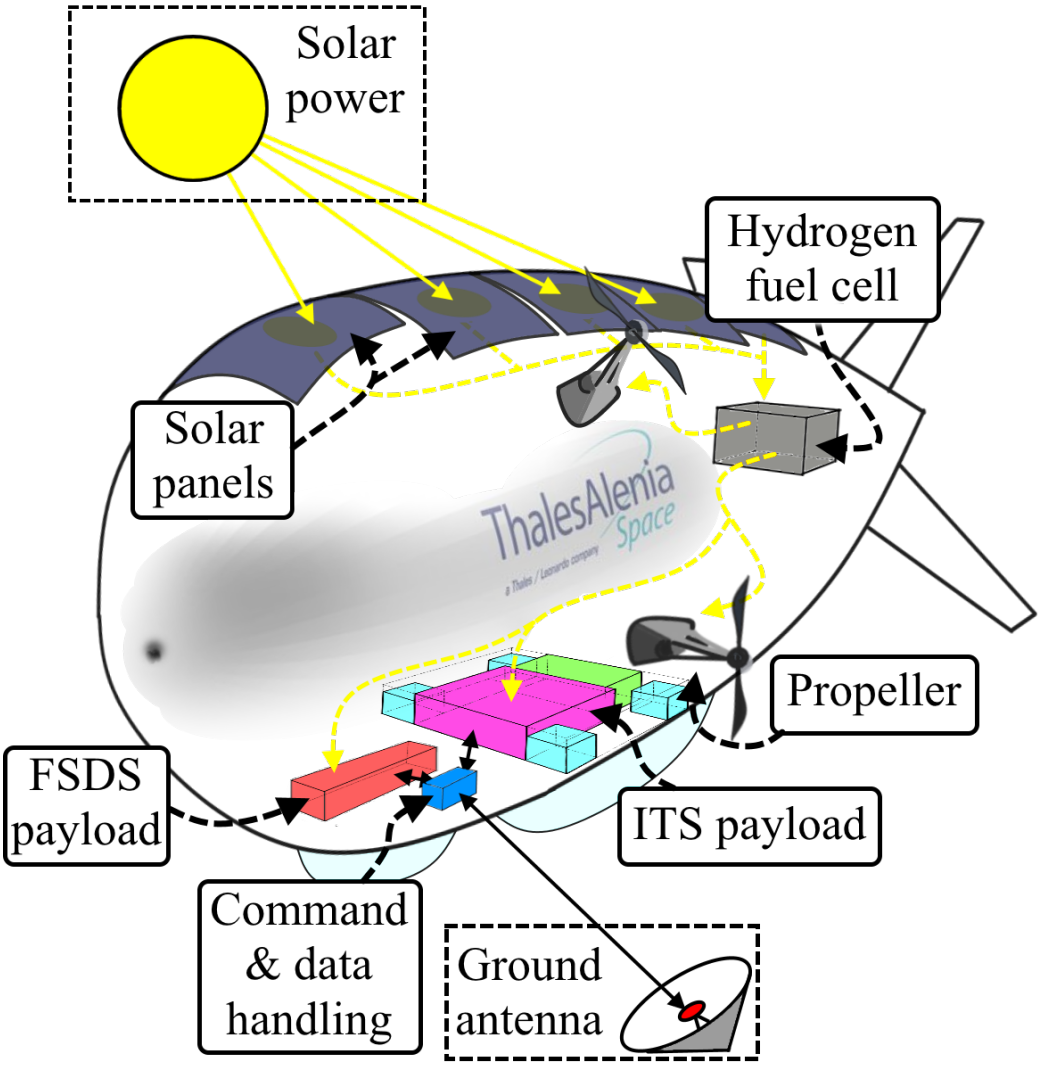

Figure 0.1: Representation of the airship with its subsystems

The airship ground base consists of a mooring mast, two hangars and a launch pad. Mission control of the NSS will be located either near the airship ground base in the middle of the Netherlands, or near VenJ in Den Haag. VenJ must determine which of these two locations serves their needs best.

Next to the airships, drones will be used as a back-up when it is cloudy or night time, as the airships have diminished visibility under these circumstances; see Figure 0.2. The Boreal GasFinder2-UAV will be used in order to perform chemical analysis where it will have an endurance of 600 minutes. The Aeryon Skyranger drone will be used in order to identify and track targets. It has a loiter time of 50 minutes. Both drones are specifically designed for performing their respective tasks. A total of 18 drones were selected in order to perform chemical analysis and 74 drones were selected in order to track targets. The drones were selected such that the drones will cover the Netherlands entirely with a temporal resolution of 10 minutes.

(a) Boreal GasFinder2-UAV (b) Aeryon Skyranger

Figure 0.2: Selected drones

A cost estimation was carried out in order to ascertain the viability of the system. The estimated material costs for the entire system will amount to €203 ± 28.5 million and the estimated annual operational costs will amount to €13.7 million for the first five years. Nearly 100% of The Netherlands will be covered by the system, which was a requirement set by the ministry. However, by covering the areas with the highest crime rates, only 8 airships need to be used in combination with one ground station. This could potentially halve the cost mentioned before and allow the system to concentrate on the more relevant areas.

A system's performance depends not only on the performance of each of its parts but also on the interconnection between them. The operations of the NSS can be divided into nominal operations and back-up operations.

The nominal operations for each airship centre around station keeping at a fixed location, constantly scanning its field of view – either searching for marked targets or for any signs of fire, smoke or gas. These are continuous operations, meaning that unless the 'safe mode' is activated, they will be continuously performed by the airship. There is an instance in which the airship might not be able to do this, and that is if the weather is very cloudy. In such a scenario, the NSS drones would come into play to support the system. With a response times of 10 minutes, these will be able to quickly reach any point in the Netherlands and perform chemical analysis and tracking of smoke or gas or tracking of a specific 'high priority' target.

The back-up operations or 'safe mode' are activated if an element fails one of the two requirements mentioned before. In case of contact loss, a contact loss protocol is initialised in which both the element and the ground station computers take corrective measures to regain connection. The other requirement involves the status reports produced by the subsystems of each element. These provide information on the several components of each subsystem and help assess at what level of performance they are operating. If any of them comes negative, the 'safe mode' is activated for that element. Naturally, a system like the NSS, as any other engineering project, is posed with a considerable number of risks. These involve technical risks associated with the payload, communications systems and ADCS of the airship but also operations risks like airship loss, hacking by a third party or just contact loss. All these were mitigated either by introducing redundancies in the system or by suggesting extensive testing, simulation and the introduction of algorithms ready to cope with them. This resulted in a set of risks that is both acceptable and manageable.

The final proposed design is a complete system, able to fulfil all the requirements stipulated by the stakeholders and even with additional capabilities that might be of great use. However, there is always room for improvement and so a series of strategies for a modified system were proposed. Cost is obviously linearly correlated with the number of airships and so the key goal of the suggested modifications was to show the achievable price range if further investigation is done to improve the system's capabilities and hence reduce its required number of airships. This can be achieved through a number of ways, like improving the airship's manoeuvrability, changing the coverage requirements to allow for different set-ups or just by improving the technology behind the detection methods. To show the findings from this research the following financial matrix is presented (Table 0.2):

Table 0.2: Financial matrix

	Coverage %	Temporal resolution (min)	Feasibility (1-5)	No. of airships	Cost (€ million)
Proposed configuration	99	1	5	15	217
Manoeuvrable configuration	75 - 100	1 - 6	1	9	135
Extended ITS FOV					
QD	99	1	2	15	217
PC	95	1	3	10	149
Alternative distribution					
Single airship	8.7	1	5	1	15
Randstad coverage	28	1	5	3	41
Crime-rate based coverage	50	1	5	8	122
FSDS only					
Airships	99	«30	5	3	41
CubeSats	99	30	5	32 (CubeSats)	20

Here the different possible configurations are shown along with their key parameters that allow to better visualise and characterise them. This table is meant to be used as a future reference for what kind of systems can be achieved depending on the requirements and the design approach. Also emphasis was put on how much the ITS drove the requirements of the proposed NSS design. A system performing FSDS operations only would be much cheaper as it would require a much smaller number of airships. Even a system using CubeSats would potentially become a strong candidate for such a design.

This project was performed in the context of a feasibility study for the ministry of VenJ. The primary task was to investigate and design a useful system for fire and smoke detection, and target identification and tracking. This project has shown that the best solution can sometimes be very different from what was initially expected. It was discovered that the identification system drove the design of the system entirely. The designed system is functional, but comes at a price of increased cost, development time, and risk. There are several potential research opportunities to continue this project further.

First and foremost, the payload has to be designed in detail. This must be done in conjunction with the ITS detection strategies as they depend on each other. Quantum dots are an emerging technology and thus require a lot of research before implementation. Research might also show that it is possible to increase the FOV determined by the Quantum Dots (QD). Further research is also required to show the true potential of the panchromatic coating.

Alternatively, in cooperation with companies such as Thales, improvements to the airship can be investigated increasing the operational range of a single airship.

Finally, the ministry should reconsider some of their requirements about the system. Cost and complexity decreases with the number of airships. If they are willing to consider separating the FSDS and the ITS it might suddenly be possible to again use satellite systems as the ministry initially expected.

The Ministry of Security and Justice can use the recommendations and conclusions presented in this report to further develop the National Safety System and ensure the continued safety of the citizens of the Netherlands.

List of Abbreviations & Symbols

Abbreviation	Definition
ADCS	Attitude Determination and Control System
AI	Artificial Intelligence
AMS	Autonomous Modular Scanner
CEA	Cryocooler Electronics Assembly
CI	Colour Imager
CIE	International Commission on Illumination
CHSI	Combined Hyper-Spectral Imager
DLR	German Space Agency
EPS	Electrical Power System
EM	Electromagnetic wavelengths
eMAS	Enhanced MODIS Airborne Simulator
FOV	Field of View
FSDS	Fire and Smoke Detection System
GNSS	Global Navigation Satellite System
GSD	Ground Sampling Distance
HAP	High Altitude Platform
HEA	Hyperion Electronics Assembly
HSA	Hyperion Sensor Assembly
IMU	Inertial Measurement Unit
IR	Infrared
IRIS	InfraRed Imaging System
ITS	Identification and Tracking System
LAS	Laser Absorption Spectrometry
LMS	Long, Medium and Short wavelengths
LTA	Lighter Than Air
LWIR	Long-wavelength infrared
MHSI	Multipurpose Hyper-Spectral Imager
MIR	Medium infrared
MLI	Multilayer Insulation
MWIR	Mid-Wavelength Infrared
MODIS	Moderate-Resolution Imaging Spectrometer
MTR	Midterm Report
NSS	National Safety System
PC	Panchromatic Coating
PHSI	Panchromatic Hyper-Spectral Imager
QD	Quantum Dot
QHSI	Quantum Dot Hyper-Spectral Imager
SAR	Synthetic Aperture Radar
SNR	Signal to Noise Ratio
SWIR	Short-wavelength infrared
UV	Ultraviolet
VenJ	Ministry of Security and Justice
VIS	Visible light

Symbol	Definition	Unit
a	Semi-major axis	[m]
A	Aperture area	[m^2]
b	Semi-minor axis	[m]
$\frac{C}{N_0}$	Carrier-to-noise ratio	[dB-Hz]
d	Pixel size	[m]
D	Aperture Diameter	[m]
D_{limit}	Diffraction limit	[m]
e	imposed error by ADCS	[°]
E	coverage length minus the length induced by the error	[m]
EIRP	Equivalent isotropic radiated power	[dBW]
f	Focal length	[m]
F	F number	[-]
$\frac{G}{T}$	Received antenna gain	[$\frac{dB}{K}$]
G_t	Gain of transmitter	[dBW]
G_r	Gain of the receiver	[dBW]
H	Altitude	[m]
L	Total coverage length	[m]
L_a	Zenith attenuation	[dBW]
L_{comb}	Loss factors	[dB]
L_l	Loss of the transmitter	[dBW]
L_{pr}	Antenna pointing loss	[dBW]
L_r	Loss of the receiver	[dBW]
L_s	Space loss	[dBW]
n	Location error	[m]
P	Power	[dBW]
R	Radiance	[ph/m^2/s/sr/m]
R_0	Base value Radiance	[ph/m^2/s/sr/m]
R	Data rate	[bits/s]
S	Signal Strength	[-]
t_i	Integration time	[s]
t_s	Shutter time	[s]
T_s	System noise temperature	[K]
Q_e	Quantum Efficiency	[-]
V	Volume	[mm^3]
V_0	Object velocity	[m/s]
$\bar{x}$, $\bar{y}$, $\bar{z}$	CIE standard observer	[-]
α	Field of View	[degrees]
$\Delta\lambda$	Wavelength Bandwidth	[m]
η	Percentage of GSD	[-]
θ_2	Rotation angle	[°]
θ	Ground Angle	[degrees]
$\theta_{stability}$	stability angle	[arcsec/s]
λ	Wavelength	[m]
$S(\lambda)$	Spectral Reflectance	
$I(\lambda)$	Illuminance	[-]
ρ	Reflectivity	[-]
τ	Optical Loss	[-]
ϕ	Radiance Angle	[degrees]
Ω	Solid Angle	[sr]

List of Figures

List of Tables

1 Introduction

In the Netherlands, under coordination of the ministry of Security and Justice (VenJ), emergency services and law enforcement agencies are working tirelessly to ensure a fair application of the rule of law and the population's safety. In order to facilitate some of the challenges faced during the operations in service of the country, with the use of satellite technology, VenJ launched the innovation programme for satellite applications.[1]

This report serves as a feasibility study that dives into the practical design of a modular National Safety System with two principal tasks in mind; the first being the identification and tracking of targets of interest, and the second is the monitoring, movement prediction, and chemical analysis of gas and smoke clouds, and the detection of fire. The current solution for the former task is relatively inefficient, as it still relies on the placement of radio beacons, which are fairly easy to detect. Moreover, these operations can require a lot of manpower, while there are over a thousand targets of interest that are deemed necessary to be tracked by the authorities.

When it comes to the Fire and Smoke Detection System (FSDS), the wish is to provide the fire brigade with reliable information and quick updates about hazardous situations. The necessity for this stems from the fact that the Netherlands is a densely populated country where the industrial zones are frequently within a stone's throw from urban areas. Currently, there is no system in place capable of providing a forecast of how smoke and gas clouds might develop, what their current effects are, and what their chemical composition is. It is therefore extremely helpful to have such a system that can determine which areas need to be evacuated, and tackle the situation on the ground efficiently, with fast and calculated reactions. Investing in the development of such systems would not only aid the authorities in ensuring the public's health and safety, it would also help exercise the rule of law, and spur innovation and research in the Dutch technological and scientific sectors.

To reach the most optimum design solution, the team went through a process of defining the system's requirements through conversation with the customers at VenJ, in order to find out which performances were expected of the system. Thereafter, a number of different techniques were studied for how a possible solution could be provided, and a number of different concepts were written out, which were filtered according to feasibility. After comparing the four final concepts in the midterm review, it was clear that using satellites would not allow for all the requirements to be met, therefore giving rise to the need for airships. This final concept is presented and worked out in detail in this report.

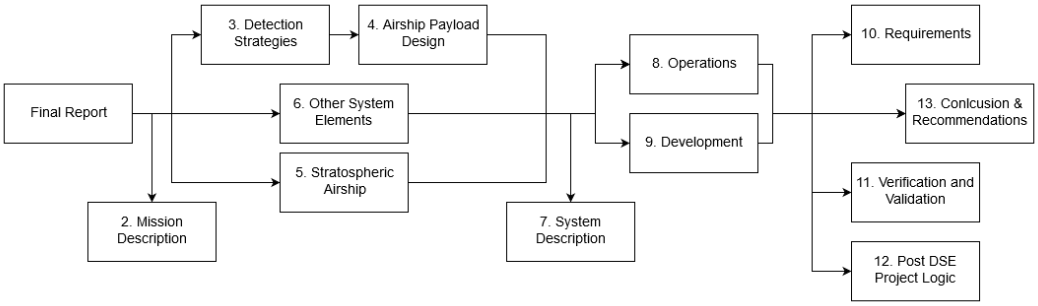

Figure 1.1: Road map of the report

[1] https://www.rijksoverheid.nl/ministeries/ministerie-van-veiligheid-en-justitie/inhoud/innovatie-veiligheid-en-justitie/innovatieprogramma-satelliettoepassingen

A road map of the report can be seen in Figure 1.1. In Chapter 2, the mission objective, the mission approach, and the design approach can be found. This chapter provides an overview of the purpose of the system. Chapter 3 discusses the different detection strategies, where both the ITS and the FSDS are explained. After the detection methods have been determined, the payload design is illustrated in Chapter 4. It is important that the payload can be supported by a platform and its subsystems, which is discussed in Chapter 5. Chapter 6 reveals the design of the remaining elements of the system. A clear overview of all the different elements of this system is presented in Chapter 7, as well as a cost breakdown and sustainability approach. After the system breakdown, risks analysis and the intricacies of the entire system's operations are discussed in Chapter 8. Then, after elaborating upon the operations of the system, its further possible developments are discussed in Chapter 9. In Chapter 10 it will be checked if all the requirements are met, which were set in the baseline phase of the project. The different tools used in the design of the National Safety System are verified and validated in Chapter 11. In Chapter 12 the different steps to be taken by the ministry of Security and Justice and other involved parties are represented in a flow chart and a Gantt chart. Chapter 13 concludes the findings of the report and discusses the recommendations presented to the ministry of Security and Justice and other involved parties.

2 | Mission Description

This chapter gives a brief overview of the mission that this project and the National Safety System (NSS) need to perform. First the mission objective is restated to give the reader an overview of what this project is about. Next, the mission objective is divided into a number of basic segments. Lastly, the design approach is explained.

2.1. Mission Objective

There are two main mission objectives the NSS is concerned with. The first mission objective relates to a Fire and Smoke Detection System (FSDS). When a fire or a gas leak occurs it is hard to predict spreading of the developed cloud, and subsequently determining the affected area. This makes it difficult to indicate where preventive measures should be taken. Secondly, the composition of such clouds has to be determined, aiding the decision whether to evacuate the affected area. Current technologies require on site measurements, which causes the response time to be low, making it hard to give predictions about an affected area during the first moments after detection. Additionally, to map the smoke cloud, teams have to drive to each location, take measurements and repeat this process, making it time consuming and slow.

This results in a demand for an alternative solution to determine the development, composition and affected area of gas and smoke clouds with a time interval of 30 minutes.

The second mission objective is concerned with the identification and tracking of objects, such as cars and containers. This functionality will be performed by the Identification and Tracking System (ITS). Currently radio beacons are primarily used for the tracking of targets (such as a certain red-white striped individual). Radio beacons have as a disadvantage that they can easily be detected. Another method used to track cars or containers is by simply following them with a car, which requires a lot of manpower. Also, the target could be lost easily, at for instance a traffic light or by human error, or the target could notice being followed.

Thus a need arises for a more accessible way to track vehicles with a high interval and accuracy without being detected and physically present.

Figure 2.1: 'DISPATCHING DRONE TO TARGET COORDINATES.' – 'Wait, crap, wrong button. Oh jeez.'

[0] https://xkcd.com/1358/ [cited 20 June 2017]

2.2. MISSION APPROACH

The mission approach describes how the mission objective will be achieved successfully. Figure 2.2 shows a general overview on the mission approach which was determined during the MTR. The approach is divided into six main segments. The first and second segment are concerned with the object of interest, being either vehicles or smoke and fire. This can be described as the method of detection, such as markings on cars or specific fire and smoke signatures. The third segment concentrates upon the payload which will detect either these markings or signatures such that the item of interest is detected. The fourth segment is the platform on which the payload will be mounted, more specifically the airships. The fifth and sixth segment contain all supporting elements such as the ground-station and the drones which will operate during cloudy conditions. Combining all the elements together will give a system description and the interaction together will be given by a set of operations. Table 2.1 contains the contents of each segment, and includes in what chapter it will be discussed.

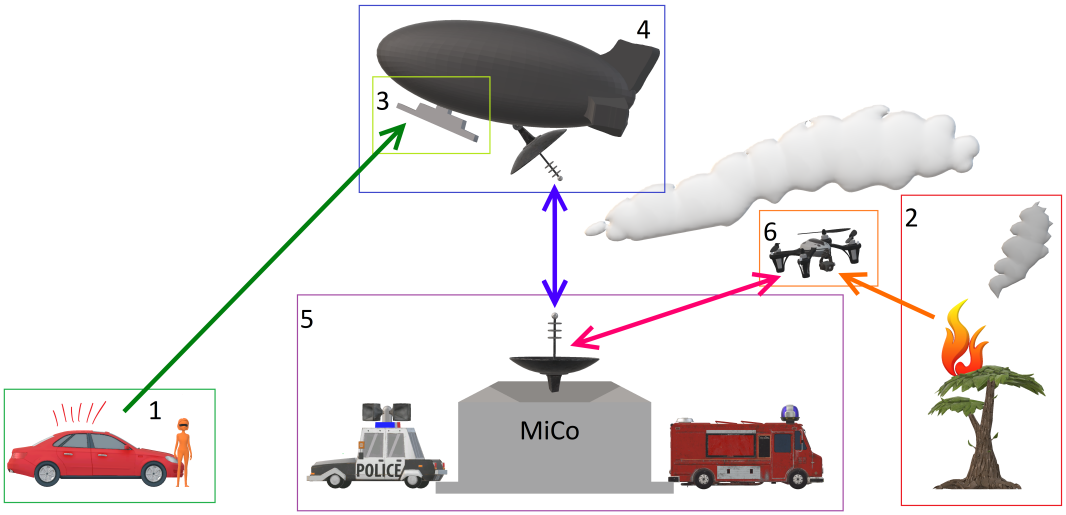

Figure 2.2: General overview of system elements

Table 2.1: Mission approach divided into six main segments, including which chapter will discuss relevant results

Segment	Contents	Chapter
1 & 2	Detection Strategy	3
3	Payload Design	4
4	Stratospheric Airships	5
5 & 6	Other System Elements	6
All	System Description Operations	7 8

2.3. DESIGN APPROACH

To design a system which will be able to achieve the mission objective, a structured design approach is required. The design approach has great overlap with the mission approach, however it is intended to show the design interaction of each segment. Figure 2.3 shows the flow diagram for the design approach which will be used for this project. This will also be reflected into the structure of the report. The flow diagram has yellow and green boxes which indicate found requirements and results respectively. It should be noted that not all results are presented in this diagram for the sake of brevity. The included results and requirements have a large impact on the following segments.

The first stage of the design process is determining the detection strategy for both ITS and FSDS.

One of the results will be the maximum achievable FOV of a single airship, as this is limited by the detection method and geometry, and will influence the amount of airships required. Requirements set by the detection method will also include GSD, the detection wavelength and the spectral resolution. These three requirements will influence the payload design, more specifically the optics. The payload design will determine the size, amount of data, weight and power of the payload. Additionally it will put requirements on the airship in the form of pointing stability, lifting capacity and data-rate. With these restrictions the airship selection, as well as the Attitude Determination and Control Subsystem (ADCS) and data handling will be investigated. The amount of airships required can be determined based on the previously found coverage area for a single airship, additionally a cost estimation can be made for the entire system, which will be based on the selected airship, the determined payload and the required amount of airships. Once the contents of the entire system have established, the operations of the entire system will be designed, such that the system achieves all set requirements. To finalise the design, all required developments from each segment will be identified.

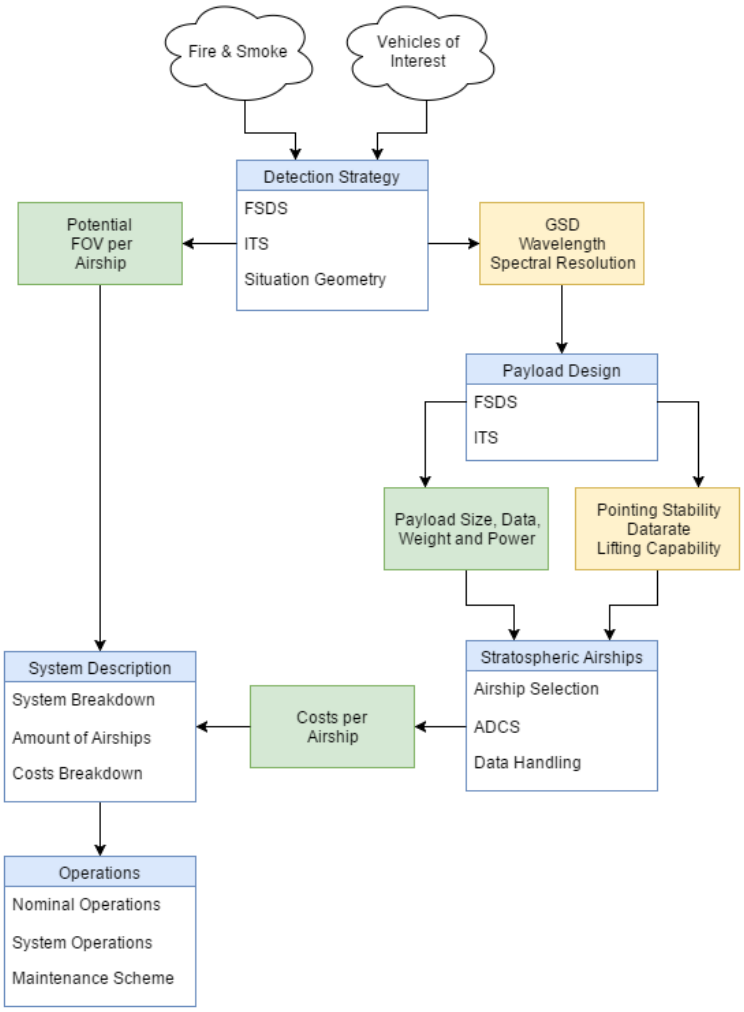

Figure 2.3: Flow diagram of the design approach

3 | Detection Strategies

One of the primary decisions of this project is to identify and select what physical mechanisms will be used to perform the FSDS and ITS functionality of the system. This chapter explains those mechanisms. Chapter 5 from the MTR has already laid the groundwork for most of the content; this chapter will restate some of the information of the MTR briefly and elaborate on some interesting points [2]. First the physical mechanisms that allow the detection of gas, smoke, and fire will be discussed. This discussion will also touch on the chemical analysis of clouds of gas and smoke.3.1 A brief overview of possible future FSDS technologies is also presented.3.1.3 After that the attention switches to the ITS where first some basics of quantum dots are restated 3.2.1. After which a new ITS detection method, called panchromatic coating, will be introduced and explained in detail 3.3. This part also contains future possibilities. Finally the geometry of the detection situation is explained. This focuses primarily on the maximum field of view of a single airship and on the radiance that arrives, from a scene on the ground, at the detectors.

3.1. Fire and Smoke Detection Strategies

Passive fire and smoke detection methods have been selected and discussed in the MTR in detail [2]. First a summary of the previous findings will be presented in this section together with the final conclusions regarding the preferable spectral bands to be used for fire and smoke detection. Then the detection strategy for specific chemicals within these clouds will be discussed. The chapter will be concluded with potential future detection strategies.

3.1.1. Fire and Smoke Detection

Fire and smoke detection are very similar in the sense that the method used for the detection of both is based on the same principle. The idea behind it is to use a spectral camera, capable of imaging around specific wavelengths, and apply algorithms to the images it captures in such way as to achieve new images that will reveal the presence of one or the other. In the previous report emphasis was put on the advantages of the use of the bands centred around $3.9\mu m$ and $10.8\mu m$ for fire detection [2]. There are several reasons to support this.

- Both of these spectral bands are located in 'atmospheric windows', meaning there is very little absorption of these wavelengths by the atmosphere [2].
- Due to its high temperature, fire emits peak radiation in the medium infrared (MIR) spectrum (around $3.9\mu m$) in accordance with Planck's theory of black-body radiation. This means that this wavelength will be the most sensitive to the presence of fire [3].
- Due to the high sensitivity of the $3.9\mu m$ band it is not uncommon for false fire detection to occur. The $10.8\mu m$ band is used to tackle this effect because it corresponds to the bandwidth of maximum emissivity of Earth. This is shown in Figure 3.1. By subtracting one from the other, false fire pixels (where no fires are present) are removed and the detection becomes more accurate [3].

Imaging around these two wavelengths would most likely be enough to have a working fire detection system. However this would not suffice for the desired application of the NSS, as the algorithms for smoke and gas detection require imaging in additional bands. An article on dust and smoke detection for multi-channel imagers proposes several different algorithms for the detection of dust and smoke over water and land [4]. The combination of all these algorithms uses spectra bands centred around 0.47, 0.64, 0.86, 1.38, 2.26, 3.9, 10.9 and $12.0\mu m$. Using these bands, the number of applications and accuracy for both fire and smoke detection increases. The possible applications of these include the filtering out of reflective surfaces or Sun glint and detection of smoke or dust over water or land.

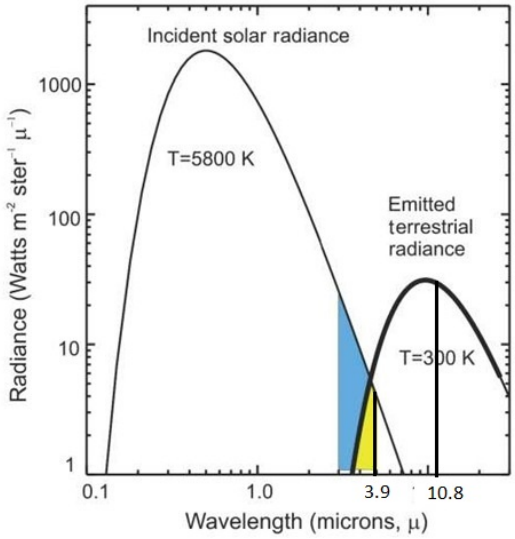

Figure 3.1: Radiance graphs of the Sun and Earth

It is clear that the addition of these spectral bands, besides the original 3.9μm and 10.8μm, would bring massive advantages for the system in terms of the features that could be potentially seen. Using info from MODIS, a payload currently operational that performs satellite imaging on all of them, it was possible to indicate typical bandwidths for each wavelength, given in the following Table 3.1.[1]

Table 3.1: Typical bandwidths for selected wavelengths

Wavelength [nm]	**Spectral band** [nm]
470	459–479
640	620–670
860	862–877
1,380	1,360–1,390
2,260	2,105–2,155
3,900	3,929–3,989
10,800	10,780–11,280
12,000	11,770–12,270

Another possibility for passive fire detection that was looked into is the use of microwave emissions from the fire. Microwave fire detection would solve an issue that was mentioned in the previous report [2], the cloud blockage. Microwaves are able to pass through clouds with ease and so their presence would not affect the FSDS operations if this type of detection was used. However, literature shows that this would not be a feasible way of detection for a stratospheric airship at 20 kilometres altitude. This is due to the low emitted energy, causing the distance at which detection is still possible to be limited at a most of 100 metres [5].

3.1.2. CHEMICAL ANALYSIS

Being able to quickly detect fire and smoke is one of two primary tasks of the NSS. However, its end purpose is to protect the citizens of the Netherlands and the stakeholders expressed another secondary task in which the NSS could assist. That is performing real-time, detailed chemical analysis of the smoke or gas clouds that are detected.

The method used for gas identification also utilises spectral imaging which is quite convenient. Its functioning is based on creating an approximation of the measured spectrum and comparing

[1] https://modis.gsfc.nasa.gov/about/specifications.php [cited 13 June 2017]

it with known reference spectra of several substances until a match is found. A spectral library is given to the system beforehand for this purpose. The correlation between the two spectra is given by 'subtracting' the two in a certain spectral windows. Also the signal-to-noise ratio is calculated by dividing the maximum brightness temperature caused by the target compound by the noise equivalent temperature difference of the spectrum. If all coefficients of correlation and the signal-to-noise ratio are greater than compound specific threshold values, the target's compound is considered to be a match [6].

This task has been previously achieved with the IMG instrument as the payload of the ADEOS spacecraft. This sensor is able to image in 3 bands, from 3.3 μm to 4.19 μm, from 4.0 μm to 5.0 μm and from 5.0 μm to 16.7 μm [7]. One of the resultant absorption spectrum from this mission is given in Figure 3.2 as an example.

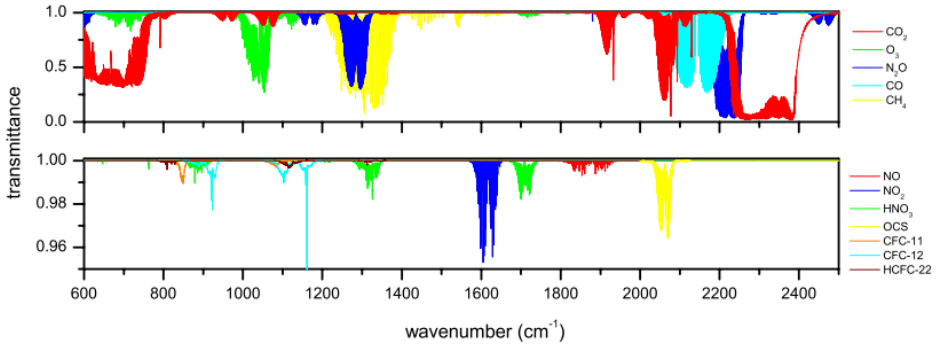

Figure 3.2: IMG spectrum (in transmittance units) in the 600–2500 cm^{-1} spectral range recorded over South Pacific (-75.24, -28.82) on 4 April 1997, 04:00:42 GMT (top) [7]

The selected spectral range is associated with the rotational transition lines related to the fundamental vibrational bands of H_2O, CO_2, O_3, N_2O, CH_4, and CO. Weaker absorption contributions occur due to the presence CFC11, CFC12, HCF22, HNO_3, OCS, NO and NO_2. There are a number of existing instruments that have been designed specifically for this purpose. An example of this is the SIGIS 2 (Scanning Infrared Gas Imaging System), a scanning imaging remote sensing system based on the combination of an infrared spectrometer with a single detector element and a scanner system. With a spectral range of 1.6 to 16 μm this imager is designed to detect gas and smoke clouds at over 10 km and with a resolution of 640 by 512 pixels [8]. This comes to show the feasibility of this detection method and how developed this technology is.

3.1.3. FUTURE FSDS POSSIBILITIES

ACTIVE DETECTION

In order to eliminate the challenge of obstructed views by clouds or the lack of a Sun above the horizon, an alternative for passive detection is active detection. This would be done using radar technology. Radar detection works as follows: there is a transmitter that emits radio waves (either in pulses or continuously), and a receiver that detects the reflected waves. Depending on the nature and characteristics of the object that reflects these waves, the receiver detects a different signal. The time interval between emission and detection is also used to determine the distance to the object, while the Doppler effect can help in determining its velocity. Radar is used to detect aircraft, ships, guided missiles, and for remote sensing of terrain and weather formations. It is the latter application that can prove to be useful to detect and monitor smoke clouds. While the radar waves would pass through clouds, one could choose the right frequency which would interact with solid aerosols, of which smoke clouds consist.

There are numerous examples of radar instruments that have been utilised in space missions for remote sensing tasks, but the payload capacities of these platforms exceed those of the available stratospheric airships. Some of these are designed by Thales Alenia. For example: the Synthetic Aperture Radar (SAR) payload instrument used on the KOMPSat-5 has a mass of 520 kilograms

and a power consumption of 600 Watts with peaks up to 1700 Watts.[2]

As mentioned earlier, the advantage would be the fact that clouds would no longer pose a problem for observation. The system will perform equally well during day and night as it will not rely on electromagnetic waves provided by the Sun, nor will it suffer from the Sun's interference during operation. On the other hand, the main issue with utilising this particular technique is the fact that it is an active detection method; meaning that it will be much more demanding in terms of energy and weight. However, the feasibility of this particular application of this technology on airships should be further studied, and eventually a design could be pushed forward which is compatible with airship placement.

Another future FSDS possibility is LIght Detection And Ranging of Laser Imaging Detection And Ranging (LIDAR). "Lidar is a high-resolution, active, airborne, remote sensing system that can provide accurate, three-dimensional models of forest structure and surface topography" [9]. This is a proactive method of fire management. The possibility is investigated to use LIDAR in wildfire management in British Columbia. Research done by J. Burns shows that LIDAR could be very beneficial for at least in British Columbia [9]. However, the disadvantage of this method is that it cannot be used on an airship, because it is an airborne system, therefore it can only be used as a back-up of the NSS. This possibility should be further investigated.

ARTIFICIAL INTELLIGENCE

Another different area in which the FSDS functionality of the NSS can be improved is not specifically related to the detection mechanisms but how the system deals with incoming signals. It is only a matter of time before these advancements become implementable in the NSS FSDS operations. There are two major advantages that the use of an improved AI system would bring to the system: as it gains experience and more and more fires are detected the system will become increasingly fast at detecting them. The first minutes of a fire are usually the most critical, and so the advantages of a faster detection are massive, even if the detection is already relatively quick. Over time, fire detection would require less and less input from the environment to accurately assess the start of a fire and this could reach levels of almost instant fire alert anywhere in the Netherlands. Another major advantage of developing the AI for this kind of operations would be the massive reduction of false positives. Again, as the AI gains experience it becomes aware of which patterns are incorrectly assesed as fire or smoke. Each of these instance generates additional costs for the system, and these costs increase the longer the false fire alarm goes undetected. As the AI is developed it would reach a level where the false detection probability would be minimal and the FSDS operations would effectively be near-optimal. Finally, the beauty of AI is that it can be implemented very easily and with very low costs associated, since it is mostly related to software development. As said before, this technology requires additional developments, but taking into account recent breakthroughs, this should be possible to do in the near future.

3.2. IDENTIFICATION AND TRACKING STRATEGIES

ITS, just like FSDS, requires signatures to be able to detect targets. As decided in the MTR the NSS will require targets to be marked in some way in order to detect them. During the MTR the focus of the marking techniques was on using a transparent quantum dot (QD) coating or paint. The midterm review showed that this method, although effective, has some limitations and thus a second marking technique is necessary to complement it. The second technique that is being considered is by using a panchromatic coating (PC) which is explained in detail in Section 3.3. But first, in this section a short summary about the QDs is given and after that some possible future ITS detection strategies are discussed.

3.2.1. QUANTUM DOT IMAGING

As already discussed in more detail in the Midterm report one of the possibilities of marking a target is using quantum dots [2]. QDs are essentially nano-crystals made out of semi-conductor ma-

[2] http://spaceflight101.com/spacecraft/kompsat-5/ [cited 09 June 2017]

terials. The size of these crystals is in the order of several nanometers which allows them to have a quantified electron energy gap between the valence band, the ground energy state (S_0 in Figure 3.3),[3] and the conduction band (S_1) This enables some interesting applications for QDs.

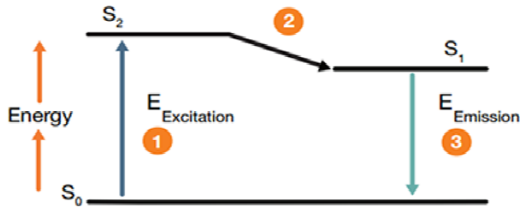

Figure 3.3: Schematic of electrons states

Incoming photons can excite electrons in the valence band to above the conduction band. This enables the absorption of photons of a wide range of wavelengths. These excited electrons then drift down towards the gap. If the electrons are conducted away before they hit the gap then electricity is generated and the QDs act as tiny solar cells. If the electrons hit the gap, they immediately fall down to the valence band and while doing so, emit a photon. The wavelength of that photon is solely determined by the size of the gap and possibilities exist to emit anywhere in the UV, VIS, and IR part of the spectrum [10]. This is generally called fluorescence. Thus, QDs are useful since they allow for the absorption of photons of a wide range of wavelengths while emitting at a very specific one. Additionally, QDs can be made soluble in water by combining it with certain biological molecules. Those two facts combined make them a versatile solution which is highly engineerable. Different size of QDs can be combined to form a unique paint that can be used to mark targets.

The technology of QDs is relatively new and thus a transparent paint or coating containing the QDs has to be developed. Scientist are currently working on transparent QD paint which would act as spray on solar panels [11, 12]. This requires the paint to also conduct electricity, something the ITS technology has no use of. Since the spray on solar panels seems to be quite possible, it can safely be assumed that making a transparent non-conducting paint is, although not trivial, not a major hurdle in this project. When such a paint will be created it must be made sure that weather conditions such as rain and wind will not degrade the QD paint too fast. It is assumed that this is possible to achieve and is considered beyond the scope of this current project.

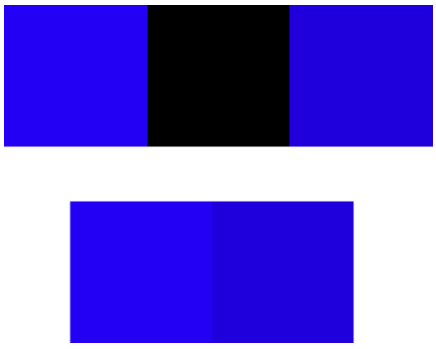

Figure 3.4: Light absorption by quantum dots – 10 % change in brightness between the left and right blue squares

This technology is, however, not magic and has some limitations. In order to emit enough energy to be able to detect the QDs require enough ambient light. Thus this technology is limited to operating during the day. In the MTR it was also decided that, because of benefits for contrast and available energy, the emission should take place in the IR. However, this makes it possible for other individuals to detect the markers as well using a camera capable of looking in the near and shortwave infrared. Another potential issue is the fact that, although the paint itself is transparent, the

[3] http://www.leica-microsystems.com/science-lab/basic-principles-of-luminescence/ [cited 20 June 2017]

QDs do absorb light. This absorption causes the colour of the object beneath the paint to change in brightness slightly. In the MTR it was assumed that the QDs absorb 10% of all incoming light. In Figure 3.4 it can be seen that, at least for dark colours, a 10% change in brightness is not visible as long as the colours are not right next to each other. These downsides put a limitation on the usefulness of quantum dots. Thus a second marking system was deemed necessary to complement the quantum dot markers. For this purpose a second marking technique is a panchromatic coating is considered.

3.2.2. FUTURE ITS POSSIBILITIES

So far, the directionality of light has not been considered yet. Polarisation is a physical property of light, describing the directionality of the oscillating electric field with respect to the direction of travel. The main advantage to using polarisation for remote sensing, lies in the additional information that it carries about the object from which it has been reflected. For instance, circular polarisation is produced by scattering from relatively high conductivity materials such as metals, carbon soot, or aerosols containing carbon. Birefringent materials such as plant leaves can also produce circular polarisation [13]. Unfortunately, polarisation is slow to find remote sensing applications. This is mainly due to the requirement for at least two (0°/90°), sometimes even three (0°/45°/90°), simultaneous photometric measurements of every point in the sensor field of view. So, for now at least, the scope of remote sensing applications is more or less restricted to power spectral densities, not polarisation, of light. With future technological developments, polarisation may become an attractive option for target marking. This requires further development of polarising paints to mark targets, as well as sensors which can discern their polarisation.

Another future possible ITS technology is Synthetic Aperture Radar (SAR), which was also mentioned in Section 3.1.3 as a future FSDS technology. SAR change detection is especially useful when clouds or the night blocks the ability to detect objects. There are different missions that have high spatial resolutions. For example there are different missions that have a spatial resolution of between 0.25-3 m. TERRASAR-X has a spatial resolution of 0.25 metres with a swath width of 4x3.7 km at an height of 514 km. This is the highest spatial resolution that can be acquired. The disadvantages of the SAR method are that it consumes a lot of power (800 Watts on average) and that the instrument is very large 5 x 0.80 metres.[4] If the Netherlands is mapped by SAR for example every week, the changes of the environment can be observed by comparing the images. By using SAR, extremely subtle changes (that cannot be seen by the human eye) of the environment can be detected. For example vehicle tracks, can be detected [14]. Due to its ability to discern vehicle tracks it is assumed that with this method also drugs dumping can be seen and a grave can be seen. SAR seems also useful when the data is directly monitored by an operator where crowd and situation monitoring can be done. However, this crowd monitoring at real time is not possible yet and this should be further investigated. At Microwave Sensing, Signals and Systems at the University of Technology Delft dr. F. Uysal is interested to grow such a project. The marking of a specific target using SAR is not possible so an intelligent system is necessary to keep track of targets. Another disadvantage of SAR is that it is needed that the platform that the instrument supports is moving with an high velocity with respect to the Earth's surface. The airship is not moving with an high velocity and therefore this should be considered as a future possible ITS technology that can be done with a satellite or an airplane. It can be used as a back-up system when clouds are present.

The possibilities of SAR evolves more and more, where one of the developments is Ground Moving Target Indicator (GMTI). SAR makes use of a single channel approach, this currently fails to detect fast and slow moving targets. This can be solved by using multiple receive channels, which will improve the detection capabilities of the system by detecting and locating moving targets. [5] This technique is very promising as it can detect fast moving vehicles and individuals at walking pace. Therefore, GMTI can be used for crowd monitoring. It still can not be used on an airship, but it can be supported by different platforms ranging from light aircraft to UAV's.

[4] http://www.intelligence-airbusds.com/terrasar-x/[cited15June2017]
[5] http://ieeexplore.ieee.org/stamp/stamp.jsp?tp=&arnumber=6217083&tag=1

3.3. PANCHROMATIC COATING

The second marking technique relies on the relative distribution of an object's light reflection of different wavelengths across the spectrum, and how people perceive this as specific colours. The working principle behind the panchromatic imaging, is that under the right conditions, two objects can be perceived as the same colour to the human eye, while in fact their optical properties are not the same since they reflect wavelengths across the spectrum in differing relative proportions. This would be noticeable for a highly accurate hyper-spectral imager which can be placed on an airship.

To better understand the physical phenomenon that is to be exploited, this section will delve into the concept of colour spaces, which aid in the objective description of colours, before explaining how this panchromatic imaging will enable the NSS in the identification and tracking of targets. This method does not come without its own challenges and chances of failure, and these will therefore be carefully elaborated upon. Finally, a practical example will be given, to show how the theory has been worked out.

COLOUR THEORY

First of all, consider two colour specimens that under normal light conditions appear exactly the same to the naked eye. However, when illuminated by a different light source, they no longer seem to match. This is called metamerism, and is caused by different spectral reflectance characteristics of the two colours, which are no longer noticeable to the human eye under the specific lighting conditions. The reason that when illuminated by a different light source, the differences might become apparent, is due to the fact that different light sources emit wavelengths across the spectrum in differing relative proportions. When this is combined with different spectral characteristics, the spectral properties of the light that is reflected will change, causing the way it is seen by the naked eye to change slightly.

But how would all of this be defined in an objective, mathematical way? First, one must look at how to define a certain colour. This can be done by something called a colour space, which usually consists of three coordinates, usually referred to as tristimulus values. Since the goal in this case is to fool the human eye, the colour space that will be used must be one that takes into account both the objective characteristics of a colour, and perception of colours by people.

In order to perceive visible light (or see) under normal lighting conditions, the human eye uses three different cone cells, each being sensitive to a different part of the visible light spectrum; long, medium, and short wavelengths (LMS). Their spectral sensitivities can be seen in Figure 3.5, with the wavelengths on the x-axis and their respective relative sensitivity on the y-axis. Combining this information with the spectral power distribution of an illuminant gives three stimulus values, together making up a tristimulus description of a colour, which has been defined as the LMS colour space.

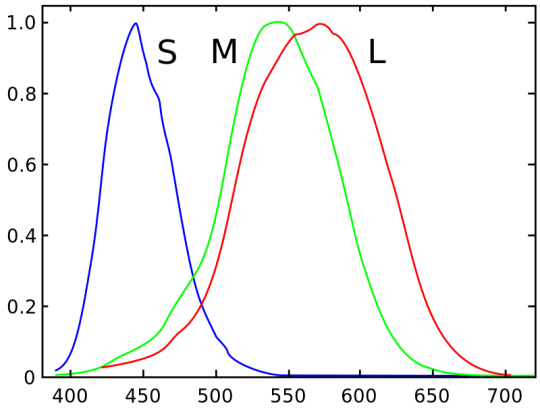

Figure 3.5: Spectral sensitivity of the different human cone cells [15]

There are a number of problems that arise in the implementation of LMS tristimulus values under certain conditions. This is, however, only one example of a colour space. Colours tend to be specified in other colour spaces.

According to Grassmann's law, the human perception of colour (trichromatic) can be described as a linear combination of different light colours or wavelenghts (panchromatic). Building on this assumption, colour matching experiments were done in the late 1920s by William David Wright and John Guild. The results from these experiments led the International Commission on Illumination (CIE) to define the so-called XYZ colour space in 1931. The XYZ colour space includes every colour sensation that the average observer experiences (and some more, but that is not relevant). From these XYZ values, the normalised x and y can be determined, which are then used to map the colour on the CIE colour space chromaticity diagram, as can be seen in Figure 3.6.

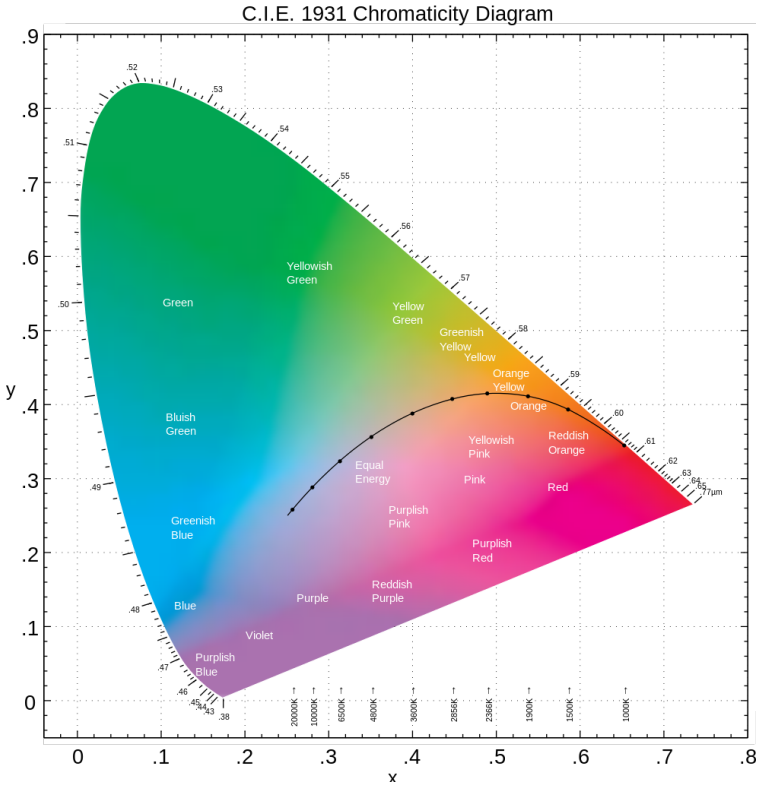

Figure 3.6: CIE 1931 colour space chromaticity diagram, with low saturation images, as can be reproduced with pigments

There are multiple ways of determining the XYZ values. For the following calculations, the reflective case will be taken into account, as the colours will be applied as a pigment on cars and reflect light from the environment (e.g. sunlight). The following equations are used.

$$X = \frac{K}{N}\int_0^\infty S(\lambda)I(\lambda)\bar{x}(\lambda)d\lambda \tag{3.3.1}$$

$$Y = \frac{K}{N}\int_0^\infty S(\lambda)I(\lambda)\bar{y}(\lambda)d\lambda \tag{3.3.2}$$

$$Z = \frac{K}{N}\int_0^\infty S(\lambda)I(\lambda)\bar{z}(\lambda)d\lambda \tag{3.3.3}$$

$$N = \int_0^\infty I(\lambda)\bar{y}(\lambda)d\lambda \tag{3.3.4}$$

Here, K is a scaling factor, being either 1 or 100. $I(\lambda)$ represents the spectral power distribution of the illuminant, for instance sunlight, which depends on the position of the Sun at different times of the day, or other environmental factors. The spectral distribution of different illuminants have

been standardised and defined by the CIE for use in colour reproduction and calculations. Examples of the emittance from different light sources can be found in Figure 3.7. As a result of the earlier mentioned experiments that were conducted, the colour matching functions $\bar{x}, \bar{y}, \bar{z}$ were defined. These are numerical descriptions of the colour response of the standard human observer; and are numerically related to the LMS tristimulus values. Finally, the $S(\lambda)$ of an illuminated pigment represents its inherent spectral reflectance; the relative distribution in which amount it will reflect different wavelengths, the combination of these wavelengths are, therefore defining its observed colour. Examples of spectral reflectance graphs of everyday objects can be found in Figure 3.8.

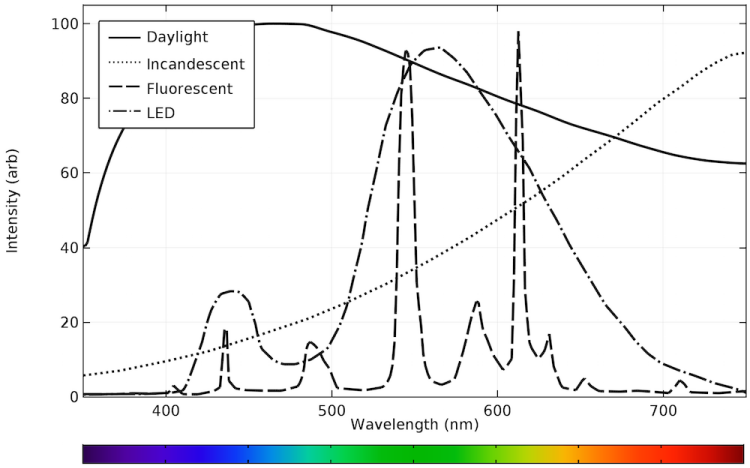

Figure 3.7: Emittance curves of different light sources[6]

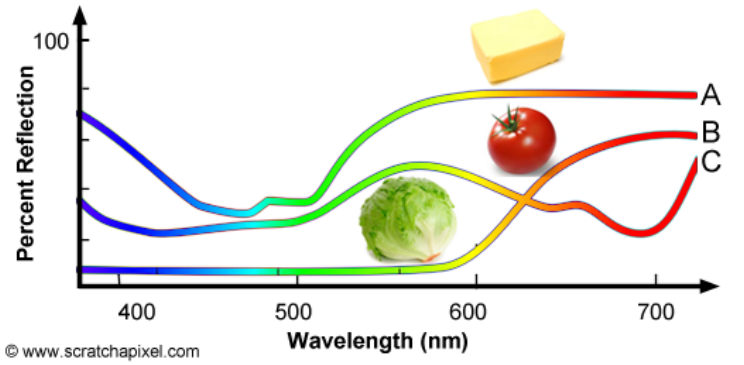

Figure 3.8: Reflectance curves of various everyday objects[7]

The last step in these calculations is to normalise the XYZ values before they can be plotted out on the chromacity diagram or converted to RGB values. This is done as follows:

$$x = \frac{X}{X+Y+Z} \tag{3.3.5}$$

$$y = \frac{Y}{X+Y+Z} \tag{3.3.6}$$

$$z = \frac{Z}{X+Y+Z} = 1 - x - y \tag{3.3.7}$$

[6] https://www.comsol.com/blogs/calculating-the-emission-spectra-from-common-light-sources/ [cited 20 June 2017]

[7] https://www.scratchapixel.com/lessons/digital-imaging/colors [cited 20 June 2017]

Of course, since these values are normalised, the final equation that applies to the z-coordinate also applies to the other coordinates.

In mathematical terms, metamerism could be described as the special case where:

$$(x, y, z)_1 = (x, y, z)_2 \tag{3.3.8}$$

while in general

$$S_1(\lambda) \neq S_2(\lambda) \tag{3.3.9}$$

Metamerism may be used as a working principle for target marking. Now that the physical workings behind this phenomenon have been laid out, the next step is to figure out how to exploit it.

IMPLEMENTATION & RECOGNITION TECHNIQUES

That brings the reader to the implementation of this theory to perform the mission. It is by controlling and observing this variable, $S(\lambda)$, that the vehicle tracking and identification can be performed. $S(\lambda)$ is determined by the chemical composition of the pigments. One could ensure that two parts of the car have colours that are metameric pairs with a different $S(\lambda)$. Using a sufficiently accurate hyper-spectral imager that would identify the differences, one may determine which target is being imaged.

For the best and most accurate results, this method would require cooperation of paint manufacturers, which would produce a specific colour that is perceived to be the same as the one of the target vehicle, but would in fact be composed of a spectrum which differs from commercially available metallic paints, hence ensuring metamerism. The next step is to apply this paint to a vehicle, having a different spectral deviation for each individual target.

The most optimal implementation would be to apply a coating to the top of the car, while maintaining the original colour on the bonnet. This way there would be a spacing between the metameric pair, making it more difficult to notice any colour differences that might appear under different lighting conditions. This is visualised in Figure 3.9 and Figure 3.10.

Figure 3.9: A metameric pair as would be seen under fluorescent light – using the F2 standard illuminant

A hyperspectral imager would then register the difference in spectral luminance, which is the reflectance multiplied by the illuminance. In Figure 3.11, the spectral luminance can be seen for the two colour pairs given in the example above. In Figure 3.12 the differences have been plotted.

As can be seen in the two previous graphs, the differences can sometimes be quite small yet present, for both optical perception and objective measurements. However, in order to ensure reliable observation from the system platform, a camera should be chosen that can measure the luminance at highly accurate wavelength intervals; based on practical experience while working out practical examples with different intervals, it was assumed that this should be in the order of 5 nm for useful results. And to be able to discern different surfaces of the car, the optics must be able to provide a spatial resolution of at least 1 metre.

Figure 3.10: A metameric pair as would be seen under incandescent light – using standard illuminant A

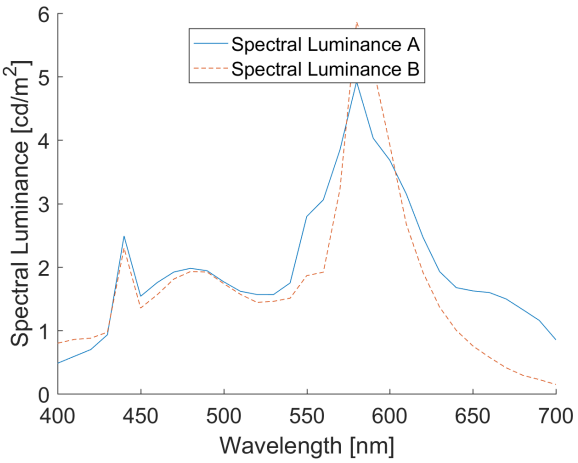

Figure 3.11: Spectral luminance for specimen A and B

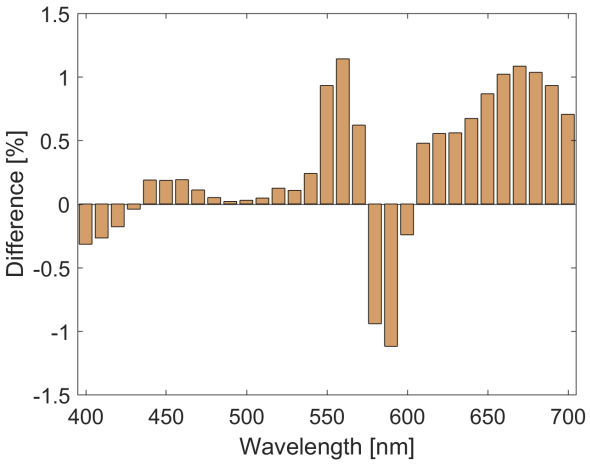

Figure 3.12: Percentage difference in spectral luminance between A and B

Another interesting design solution would be to apply the paint similarly to a bar code. Much in the same way as the previous method, there would be an invisible pattern constructed by a metameric pair for the purpose of identifying targets. These transitions between the two colours would be unique to every target, giving the possibility for identification. This would be in order to more easily identify a target, and quickly and reliably distinguish them from the 1000 other targets that will be tracked (as requested by the customers). Moreover, this technique could also be used to provide some additional information to the ground operations once it has been spotted by the system, by a recognition pattern can be applied on top of the target. There are multiple

solutions available, such as bar codes, or other generic recognition patterns that are unique to each target.

If one would opt for bar codes, there is a choice between 1D bar codes, and 2D bar codes, also known as QR codes. The latter are physically smaller - only 1/10th their size - and are therefore able to carry more information. This larger amount of data can also be segmented in different parts of the QR code. The kind of information that QR codes can carry is also more diverse; including characters, numbers, symbols, text, and control codes, while regular bar codes are limited to alphanumerical characters. In order to optimally use the space available on a vehicle, the QR codes can also be represented in a rectangular matrix.

Another issue to address is a decreased readability due to paint damage or accumulated dirt. While a bar code can quickly become illegible, QR codes still are more reliable, and the damaged part can even be recovered for up to 30%, with the use of Reed-Solomon error correction.[8]

Currently the spatial resolution that can be achieved is too limited to allow for the observation of such a small, intricate recognition pattern, for the system to make use of this technique. This could be a focus of development for the future. While the feasibility of these solutions would be limited, whether or not such a complex solution would be necessary is another story; it would partially depend on the amount of unique identifying metameric pairs that can be produced, and whether or not simple identifying markers would suffice to distinguish targets.

POTENTIAL CHALLENGES & METAMERIC FAILURES

While these methods and physical phenomena are promising and offer numerous possibilities to fulfil the mission, they also come with their challenges and possible obstructions during implementation.

Metamerism occurs more often for neutral colours, tending towards grey, dark, or white-ish. The brighter and more saturated the colours become, the smaller the range of possibilities to create a metameric match. More so for colours that are applied to a surface, as the colour appearance also relies on the spectral emittance of the light source, besides its own spectral characteristics.

One problem with metameric matches is the fact that they might appear to be matches under a certain light source, but not another, as has been mentioned numerous times. This is particularly, but not necessarily always, the case with fluorescent light. Fluoresce irregular spectral emittance, defined by multiple peaks at different wavelengths, whereas other light sources have smoother emittance curves, as can be seen in Figure 3.7. Since it was mentioned before that the colour appearance depends both on the spectral characteristics of the material itself, but also on the spectral emittance of the light. Due to this, if one chooses to illuminate the reflective surface with particular a light, the colour differences that weren't seen before might suddenly become apparent. This is called illuminant metameric failure.

On top of that, there is observer metameric failure, which occurs due to a difference in colour perception by different people. This is usually caused by colourblindness, which is caused by people having a fault in one of their colour sensitive cone cells. To give an example of how this would influence colour vision, during World War II the US army would take colourblind people on reconnaissance flights as they weren't susceptible to camouflage thanks to their red-green colour deficiency; allowing them to easily spot artillery and tank positions whereas others couldn't. However, colourblindness is not always at the root of this, as an observer's colour perception also depends on many personal variables: the relative proportion of different cones in one's eyes, the light sensitivity profile of each cone, etc.

One final example of metameric failure is field-size metameric failure. There exists a different proportion of cones in the centre of the eye compared to the periphery. As a result, colours that appear to be the same when seen as small areas fixed in the centre of one's vision, might be noticeably different when seen in larger areas.

This gives rise to numerous circumstantial challenges in the implementation of this technique that must be taken into account in the risk mitigation. In order to mitigate the risk of compromise the

[8] http://www.qrcode.com/en/about/error_correction.html [cited 13 June 2017]

feasibility of the different detection techniques will have to be worked out and verified. So based on these risks and the exact circumstances wherein the identification and tracking shall be used, the implementation and the specific method can be given a green light or fine-tuned if necessary; thereby maximising the efficiency of the system.

To conclude, while this method is very promising, it is prone to being discovered in multiple ways. However, something which works in the advantage of this system's functioning, is the general population's preference for car colours leans towards blue, grey and black. These colours together constitute 71% of cars – when including red this figure comes to 81.5%.[9] This percentage is even higher among criminals as they have a high tendency to acquire neutrally coloured cars – whether these are stolen or not.[10]

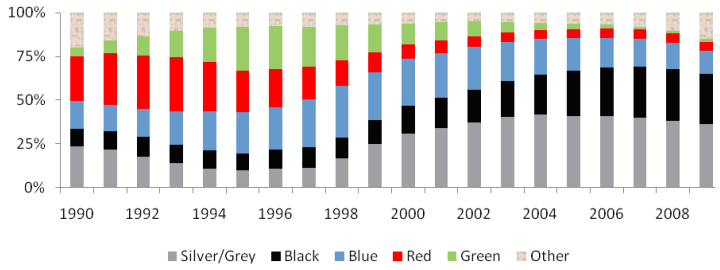

Figure 3.13: Relative prevalence of different car colours
Source: CBS/RDW

Thanks to these pieces of information, the scope and requirements of the system can be narrowed down, allowing for a more specific and targeted analysis of the colour sensitivity analysis and bandwidth determination.

WORKING CONCEPT

In order to show the workings of this concept, a tool was written in Matlab for the specific purpose of performing the calculations from the section *Colour Theory*. The point of this tool is to show the possibility of making colours match better by making use of their properties, external conditions, and human perception, while their optical properties are measurably different.

For this specific example that has been worked out, there are two colour specimens with different reflectance spectra, as can be seen in Figure 3.14. These were found on the internet and are allegedly a metameric pair. Specific information about these graphs is relatively difficult to find online, so these graphs were approximated at increments of $10nm$.

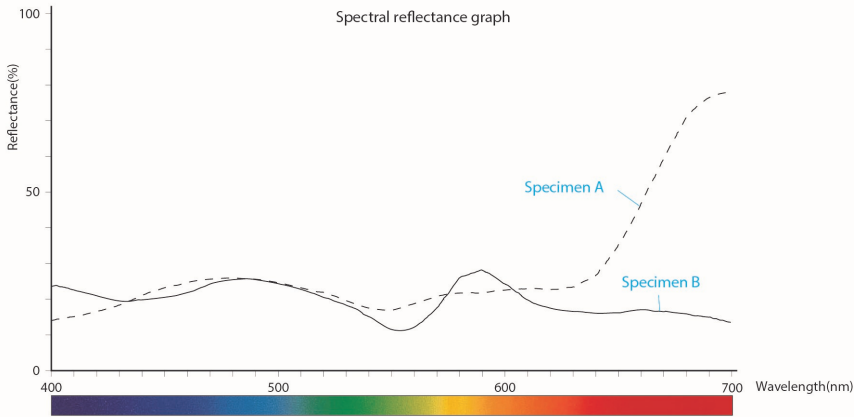

Figure 3.14: Spectral reflectance of specimen A and specimen B [11]

[9] http://statline.cbs.nl/StatWeb/publication/?VW=T&DM=SLNL&PA=71405NED&D1=54-68&D2=0&D3=0-11&HD=090325-1555&HDR=T&STB=G1,G2[cited 13 June 2017]
[10] http://voxeu.org/article/car-thieves-not-too-bright-please [cited 13 June 2017]

Thereafter data was accumulated about the spectral power distribution of different light sources, as defined by the standard illuminants published by the CIE. The illuminants that were used are D65 – representing average daylight conditions –, D50 – horizon light –, F2 & F11 – fluorescent light –, incandescent light (standard illuminant A), and an equal energy distribution across the entire visible spectrum. Luckily this information was more freely available, as these are defined by conventions.

Then, the above calculations were performed with Matlab to find the tristimulus values of specimen A and B under different light conditions. and convert the resultant colour coordinates into RGB values so that they can be represented on computers in order to be both visually and numerically compared with one another.

With the generated data, the following graphs (Figure 3.15 - Figure 3.20) were produced for each standard illuminant; the spectral luminance of specimen A and B, the relative difference between the spectral luminance, and an overlay of the standard observer graph with the relative difference in spectral luminance to indicate where the differences have the largest impact on the human perception.

[11] http://sensing.konicaminolta.asia/2016/01/metamerism/ [cited 20 June 2017]

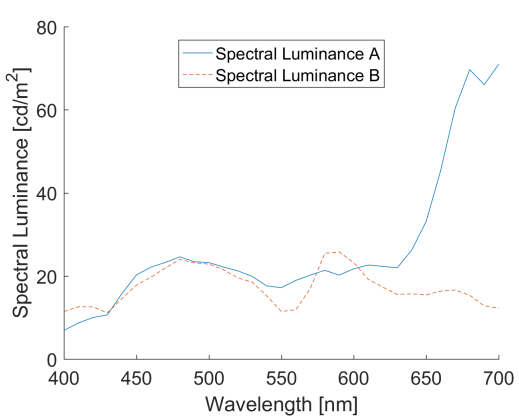

(a) Spectral luminance graphs for specimen A and B

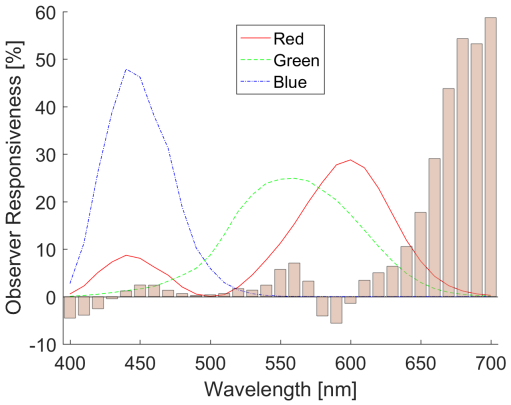

(b) Relative difference in luminosity overlaid with observer responsiveness

Figure 3.15: Spectral information for D50 standard illuminant

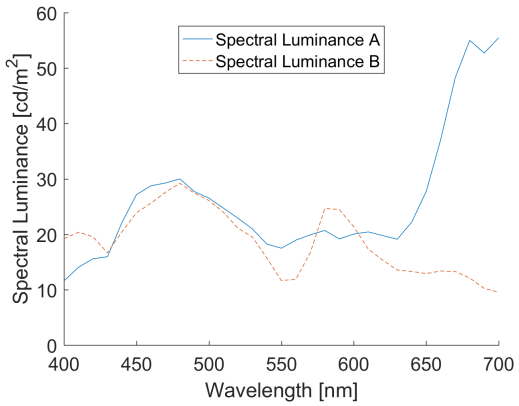

(a) Spectral luminance graphs for specimen A and B

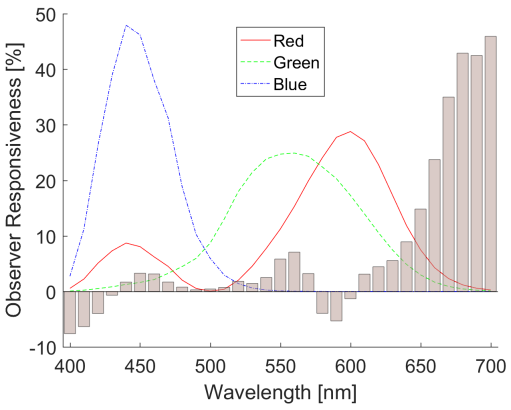

(b) Relative difference in luminosity overlaid with observer responsiveness

Figure 3.16: Spectral information for D65 standard illuminant

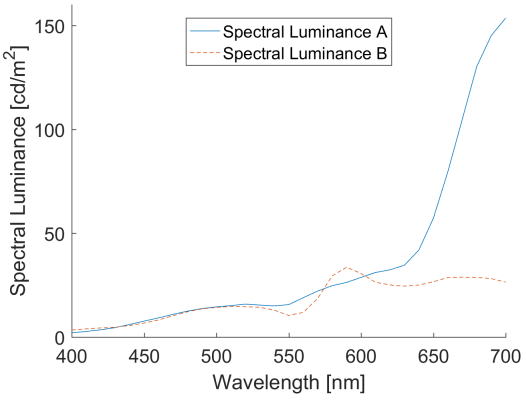

(a) Spectral luminance graphs for specimen A and B

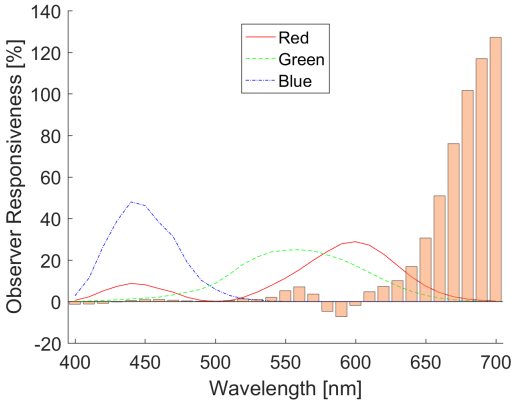

(b) Relative difference in luminosity overlaid with observer responsiveness

Figure 3.17: Spectral information for standard illuminant A – an incandescent light bulb

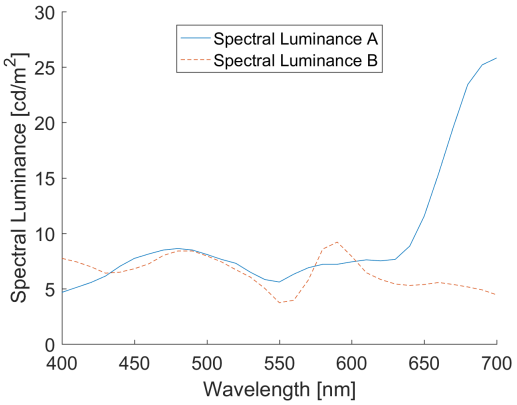

(a) Spectral luminance graphs for specimen A and B

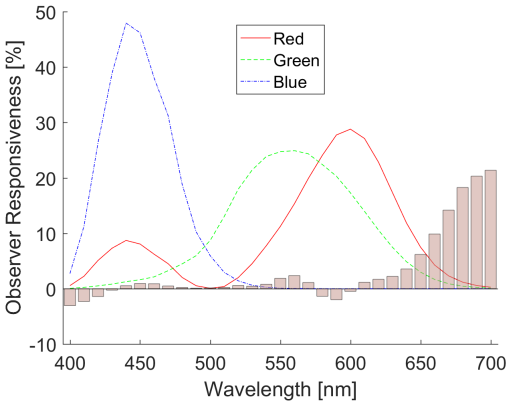

(b) Relative difference in luminosity overlaid with observer responsiveness

Figure 3.18: Spectral information for an equal energy distribution

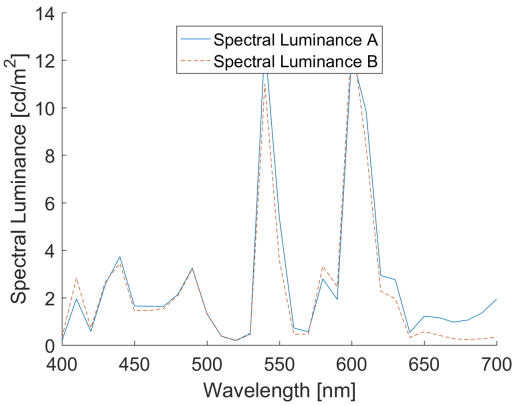

(a) Spectral luminance graphs for specimen A and B

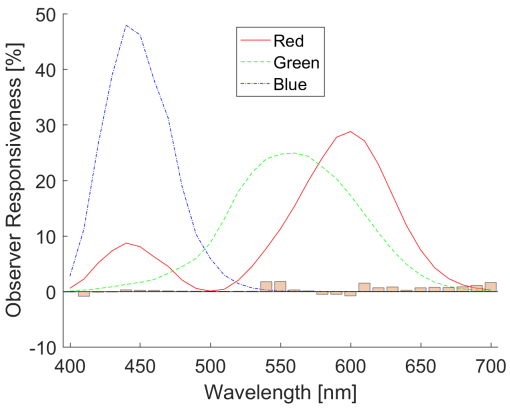

(b) Relative difference in luminosity overlaid with observer responsiveness

Figure 3.19: Spectral information for fluorescent light source F11 – a narrow triband illuminant

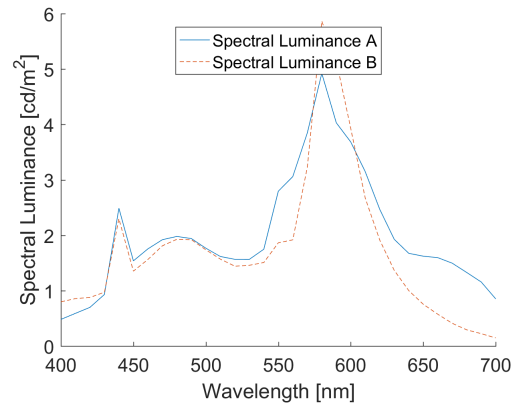

(a) Spectral luminance graphs for specimen A and B

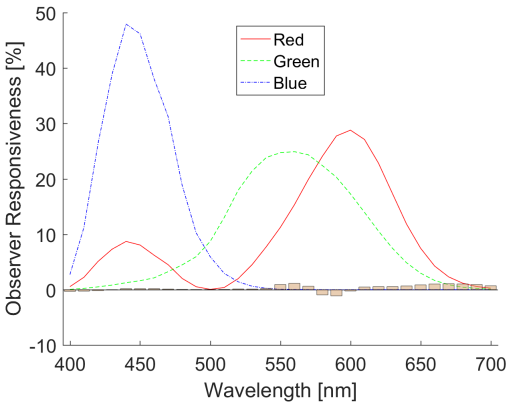

(b) Relative difference in luminosity overlaid with observer responsiveness

Figure 3.20: Spectral information for fluorescent light source F2 – a standard illuminant with two semi-broadband emissions

The colour specimens under each light source can be seen in Figure 3.21 and Figure 3.22.

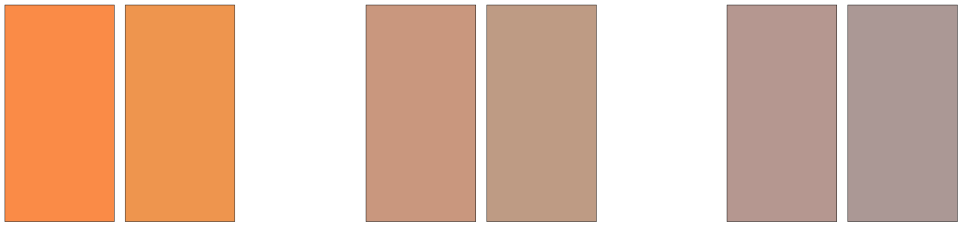

(a) Standard illuminant A (b) Standard illuminant D50 (c) Standard illuminant D65

Figure 3.21: Metameric pair under different light sources (1/2)

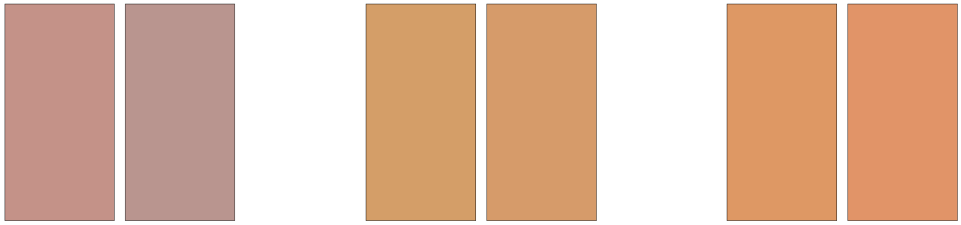

(a) Equal energy distribution (b) Standard illuminant F2 (c) Standard illuminant F11

Figure 3.22: Metameric pair under different light sources (2/2)

In order to have a better idea of the deviations between the two specimens for each illuminant, the standard deviation was calculated for each case and summarised in Table 3.2. This was done for both the difference between the spectral luminance and the RGB values. The ratios between $\sigma_{\Delta luminance}$ and σ_{RGB} were also calculated. The former value indicates how easily the differences are noticeable to an instrument, while the latter has an effect on how well the eye can see it. While these values are specific to this case, but they indicate a clear trend. Under daylight, the differences would be better observable to the instruments, while not sacrificing too much perceivable colour difference. The implication would be that the spectral reflectance curves, which is at the core of these deviations, could be optimised to ensure true metamerism, while maintaining a certain $\Delta_{luminance}$ such that it would still be visible to the panchromatic imager under daylight.

Table 3.2: Standard deviations of the luminance and RGB values between specimens A and B for different illuminants

	$\sigma_{\Delta luminance}$	σ_{RGB}	**Ratio**
Incandescent	36.7	0.0446	823
D50	18.3	0.0359	508
D65	14.7	0.0324	453
Equal Energy	6.54	0.0370	177
F2	0.560	0.0088	63.9
F11	0.690	0.0167	41.2

As an important sidenote, however, due to some limitations in available information and technology, the examples might not represent what exactly is achievable. For instance, the number of colour representations on computer screens and on the internet is very limited compared to the complete colour range that the human eye can observe. Another challenge that limited the number of case studies that could be performed, was the lack of numerical data regarding the spectral reflectance graphs for metameric pairs. Even the pair that has been used in this example was acquired from a graph by measuring the coordinates of data points at intervals of 10 nm. However, in that way data is lost in the process, causing discrepancies between the final RGB values.

On the other hand, the tool is representative of how the difference between the colours becomes more or less apparent under changing light conditions. The tool also gives an indication of the

difference in illuminant power provided by the reflection from metamers, giving an idea of how accurate measurement tools should be. Therefore, when looking at what is possible to work out with rudimentary tools, the possibilities are much greater with expert painting tools and access to both higher quantity and quality of information.

LITERATURE STUDY AND CONCLUSION

There are many instances where metamerism appears in daily life, most of the time this occurs unintentionally. Having a good knowledge of the spectral reflectance of different pigments, and the exact mixes used to produce a particular paint, will make it possible to create a metameric coating. The more accurate and sensitive the measurement can be, the less noticeable the difference between the metameric pair will be. But by definition, a metameric pair will appear differently under different light sources, so this is an inevitable obstacle. This effect can however be minimised by measurement and testing under colour matching lamps, such as the one in Figure 3.23.

Figure 3.23: Metameric pairs of fabric under colour matching lamps to indicate their metameric failure

All in all, panchromatic coatings bring some new tracking solutions, but at the cost of a major structural flaw. The possibility is definitely there, and it is inexpensive to create some real-world examples to further work out the concept. In order to make good use of it though, the camera that will be used should have an accurate spatial resolution and sensitivity.

3.4. SITUATION GEOMETRY

Although the physical phenomena for the detection strategies are important, they do not tell the complete story. The detection methods determine what the maximum field of view (FOV) and radiance of the observed objects are.

3.4.1. FIELD OF VIEW ITS

There are are two things to consider when estimating the ITS coverage area of an airship. The first being the field of view of the airship itself as illustrated in Figure 3.24a, indicated with α, and the ground angle indicated with angle θ. The second is the angle at which the object radiates its signature wavelength as seen in Figure 3.24b indicated with the angle ϕ and the opposite ground angle θ. The angle ϕ depends on the detection method.

With the approach of QDs, the angle ϕ depends on the radiance angle of the QDs. Considerable research is conducted with respect to radiance patterns for QDs and specifically how to manipulate these [16]. However, manipulating these radiance patterns requires specific structures. In theory this is possible using self assembling structures but lies for now in the future and is not considered further. Thus it will be assumed that the QDs will be in plane. The radiance pattern for in plane QDs can be seen in Figure 3.25 and from the figure can be seen that most of the radiance

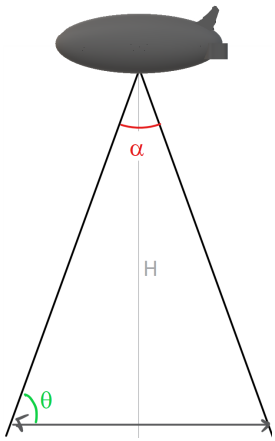

(a) Airship FOV α and ground angle θ

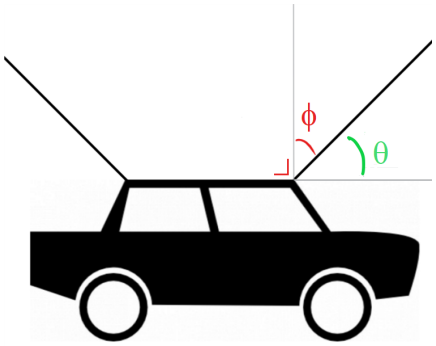

(b) Radiance angle ϕ

Figure 3.24: Angles defining the ITS situation geometry (1/2)

is emitted in an angle of 45° from the plane normal. Thus it can be concluded that the angle ϕ is equal to 45° and thus sets the maximum ground angle θ to 45°. The covered ground diameter can be calculated, and is equal to twice the altitude of the airship, or put differently: it can cover an area with a radius equal to the altitude the airship is floating at. Having an airship at an altitude of 20 km would mean a 20 km coverage radius.

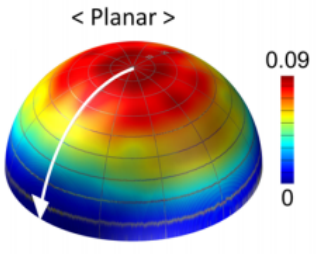

Figure 3.25: Radiance pattern of planar quantum dots [16]

Identifying a car on colour and geometry or more specifically, the panchromatic approach, relies on detection of diffusely reflected light. To fully describe the situation geometry, it is important to know the radiance pattern. It will be assumed that the vehicle is a so-called Lambertian emitter, meaning that all light will be emitted uniformly from the source. To determine the signal in a specific direction, the Lambert's cosine law should be considered. This law states that the perceived brightness of a surface is independent of viewing angle. Because the emitted power from a given area is reduced by the cosine of the incidence angle with respect to the surface normal, while the perceived area is reduced by the same amount, the brightness remains the same. From this, it can be concluded that the emitted power of a surface is reduced by the cosine of the incidence angle ϕ as seen in Figure 3.26a, which shows the law for incoming light. The emitted power is thus dependent on the angle with which the observer is looking at the object and therefore the signal decreases in strength as the angle of the observer increases. Theoretically speaking the aperture size can be increased to acquire a required signal strength. However, if the object is obstructed by e.g. houses or trees, it is no longer limited due to optics but rather due to the height of the platform and the size of the obstructions. This is illustrated in Figure 3.26b. Another thing to consider is the maximum visibility distance, the Netherlands had an average minimum and maximum daily visibility in 2016 of respectively 31 and 57 km.[12] The average visibility was around 44 km and should not be exceeded as maximum distance of the diagonal between the ground and the airship. Considering all these factors the ground angle θ was set to be 30°, giving a FOV α of 120°. This gives a

[12] http://www.sciamachy-validation.org/climatology/daily_data/selection.cgi [cited 07 June 2017]

ground coverage radius of 34 km for the panchromatic solution.

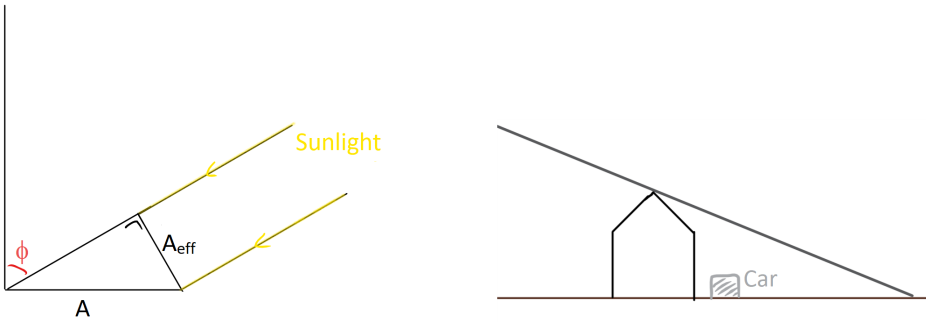

(a) Visual representation of the Lambert's cosine law (b) Obstruction of viewing angle due to objects

Figure 3.26: Angles defining the ITS situation geometry (2/2)

3.4.2. FIELD OF VIEW FSDS

When investigating the coverage area for fire and smoke it is important to know how high typical smoke clouds rise above the terrain. Figure 3.27 shows smoke altitudes from fires in America over the course of 5 years, although these fires are primarily forest fires it is assumed that other fires will have similar characteristics. It can be concluded that it is very rare for smoke to exceed an altitude of 2 km. The coverage area for FSDS can be higher than that for ITS, however, it is not interesting to make it considerably larger than that of the ITS if the adjacent area is already being covered by a different airship. What is worth mentioning, if a fire happens right on the border of two adjacent airships, the ground distance must be larger the ITS ground distance. This is to account for the developed smoke rising up and leaving the field of view. Although the airship could be moved if this were to happen, it would be preferable to have a slightly larger FOV than the ITS, as depicted in Figure 3.28. Using a cloud height of 2.5 km, allowing to see over it, and the found ITS coverage radii of 20 and 34 km yield a required FSDS FOV of 98° and 126°, respectively. The latter will be used, as it is the larger and thus will be the driving requirement.

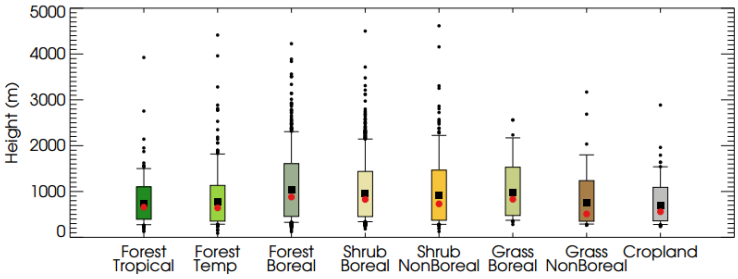

Figure 3.27: Median height above the terrain for smoke plumes in each biome (colour coded box and thin black lines: central 67% and 95% of data) [17]

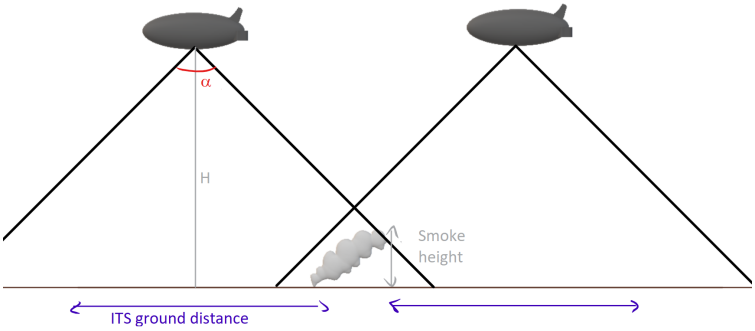

Figure 3.28: Coverage area for FSDS with FOV α

3.4.3. RADIANCE

The radiance of an object and the associated EM radiation that makes it to a detector is governed by the geometry of the situation, the black body radiation of the light source, the attenuation of the atmosphere, and the reflection or fluorescent properties of the target object. All the physics behind this was discussed in the MTR. In that same report it was calculated that the radiance of a quantum dot paint in perfect conditions is $R_{QD} = 1.94 \cdot 10^{15} [ph \cdot cm^{-2} \cdot s^{-1} \cdot sr^{-1} \cdot \mu m^{-1}]$[2].

The size of all optical payloads has a direct relation with the radiance and therefore it is necessary to also get a value for the other required radiance. In this situation the radiance for the panchromatic coating, regular colour imaging, and infrared imaging is required. These last two allow for the design of potential supporting imagers.

Estimating the radiance for the panchromatic solution is a bit more difficult since it relies on reflection which, contrary to what one might expect, is a lot more complicated than fluorescence. A rough first order estimate for the radiance was constructed using the following assumptions.

- All of the atmospheric attenuation takes place below 20 km altitude.
- The reflectivity of the tracked objects is 65%.
- The maximum allowable Sun angle from the normal is 75°.

The first assumption allows for the use of the AM0 value ($1.66 \cdot 10^{26}$ $[ph \cdot cm^{-2} \cdot s^{-1} \cdot sr^{-1} \cdot \mu m^{-1}]$ which is also calculated in the MTR) as the basic value that reaches the detector with 100% reflection. This assumption is considered valid since at 20 km altitude more than 90% of the atmosphere is below the stratospheric airship (as can be seen in Figure 3.29)[13] and prevents the need of integrating the attenuation over the entire atmospheric domain.

The second assumption yields a ratio between the radiance that actually reaches the detector and the AM0 value. Estimating the reflectivity of objects is difficult since it relies on a lot of factors, but for a car with a metallic paint is typically around 65% [18].

The last assumption gives another factor using the aforementioned Lambert's Cosine rule, which lowers the energy emitted by the object even further in proportion to the angle with which the Sun deviates from the normal. This was set to 75 degrees, since this is the minimum angle that the Sun reaches during mid-day in the winter in the Netherlands. This then makes objects detectable when the Sun is 15 degrees above the horizon.[14] The Lambert's cosine rule is also applied to the QD technique, because it is also affected by lower Sun instances. This means that the radiance R is dictated by Equation 3.4.1.

$$R = R_0 \cdot \rho \cdot \cos(\theta) \tag{3.4.1}$$

Where R_0 is the initial radiance, ρ is the reflectivity (which is not applicable for QDs), and θ is the Sun angle which is 75 degrees. The inputs and results are summarised in Table 3.3.

[13] http://climate.ncsu.edu/edu/k12/.AtmStructure [cited 20 June 2017]
[14] http://www.weerstationuithoorn.nl/weer/zonnestand.htm [cited 20 June 2017]

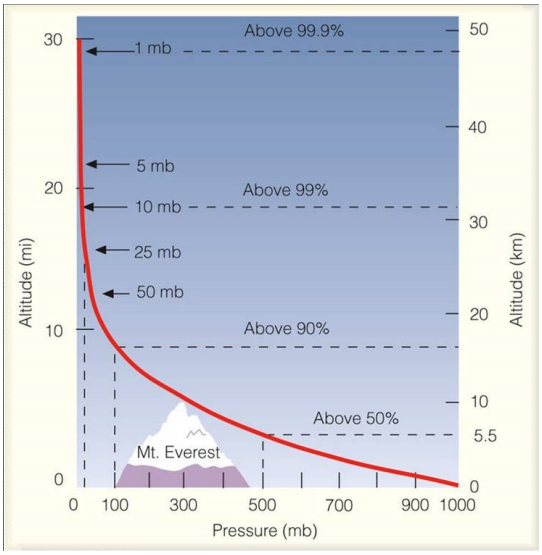

Figure 3.29: Pressure plotted against altitude

Table 3.3: ITS radiance summary

Technique	$R_0 [ph \cdot cm^{-2} \cdot s^{-1} \cdot sr^{-1} \cdot \mu m^{-1}]$	ρ	$R\ [ph \cdot cm^{-2} \cdot s^{-1} \cdot sr^{-1} \cdot \mu m^{-1}]$
Panchromatic	$1.66 \cdot 10^{26}$	0.65	$2.79 \cdot 10^{25}$
Quantum Dots	$1.94 \cdot 10^{25}$	1	$5.02 \cdot 10^{24}$

As can be seen in this table, the radiance for the panchromatic solution is, as expected, much higher than the quantum dot solution. Conveniently, for regular colour imaging the same radiance is used as for the panchromatic solution since it relies on the same reflectivity and incoming solar energy. Radiance in the infrared rely on the energy radiated by the temperature of a certain object. It is assumed that the object that is being observed is about 15°C. This results in a radiance R of $1.05 \cdot 10^{21}$ $[ph \cdot cm^{-2} \cdot s^{-1} \cdot sr^{-1} \cdot \mu m^{-1}]$ in the MWIR.

3.5. CONCLUSION

Although the NSS has only two main functions, FSDS and ITS, and will only detect objects of interest by way of remote sensing, it requires capabilities to image in many different parts of the electromagnetic spectrum. FSDS contains three different aspects. Fire detection, smoke and gas detection and tracking, and remote chemical analysis. In order to accurately detect fires, information about smoke, gas, and clouds is necessary. Thus fire detection and smoke/gas detection and tracking is performed by analysing the same specific wavelengths where the bands centred around 3.9 and 10.8 μm are the primary fire detection bands. The other spectral bands enable the system to identify clouds of smoke, gas, and water droplets in different conditions and environments. The chemical analysis of smoke and gas clouds, on the other hand, requires the use of a hyper-spectral imager. The larger the range in which the hyper-spectral imager can see, the more chemicals can be detected.

In the mid-term phase of this project, it was decided that the ITS will rely on the application of quantum dot markers. However, these fluorescent nano-crystals do have some limitations as it might be possible to detect them using regular near or shortwave infrared cameras. Thus a second marking technique was deemed necessary; for this a panchromatic coating was chosen. This detection method relies on the fact that it is possible to have two surfaces which have the same colour but a different radiation pattern. A sensitive hyper-spectral imager is able to detect these differences while a regular human eye or camera cannot. Thus to perform the ITS functions, a hyper-spectral imager that can image in the visible part of the EM spectrum (to detect the panchromatic coating) and in the near and shortwave infrared part of the spectrum (to detect the quantum dots)

is necessary. For the panchromatic coating a bandwith of about 5 nm is required while for the quantum dot paint a bandwidth of 10 nm would already be sufficient.

All the objects and phenomena that need to be detected radiate away electromagnetic radiation. However, how much of that radiation actually arrives at a detector depends on the geometry of the situation. It was calculated that in the worst case scenario the maximum coverage area, for which a single airship is still able to detect all the different kinds of radiation, is a circle centred directly beneath the airship and with a radius of 34 km.

4 | Airship Payload Design

Now that the detection methods have been determined, the payload has to be designed to actually detect it. This chapter will deal specifically with the final payload design of a single NSS stratospheric airship. This chapter contains two main parts. First the FSDS imager is discussed and selected using a trade-off. Then the ITS imagers are designed by using some basic optics equations and the information about the detection strategies from the previous chapter.

4.1. Fire and Smoke Detection Payload

This section will discuss the FSDS payload. Using the previously determined FOV the payload composition will be determined, which will decide whether an integral solution will be used or separate systems with respect to the smoke detection and composition analysis. Once the payload composition has been determined a small discussion will follow on current existing imagers for FSDS. Finally, a trade-off will be made considering the previously discussed imagers.

4.1.1. Payload Composition

The FSDS operations of the NSS can be divided into (1) fire and smoke detection and (2) chemical analysis of smoke or gas clouds. As explained earlier in Section 3.1, the basic principle behind both tasks is similar in the sense that both of them require the analysis of specific spectral bands. This leads to two possibilities regarding the set-up of the cameras: have one camera perform all tasks or split them between more cameras such that there is a main camera for constant fire and smoke detection operations and a different one specifically for chemical analysis of gas clouds, when necessary.

To properly determine the best option, it is relevant to look back at the theoretical basis for the two. As explained in Chapter 3, FSDS is performed by applying algorithms to a combination of spectral bands, while the chemical analysis requires a recreation of the spectrum of the substance under analysis. This fundamental difference leads to the necessity to separate the payload operating the two tasks, since the fire detection algorithms need only data related to specific wavelengths while recreating a spectrum benefits from having data on a bigger number wavelengths (ideally continuous data from one wavelength to another, although this is not possible in practice).

It is safe to conclude that the two tasks will, optimally, be separated from each other due to the nature of their methods. In this section there will be further investigation of commonly used spectral imagers and their specifications will lay the path to choose the best design option for each task.

eMAS

The Enhanced MODIS Airborne Simulator (eMAS)[1] is a multispectral scanner meant to operate to similar fashion as the Moderate-Resolution Imaging Spectrometer (MODIS), one of NASA's operational spectrometers. It is able to acquire images in 38 different spectral bands with a spatial resolution of 50 m at a 20 km altitude. There are 9 bands in VIS (445 - 967 nm), 16 bands in SWIR (1.616 - 2.425 μm), 2 band in MWIR (3.647- 3.830 μm), and 12 bands in LWIR (6.589 - 14.062μm). This is obviously a very good selection of spectral bands that would allow the application of many different algorithms for fire and smoke detection. Also, this camera has been used extensively in operations at 20 km altitude which is exactly the planned altitude for the NSS airships.

[1] https://asapdata.arc.nasa.gov/asf/sensors/emas.html [cited 14 June 2017]

Table 4.1: Specifications eMAS [19]

Name	Enhanced MODIS Airborne Simulator
Manufacturer	NASA (Customised MODIS)
Sensor type	Optical Imaging Line Scanner
Bits/pixel	12
Frame rate	6.25 Hz
Size	59.7 cm x 45.7 cm x 48.2 cm
Mass	96 kg (including heater, data handling and stabiliser)
Power	Unknown
Pixels	716 x 16 (spatial x spectral)
Pixel size	1.25 mrad
Aperture diameter	15.2 cm
Focal length	15.2 cm
GSD	50 m
Design Temperature range	Unknown
Comments	None

AMS WILDFIRE SENSOR

The NASA Autonomous Modular Scanner (AMS) Wildfire sensor[2] is a 16-band VIS-IR-MIR-TIR line scanner. It has been used extensively in several different aircraft for missions related to disaster support, active fire smouldering and post-fire conditions. It has a swath width of 716 pixel across (50 m spatial resolution) yielding angular widths of 86° and scan rates can vary between 2-scans/sec to 33-scans/sec. Its spectral bands are given in Table 4.2. The AMS wildfire is a complete system and includes a spectrometer, optical telescope, data handling unit, data storage unit, and a stabilisation mechanism. The scan-head includes a rotating mirror which allows the system to direct its smaller FOV. The stabilisation system provides up to ±15° roll correction and active stabilisation of up to 3.1 mrad/s [20, 21]. The mass of the sensor is approximately 57 kg which includes the heater, data handling, data storage and stabilisation systems. The entire system has a nominal power consumption of 140 W [22].

Table 4.2: AMS Wildfire Spectral Bands

Spectral Band No.	Spectral band μm
1	0.42- 0.45
2	0.45- 0.52 (TM1)
3	0.52- 0.60 (TM2)
4	0.60- 0.62
5	0.63- 0.69 (TM3)
6	0.69- 0.75
7	0.76- 0.90 (TM4)
8	0.91- 1.05
9	1.55- 1.75 (TM5) (high gain)
10	2.08- 2.35 (TM7) (high gain)
11	3.60- 3.79 (VIIRS M12) (high gain)
12	10.26-11.26 (VIIRS M15) (high gain)
13	1.55- 1.75 (TM5) (low gain)
14	2.08- 2.35 (TM7) (low gain)
15	3.60- 3.79 (VIIRS M12) (low gain)
16	10.26-11.26 (VIIRS M15) (low gain)

Table 4.2 shows that the available spectral bands, despite being less than the eMAS camera, are still very suitable for the FSDS operations. This imager was also specifically designed to operate at an altitude of 20 km.

[2] http://www.isprs.org/proceedings/2011/ISRSE-34/211104015Final00468.pdf [cited 14 June 2017]

TELOPS HYPER-CAM AIRBORNE

The Hyper-Cam is a hyperspectral imaging camera used for hyperspectral mapping of surveyed areas.[3] Its spectral range is centred on the MWIR and LWIR (3-5 and 8-12 μm). Its power consumption is around 680W and the swath angles are 6.4°x5.1°. This camera has been used in several different missions, most of which were performed on unpressurised aircraft platforms at a max altitude of 3000 m.

Table 4.3: Specifications TELOPS Hyper-cam Airborne

Name	**TELOPS Hyper-cam thermal airborne**
Manufacturer	TELOPS
Sensor type	Hyperspectral imaging camera
Bits/pixel	Unknwon
Frame rate	Unknown
Size	591mm × 566mm × 613mm
Mass	68 kg (including heater, data handling and stabiliser)
Power	680 W
Pixels	320 × 256 pixels
Pixel size	0.02°
Aperture diameter	Unknown
Focal length	Unknown
GSD	30 m
Design temperature range	0 - 40 °
Comments	Built-in geolocation system with accuracy of 5m

DAEDALUS SCANNERS AIRBORNE SCANNER

DaedalusScanners's Airborne scanner for oil and fire mapping is a commercially available dual optical port scanner specifically created for aircraft operations. It is able to image in the ranges of UV (0.32-0.38 μm), MWIR (3.5-5.5 μm) and LWIR (8-12.5 μm). It has been used and tested previously at maximum altitudes of 15.2 km and it has its own software installed that allows it to immediately generate geo-rectified imagery.

Table 4.4: Specifications DaedalusScanners Airborne scanner

Name	**ABS**
Manufacturer	DaedalusScanners
Sensor type	Airborne Scanner
Bits/pixel	16-bit
Frame rate	100, 50, 25, 12.5 scans/sec
Size	38cm x 38cm x 38cm
Mass	25 kg
Power	300 W
Pixels	1500 x 1 pixels
Pixel size	1.25 mrad
Aperture diameter	Unknown
Focal length	Unknown
GSD	30 m
Design temperature range	5 to 50°C
Comments	Built-in geolocation system with accuracy of 5m

[3] http://telops.com/products/hyperspectral-cameras [cited 14 June 2017]

4.1.2. FSDS CAMERA TRADE-OFF

The presented trade-off focuses on the performance of each of the scanners when applied to the FSDS operations. The chosen criteria are technology readiness level (TRL), spectral bands, optimal altitude performance, weight, ground sampling distance and swath width. TRL indicates the maturity level, TRL-9 being the maximum and corresponding to a 'flight proven' design. The spectral bands score refers to the number and placement of the bands that the sensor is able to detect. Since all the considered sensors have their spectral ranges around similar wavelengths as the fire detection algorithms require, this score will be mainly based on the number of bands they are able to image (more spectral bands means better detection algorithms can be used). The design optimal altitude indicated the altitude for which the sensors have been designed for, and the closer it is to 20 km the higher the score (since the airships loiter at around 20 km). The weight is taken as another important criteria to consider in the selection as there is a limited amount of payload mass. The ground sampling distance (GSD) and swath width are included as these parameters are always highly relevant when comparing imagers (the lower the ground sampling distance and the bigger the swath width, the better).

By looking at the trade-off matrix (Table 4.5), it becomes apparent that the AMS scanner is superior in performance when compared to the other sensors. This is explained mainly due to the extensive spectral band selection and the fact that it has been designed to operate at around 20 km. It is only slightly outperformed by the eMas sensor which has almost double the weight. The values of GSD, although relevant, do not affect the trade-off in a significant way since they all comply with the 100m requirement (= 50m spatial resolution). It is important to note that power consumption was not taken into account in this trade-off, due to the massive expected capabilities of power generation of one airship of the NSS when compared to the average power consumption of these sensors (< 1kW), as was discussed in the mid-term report[2].

Table 4.5: FSDS sensor trade-off matrix

Spectral sensors	Criteria						
	TRL	Spectral bands (number and placement)	Design optimal altitude	Weight	GSD	Swath width	Comments
Sensor: eMAS	20% Excellent 9	15% Excellent 36	15% Excellent 20000m	30% Unacceptable 96kg	10% Excellent 100m	10% Good 716px	Exeptionally good spectral band selection
Sensor: AMS Wildfire	20% Excellent 9	15% Good 18	15% Excellent 21000m	30% Good 57kg	10% Excellent 100m	10% Good 716px	
Sensor: TELOPS Hyper-Cam Airborne	20% Excellent 8	15% Acceptable 12	15% Unacceptable 3000m	30% Excellent 31kg	10% Excellent 56m	10% Acceptable 320px	
Sensor: DaedalusScanners Airborne Scanner	20% Excellent 8	15% Acceptable 12	15% Acceptable 15000m	30% Excellent 25kg	10% Excellent 100m	10% Excellent 1500px	Integrated sofrware for geo-rectified imagery

Excellent: exceeds requirements	Acceptable: correctable deficiencies
Good: meets requirements	Unacceptable: major deficiencies

Table 4.6 shows some basic characteristics of the AMS Wildfire scanner when applied to the NSS system, meaning at an altitude of 20km. Unfortunately, no data is available on the sensor itself or on the specific optics, specially regarding focal length or aperture diameter which would have been interesting dimensions to know. However, the sources showed that a spatial resolution of 50m minimum, at an altitude of 20km achievable.

Table 4.6: Specifications AMS Wildfire [20, 21]

Name	Autonomous Modular Sensor - Wildfire
Manufacturer	NASA (Customised Daedalus Scanner)
Sensor type	Unknown
Bits/pixel	8
Frame rate	<100 fps
Size	38 x 38 x 38 mm (scanhead)
Mass	57 kg (including heater, data handling and stabiliser)
Power	140 W (approximated, including heater and stabiliser)
Pixels	716 x 16 (spatial x spectral)
Pixel size	1.25 mrad
Aperture diameter	Unknown
Focal length	Unknown
GSD	25 m
Design temperature range	$-55°C$ to $70°C$
Comments	Stabilised system. Scan-head rotation allows full FOV command

4.2. IDENTIFICATION AND TRACKING PAYLOAD

Chapter 3 shows that target marking uses the panchromatic coating (PC) and quantum dots (QDs). Both these methods rely on specific markers in the Electromagnetic (EM) wavelengths that emanate from the target objects. In order to detect these EM patterns a hyper-spectral imager is necessary. The PC radiates in the visible part of the spectrum while the QDs radiate in the near and shortwave infrared. Combining the detection of PC and QDs using the same imager would be beneficial as it would only include one imager capable of doing both instead of two doing nearly the same tasks. From literature it is known that these instruments, hyperspectral cameras, have a tendency to be heavy and have a limited instantaneous FOV. This makes it difficult for a hyperspectral camera to scan the entire coverage area of a single airship in a limited amount of time such as 1 minute.

By adding a second ITS imager to the payload of this system, it is possible to circumvent this difficulty. A regular colour imager (CI), in combination with a smart computer system, is capable of making a rough indication of possible targets. That is: the CI is then capable of identifying a number of potential targets after which the CHSI will scan only the potential targets for a specific marker. The CI can then keep track of the targets in the FOV while the CHSI intermittently confirms the target using the marker. This has the added benefit that the CI, which is also known as a regular camera, can be used to have an operator manually observe the coverage area if the need arises.

In the Netherlands it is night about half of the time and a system that has no ITS functionality during the night is only of limited value. Both target markers rely on the energy of sunlight in order to be visible from great heights. Therefore, it is impossible to detect the markers during the night. An infrared camera, however, does give limited functionality during nighttime. If targets are considered of high enough importance either an operator or a complex computer algorithm can still keep track of individual targets. But this is limited to 1 target per IR camera. Infrared imagers typically image either in the MWIR (3 - 5 μm) or TIR (8 - 12 μm). However, since most operate in the MWIR and since that range has a better spatial resolution, it is selected for the InfraRed Imaging System (IRIS).

Table 4.7 gives an overview of these three imagers and the estimated spatial and spectral resolutions necessary for these systems to operate. The estimates were created based on the currently available knowledge of the marking techniques. The table also contains a shorthand notation for referring to those imagers.

Table 4.7: ITS imager type overview

Imager	Acronym	Required spatial resolution [m]	Required spectral resolution [nm]	Required wavelength range [nm]
Combined Hyper-Spectral Imager	CHSI	0.5 - 1	< 20	400 - 2500
Colour Imager	CI	0.3	< 100	400 - 700
InfraRed Imaging System	IRIS	0.8	-	3000 - 5000

The lower bound of the required spatial resolution for the CHSI was based on the possibility of wanting to mark a target also using a specific pattern. The available patterns decreases when the required spatial resolution is increased. IRIS will, like most infrared, operate best when imaging in either the MWIR or TIR since in those ranges there still is enough EM radiation available to detect. This also means that even if the QDs emit during the night IRIS will not detect their radiance.

4.2.1. ITS OPTICS SIZING

Now that three ITS imagers have been selected their required parameters should be investigated. This means that they have to be sized in order to meet the signal to noise ratio (SNR) and spatial resolution requirements. Short back-of-the-envelop calculations showed that the optical systems are no long diffraction limited, so now the SNR is mainly limiting. Thus the central equation is Equation 4.2.1

$$S = R \cdot \Omega \cdot A \cdot t_i \cdot \Delta\lambda \cdot \tau \tag{4.2.1}$$

Using the SNR requirement one can calculate the amount of signal the system needs to detect. This is the same for all three imagers and can be done using Equation 4.2.2.

$$S = SNR^2 = 80^2 = 6400 \tag{4.2.2}$$

This means that Equation 4.2.1 can be rewritten to Equation 4.2.3 where the necessary aperture diameter, D, is calculated.

$$D = \sqrt{\frac{4 \cdot S}{\pi \cdot R \cdot \Omega \cdot t_i \cdot Q_e \cdot \tau \cdot \Delta\lambda}} \tag{4.2.3}$$

R is given in Table 3.3, Q_e is the quantum efficiency which is 0.7 (the average for the visible light detectors evaluated in the MTR), τ is the optical loss of the system (which was calculated in the MTR to be approximately 0.886), and $\Delta\lambda$ is the wavelength bandwidth. The integration time t_i is calculate using Equation 4.2.4, and the solid angle Ω by Equation 4.2.5.

$$t_i = \frac{1}{2} \cdot \frac{GSD \cdot 3.6}{V_0} \tag{4.2.4}$$

Where V_0 is the velocity of the object in km/hr. This then gives t_i as the time in seconds that it takes the object to move half the distance of the GSD.

$$\Omega = \frac{GSD^2}{\left(H/\cos(0.5 \cdot \alpha)\right)^2} \tag{4.2.5}$$

Where GSD is the desired Ground Sampling Distance, H is the altitude and α is the FOV of the instrument. A summary of the fixed input variables is given in Table 4.8.

Table 4.8: Aperture calculation inputs (1/3)

Parameter	Value	Units
SNR	80	[−]
$\mathbf{Q}_e$	0.7	[−]
$\boldsymbol{\tau}$	0.886	[−]
H	20000	$[m]$
$\boldsymbol{\alpha}$	120	$[degree]$
$\mathbf{V}_0$	120	$[km/hr]$

The other values of the input parameters depend on the specific imager that is being considered. Table 4.9 lists those values.

Table 4.9: Aperture calculation inputs (2/3)

Imager	GSD [m]	$\Delta\lambda$ [nm]	$R\ [ph \cdot cm^{-2} \cdot s^{-1} \cdot sr^{-1} \cdot \mu m^{-1}]$	$\lambda_{max}\ [nm]$
CHSI	0.5	10	$2.79 \cdot 10^{25}$	2500
CI	0.3	100	$5.02 \cdot 10^{24}$	700
IRIS	0.8	2000	$1.05 \cdot 10^{21}$	5000

Note that the CHSI will be calculated using both the QD radiance and the reflection radiance for the PC. In the results the limiting value will be given. IRIS will be calculated using the radiance from infrared emissions. Using the above mentioned equations and tables one can use Equation 4.2.6, 4.2.7 and 4.2.8 to calculate a focal length (f) associated with an F# of 2, minimum pixel size (d), and the diffraction limit (D_{limit}) for each of the imagers. The F# of 2 is selected as it is a lower bound that maximises the FOV but keeps the system diffraction limited. The results for each of the imagers are listed in Table 4.10.

$$F\# = f/D \rightarrow f = F\# \cdot D \tag{4.2.6}$$

$$\frac{GSD}{H} = \frac{d}{f} \rightarrow d = \frac{GSD \cdot f}{H} \tag{4.2.7}$$

$$D_{limit} = 1.22 \cdot H \cdot \frac{\lambda}{D} \tag{4.2.8}$$

Table 4.10: Aperture calculation inputs (3/3)

Imager	Aperture Diameter [m]	Focal length [m]	Diffraction limit [cm]	Min. pixel size [μm]
CHSI	0.12 (0.2)	0.24 (0.4)	17 (103)	15 (15.9)
CI	0.14	0.27	25	2
IRIS	0.33	0.66	74	13.1

Note that for the CHSI the values between parentheses are the results when applying the QD solution and thus imaging around 2500 nm.

4.2.2. ITS IMAGER SELECTION

All the calculations done above are approximations and serve to give a first estimate of the size of the optical systems. A more detailed analysis must be performed to refine those numbers. To get an idea of what is possible some systems will be presented. Those systems will be included in the final design presented in this report. However, it is likely that a more detailed analysis of the optics, which is beyond the scope of this project, will require the optical systems to be either heavily customised (also to perhaps reduce mass) or newly designed.

The system selection has been performed by using the results from Table 4.10 to look for comparable systems on the internet. For the CHSI complete system will be selected. The CI and IRIS will be assumed to be simple lens systems and as such for these systems a sensor will be selected and the basic characteristics will be calculated.

Some basic information about the CI can thus be calculated. First order of business is to select the sensor. During the MTR phase of this project a large database of available sensors was created and this shows that in the VIS part of the EM spectrum the CMOSIS CMV50000 has the best performance while having pixel sizes larger than the minimum needed. This sensor has a different pixel size so some other basic values about the CI which relate to the sensor and optics have to be recalculated. This sensor has a different pixel size and thus this will have an impact on the GSD of the imager. The data of the sensor and the calculated values about the optics are summarised in Table 4.11.

Table 4.11: Specifications CMOSIS CMV50000 [23]

Name	Colour Imager	DSC-RX10M3
Sensor Name	CMV50000	-
Manufacturer	CMOSIS (sensor)	Sony
Sensor type	CMOS	Exmor RS CMOS
Pixels	7920 x 6004 (48 Mpixel)	20.1 Mpixel
Bits/pixel	12	Unknown
Maximum full frame sample rate	30 fps	240 fps
Binning possible	Yes	Yes
Chroma	sRGB	sRGB
Sensor Size	36.42 x 27.62 mm	13.2 x 8.8 mm
Pixel size	3.5 μm	1.4 μm
Q_e	60%	Unkown
Power consumption	3.05 W	2.03 W
Temperature range	-30°C to 70°C	0°C to 40°C
SNR	FOV Edge: 74, Nadir: 149	Edge: 25 Nadir 49
GSD	0.32 m	0.12 m
Diffraction limit	0.16 m	0.19
Focal length	0.22 m	0.22 m
Aperture diameter	0.11 m 0.09 m	
Mass	3 ± 1 kg	1.1 kg
Dimensions	12 x 12 x 22 ±4 cm^3	13.3 x 9.4 x 12.7 cm^3

Using again Equation 4.2.7, one can calculate the new GSD of the CI to be 0.32 metre. To get the approximate mass of the optical system, it was assumed that a simple optical system weighs about 1 kg/L [24]. The dimensions were estimated based on the aperture size and focal length and by assuming that the system is just a cylinder. This introduces some uncertainties which were estimated to be about 25%. As stated at the beginning of this section, the CI is designed to be able to scan the entire coverage area of a single airship in a limited time. The requirements demand that this is done in one minute. Since the CI is relatively lightweight, up to four cameras can be installed on the airship. This means that a single CI only has to image one quadrant of the coverage area of the airship.

Table 4.11 also contains the information of the SONY DSC-RX10M3 camera which acts as a sanity check on the calculations. When it comes down to SNR, the CI performs much better due to the significantly larger pixel size. Other than that, the performance seems to be comparable. The CI is a little bit larger and thus heavier.

For the CHSI such an approach is not really feasible since hyper-spectral imagers are rather complicated pieces of equipment. Luckily such devices fall in the category of 'high-end scientific camera' and as such, plenty of information is available about such devices. The search was confined to space and airborne systems for the most part. From the found hyper-spectral imagers the Hyperion Imaging Spectrometer, which flew on the EO-1 mission from 2000 to 2017, was selected as

it meets the calculated CHSI performance adequately [25]. Details are listed in Table 4.12. When designing the payload in further detail a new or modified version of such a hyper-spectral imager needs to be designed.

Table 4.12: Specifications Hyperion Imaging Spectrometer [26]

Name	**Hyperion Imaging Spectrometer**
Manufacturer	NASA
Sensor type	VISNIR: CCD, SWIR: HgCdTe
Pixels	250 spatial x 220 spectral
Bits/pixel	12
Maximum full frame sample rate	225 fps
Binning possible	Yes (Applied)
Chroma	Multispectral
Sensor Size	Unknown
Pixel size	VISNIR: 60 μm (3x3 aggregate of 20 μm), SWIR: 60 μm
Q_e	Unknown
Power consumption	51 W
Design Temperature	157 K
SNR (Calculated)	QD (FOV Edge): 65 , PC (FOV Edge): 119
GSD (Calculated)	0.85 m
Diffraction limit (Calculated)	VIS: 0.14 m, SWIR: 0.51 m
Focal length (Calculated)	1.32 m
Aperture diameter	0.12 m
Mass	49 kg
Dimensions	39 x 75 x 66 cm^3

The Hyperion imager contains three different and seperate assemblies. The Hyperion Sensor Assembly (HSA), the Hyperion Electronics Assembly (HEA), and the Cryocooler Electronics Assembly (CEA) [27]. These three assemblies together weigh 49 kg, however only the HSA needs to be stabilised. No mass breakdown of the hyperion system was given thus the mass and dimensions of the HSA need to be estimated. From engineering drawings it is known that the HSA has approximately the same dimensions as the HEA and CEA combined [28]. If it is assumed that the average density of the imager is relatively uniform, then the mass of the HSA is 25 kg. However, some margins have to be taken into account for the uncertainties. A margin of 20% was deemed justifiable. It is unknown along which axis the dimensions have to be reduced. Estimating the dimensions of the HSA was based on Figure 4.1 and the given total dimensions. The mass and dimensions are summarised in Table 4.13.

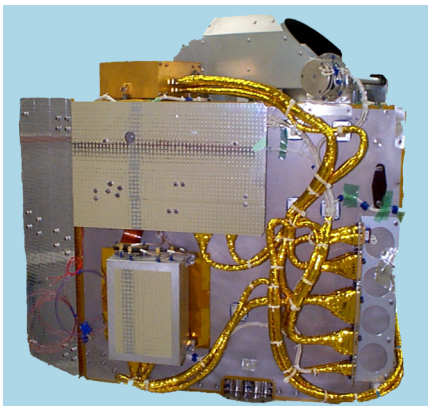

Figure 4.1: Hyperion sensor assembly [27]

Name	**Hyperion Sensor Assembly**
Mass	25 ± 5 kg
Dimensions	75 x 66 x 20 cm^3

Table 4.13: Specifications Hyperion sensor assembly

From Section 3.3 it is shown that the optimal spectral resolution for panchromatic imaging is smaller than or equal to 5 nm. The Hyperion was primarily selected based on the aperture size

and total spectral range. This makes the Hyperion, with its spectral resolution of 10 nm a good candidate for a combined imager that can both detect PC and QDs. However, further analysis is required in order to say for sure what the effectiveness of Hyperion is when it comes to detecting the panchromatic coating. Fortunately, such systems formally consist of two components, the telescope and the spectrometer. From Table 4.12 it is clear that the telescope aspect of the HSA is capable of performing the required tasks. It might prove possible to attach that, or a similar, telescope arrangement to a different spectrometer that has better performance in parts of the EM spectrum where the panchromatic coating can be detected. A good potential candidate for such a different spectrometer is the TROPOLITE instrument which is currently being developed by TNO. The advantage of TROPOLITE is that it is an instrument that is being developed for small spacecraft and is thus designed to measure less than 20 x 20 x 40 cm^3 and weigh less than 20 kg while still having a spectral resolution of 0.5 nm (which is the current spectral resolution of the TROPOMI instrument of which TROPOLITE will be a lighter and smaller version) [29, 30]. This means that the TROPOLITE spectrometer will, most likely, have a smaller mass when compared to the Hyperion spectrometer. Having a lower mass brings some benefits such as lighter and smaller stabilisation systems and the potential of having multiple spectrometers on board per stratospheric airship. However, the analysis showing the possibilities of combining different spectrometers with different telescope arrangements is beyond the current scope of this project.

Finally, IRIS needs to be designed. From the previously mentioned sensor database, a MWIR sensor was selected. The selection was done by selecting the sensor with the most pixels and had a pixel size larger than the required pixel size as mentioned in Table 4.10 (13 microns). This turned out to be the Jupiter MW sensor manufactured by Sofradir-EC. By applying the same steps as when calculating the CI the following preliminary IRIS design can be created.

Table 4.14: Specifications IRIS [31] and RS8300 [32]

Name	**IRIS**	**FLIR RS8300**
Sensor Name	Jupiter MW	-
(Sensor) Manufacturer	Sofradir-EC	FLIR
Sensor type	HgCdTe CMOS	InSb
Pixels	1280 x 1024	1344 x 784
Bits/pixel	Unknown	14
Maximum full frame sample rate	120	125
Binning possible	Yes	Yes
Spectral Range	3700 - 4800 nm	3000 - 5000 nm
Sensor Size	19.2 x 15.63 mm^2	-
Pixel size	15 μm	14 μm
Q_e	Unknown	Unknown
Power consumption	0.75 W (including microcooler)	Unknown (24 V_{DC} (total power consumption)
Sensor mass	0.8 kg (including microcooler)	-
Design Temperature ranges	77 - 110 K (Sensor only)	$-40°C$ - $50°C$
SNR	FOV Edge: 60, Nadir: 121	FOV Edge: 53, Nadir: 107
GSD (Calculated)	0.45 m	0.25 - 2.5 m
Diffraction limit (Calculated)	0.36 m	0.42 m
Focal length	66 cm	12 -120 cm (10x optical zoom)
Aperture diameter	33 cm	29 cm (approximately)
Mass	35 ±9 kg	35 kg
Dimensions	34 x 34 x 66 cm^3	31.5 x 29.0 x 92.7 cm^3

In Table 4.14, the data of the FLIR RS8300 is included as a sanity check. This shows that the design of IRIS makes sense when compared to the RS8300. With respect to volume, IRIS is a little smaller than the RS8300 while it does have a slightly larger aperture. These two effects would logically cancel out and thus it makes sense that they have approximately the same mass. For the amount of bits/pixel the value of 14 is taken over from the RS8300.

4.3. RISKS ASSOCIATED WITH PAYLOAD

A proper payload design is absolutely crucial for the success of the NSS operations due to the nature of the detection methods. The design was mainly driven by the spatial resolution requirements and signal to noise ratio values. Despite, there were several factors that had a major influence on the type and number of cameras used. One of them was the necessity of performing ITS operations during night time which, as it has been discussed, is not possible using the Hyperion camera. This was tackled by introducing IRIS, the infrared imager that can continue ITS operations at night with the downside of not being able to identify the target. Also, knowing that instruments that are able to detect PC and QD are usually heavy and have a limited instantaneous FOV lead to the addition of a colour imager that is capable of detecting potential targets. This will severely limit the FOV that the CHSI needs to scan and helps reducing the risks associated with having a heavy payload with high manoeuvrability (mechanical wear off for example).

4.4. CONCLUSION

The payload composition was determined from the requirements. For FSDS, the payload consist of a spectral imager in specific bands used for the detection of fire, smoke-, and gas clouds and a hyper-spectral imager to determine the composition of clouds. The optimal ITS payload will consist of a custom CI, a CHSI in the form of Hyperion, and IRIS. The CI will allow the tracking of already identified targets based on colour and Hyperion will allow to identify a target based on a panchromatic mark or QDs. Additionally, the hyper-spectral imager is also able to determine the chemical composition of clouds of gas and smoke, which minimises the number of needed imagers. Finally, IRIS will allow for limited night-time operations. A summary of the relevant data regarding the four imagers is given in Table 4.15.

Table 4.15: Payload summary

	AMS Wildfire	**CI**	**Hyperion**	**IRIS**
FOV [arcmin]	5154 x 8.6	433 x 329	36.5 x 0.15	99 x 79
Swath width [m]	37250 x 50	2534 x 1921	213 x 0.9	576 x 461
Mass [kg]	57	3 ± 1	49	35 ± 6
Power [W]	140 (approximated)	3	51	0.75
Size [cm^3]	38 x 38 x 38	13 x 13 x 22	20 x 75 x 66	34 x 34 x 66
Bits/pixel	8	12	12	14
Pixels	716 x 1	7920 x 6004	250 x 1	1280 x 1024
No. Bands	16	3	220	1
GSD [m]	50	0.32	0.85	0.45
Spectral Range [nm]	420 - 11260	400 - 700	400 - 2500	3700 - 4800
SNR	-	74 - 149	> 65	60 - 121

5 | Stratospheric Airships

To determine the cost and explore the different options for the main platform of the NSS, further investigation upon airships is needed. In the mid term phase of the project, airships were selected as the main platform for the NSS. This chapter elaborates on the airship platform and its subsystems. This chapter starts with some basic airships characteristics. Subsequently an airship will be selected which will serve as a platform for the payload. Afterwards the subsystems will be discussed. In order of appearance they are the payload ADCS, propulsion, navigation, station keeping, command and data handling, communications, thermal control, and the EPS. When all subsystems are presented, their integration is explained. Finally risks of the airship platform are mentioned and a short concluding section of this chapter is given.

5.1. Characteristics

First of all, it is important to know what payload mass the airship is capable of carrying. Looking at current projects or previous airship missions, data about airship characteristics is gathered. The Thales Stratobus is capable of carrying a payload of 250 kg.[1] Lindstrand technologies also launched a couple of airships in the past, of which some characteristics are summarised in Table 5.1.

Table 5.1: Airship characteristics for previous Lindstrand technology missions [1]

Year	Contractor	Payload	Altitude	Duration	Outcome	Additional Information
1958	General Mills	100 kg	18 – 20 km	8 hours	Study only	-
1970 High Platform 2	Raven	nil	20 km	2 hours	1 flight only	-
1976 HASPA	Martin / Sheldahl	100kg	Hangar testing only	-	-	-
1982 Hi-Spot	Lockheed Martin	Gross weight 11.7 tonnes	21 km	30 days	No flight	4 piston engines
1992 Japan Science Foundation	Halrop	nil	10,000 feet	-	4 short duration flights	
1995 Sky Station	LTL	600 kg telecom platform	21 km	5 years	No flight	
2004	JAXA/ NICT	100kg	13,000ft	5 years	1 flight	Severely underpowered
2011	Lockheed Martin	500kg	21 km	2 hours	'crashed & burned'	

In this table, typical altitudes can be found, which is important to determine some optical parameters. Duration of the flight can also be found in this figure and it could be seen that a total flight of 5 years is realistic. The D15 and D20 concepts from Lindstrand are capable of carrying 100 kg and 500 kg, respectively.

Another characteristic of the airships is its size, in terms of length, diameter and volume. The volume for the ESA-HALE concept is approximately 320,000 m^3, which carries a payload of 1000 kg [1]. The D20 and D15 series have a volume of 180,000 m^3 and 16,000 m^3, respectively. The maximum diameter of the ESA-HALE D20 concept is 42 m with a total length of 203 m. The volume of this D20 concept is slightly different than the initial D20 concept, the volume of this airship is 181,200 m^3, with a total area of 20,750 m^2.

[1] https://www.thalesgroup.com/en/worldwide/space/news/whats-stratobus [cited 1 June]

Drag should also be taken into account. In Figure 5.1, a graph can be seen for a drag coefficient as a function of angle of attack. This is the drag curve for the ESA-HALE D20 airship. However, the shape of airships is the same in general, therefore it can be assumed to be applicable to any airship of approximately the same shape. Notice that only the shape matters and not the overall volume, since drag coefficient depends on the perpendicular area and not on the total volume. The angle of attack is given in gradients, which is a percentage. The percentage represents the altitude gained over the horizontal distance travelled.

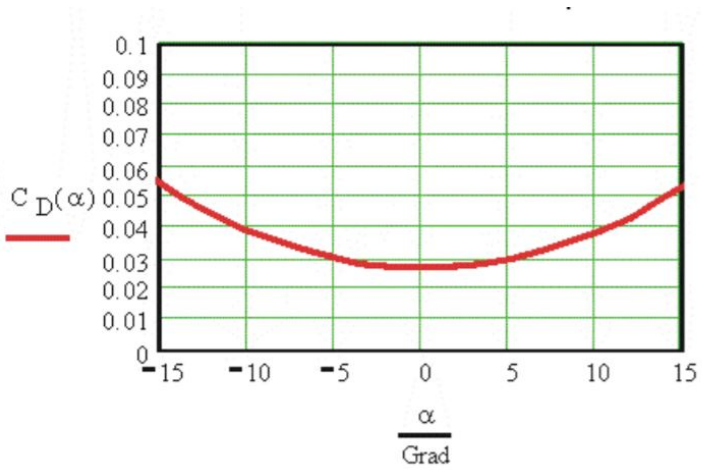

Figure 5.1: Drag coefficient as a function of α for the ESA-HALE D20 airship [1]

The graph has symmetric shape, as expected, because the airship is approximately symmetric as well. The maximum drag coefficient is 0.055 and the lowest drag coefficient is approximately 0.026 at an angle of attack of zero. The total drag force depends on the speed at which the airship flies, as well as the air density and the frontal area of the airship.

5.1.1. STRATOSPHERIC WINDS

A challenge that the airship will face, is the phenomenon of stratospheric winds. These are much more predictable than winds at sea level, and there's documentation providing accurate data on this [33]. The exact numbers depend on the geographical positions, mostly on the latitude. The data for the Netherlands has been summarised in Table 5.2.

Table 5.2: Different stratospheric wind speed situations at an altitude 20 km, and a latitude of 52° North

	Wind Speeds [m/s]	**Influence on Manoeuvrability**
Absolute maximum	30	Stationkeeping no longer possible
Nominal maximum	25	Stationkeeping possible
Nominal	10 - 20	Increased manoeuvrability

The situation indicated as absolute maximum only lasts for 1-2 weeks per year, but it does have an impact on operations, due to the fact that the airship can only provide an airspeed of 25 m/s. This would bring some uncertainty regarding the airship's ability to maintain a specific position, for certain periods of time. This would, however, not be an unprecedented occurrence for stratospheric airships; for instance, the Lockheed Martin High Altitude Airship had been set a requirement to maintain stationkeeping with an accuracy of < 2 km during 50% of the time, and < 150 km for 95% of the time [34]. It is as of yet unknown what requirements Thales has set for its Stratobus airship.

5.2. AIRSHIP SELECTION

To be able to choose an appropriate airship, existing projects or prototypes will be described and the most appropriate one chosen. The driving criteria for the selection is the payload mass capability that should be able to support the payload found in Chapter 4.

5.2.1. DIFFERENT AIRSHIPS

There are not many stratospheric airship in existence, however extensive research and experimentation has been done regarding these airships. Research revealed that five stratospheric airships have been designed that could be used in the NSS [35]. These will shortly be described and shown below.

SENTINEL80 This airship was developed as an unmanned airship which is capable of carrying 9 to 90 kg at 20 km for 30 days. Only one test has been performed and the airship crashed in November 2010 during this flight. The program was terminated in 2010 [35].

SPF This was a feasibility study conducted by JAXA. The airship would fly at 20 kilometres altitude at 30 m/s, have a length of 245 metres, weigh 32 tons and have a payload carrying capacity of 1000 kilograms. This program was terminated in 2005 after 2 test vehicles were tested and underperformed [35].

VIA200 This airship was designed by the Korean Stratospheric Airship Program. It would have been 200 metres long with a total weight of 22000 kilograms and 1000 kilogram payload. The airship would be able to fly at 20 kilometres with winds up to 12 m/s. The project was halted in 2005 [35].

HALE-D This airship was produced by Lockheed Martin. The HALE-D has a total length of 73 metres, a total mass of 1361 kilograms and payload capacity of 36 kilograms. It was designed to have an altitude of 18 kilometres and a flight duration of 2 weeks. This project has also been terminated after a failed test flight. However it is estimated that this project could be successful if resumed [35].

Stratobus Potentially produced by Thales, the airship weighs 7000 kilograms, is 115 metres long and 34 metres wide. Flying at 20 kilometres, the Thales Stratobus can carry 250 kilograms payload. This payload has the possibility to consume 5 kW of power. Thales is planning to test the Stratobus in 2018 and the plan on delivering it in 2020.[2]

To be able to decide which airship is going to be selected, normally a trade-off is performed. However in this case it can be easily distinguished which airship cannot be used because they fail to meet the requirements. The first airship, SENTINEL80, cannot hold the payloads of in total 100 kilograms so it can be discarded. The SPF airship of JAXA cannot be used since the program has been terminated by the Japanese government. The third airship, VIA200, is discarded for the same reason as the airship from JAXA. The HALE-D airship also is unable to carry the payload for NSS. The last option would be the Stratobus. This airship meets the payload weight requirement of at least 100 kilograms and is already being developed for several customers.[3] This is why the Thales Stratobus is chosen as the main platform of NSS. In the section below the Stratobus is further evaluated.

5.2.2. THALES STRATOBUS

The Thales Stratobus, see Figure 5.2 will have its first scaled test flight in 2018. It is expected that full production will start in 2020 or 2021. As can be seen in the figure below, the airships are able to communicate with each other. Next to that, the Stratobus is supposed to be serviced annually and after five years it would need a complete overhaul. The costs of the system are also not made

[2] https://www.thalesgroup.com/en/worldwide/space/news/whats-stratobus [cited 15 June 2017]
[3] http://www.janes.com/article/68513/stratobus-demonstrator-set-for-2018-launch [cited 15 June 2017]

available yet. Not much more is known about the Thales Stratobus, however what is known is displayed in Table 5.3. In Figure 5.2 a picture of the Thales Stratobus is displayed.

Table 5.3: Characteristics Thales Stratobus[4, 5]

Characteristics Thales Stratobus	
Lifting gas [-]	Hydrogen
Volume [m³]	50,000
diameter at widest point [m]	34
Length [m]	115
Propulsion system [-]	electric
Max wind speed [m/s]	25
Total weight [kg]	7000
Altitude [km]	20
Payload bay volume [m^3]	TBA
Payload power available [w]	5000
Payload capability [kg]	250

Figure 5.2: Artist impression of the Thales Stratobus[6]

5.3. PAYLOAD ATTITUDE DETERMINATION AND CONTROL SYSTEM

For an operational NSS, the payload of the Thales Stratobus must accurately point at the target. This is ensured by the Attitude Determination and Control System (ADCS). First, it is important to clearly define the three different characteristics mentioned earlier.

- **Pointing Accuracy** is the ability of the ADCS to accurately point the camera in a certain position. This is measured in arcseconds.
- **Pointing Stability** is the angular displacement over time. If this angular displacement over time is high, a blurry picture might be taken. This characteristic is measured in arcseconds per second.
- **Pointing Knowledge** is the capability of the system to know where it is pointing at. This is measured in arcseconds.

[4] https://www.thalesgroup.com/en/worldwide/space/news/whats-stratobus [cited 16 June 2017]
[5] http://spacenews.com/thales-alenia-space-stratobus-eyes-contract-in-2017-kuka-band-frequency-ok-in-2019/ [cited 16 June 2017]
[6] https://www.thalesgroup.com/en/worldwide/space/news/whats-stratobus [cited 16 June 2017]

The higher the pointing accuracy, pointing stability and the pointing knowledge that can be obtained by the ADCS, the lower the difference is in the actual location and the measured location of the object. The error is defined as the actual position minus the measured location, or the other way around, whichever one is greater.[7] This error is defined by three pointing characteristics: pointing accuracy, pointing stability and pointing knowledge. The requirements for the ADCS for the payload will be calculated in this section. The best system that could be found, which is Gyro-Stabilized Systems, is taken as the base of the ADCS. The requirements will be obtained from there. This means that a bottom up approach is used. The location of the target should be accurate in order to distinguish on which road it is. The minimum distance between two different lanes of a road is 2.75 metres.[8] Therefore, this is set to be the minimum requirement. The stabilisation of the sensor of the AMS Wildfire is controlled by the AMS's own system. It can be assumed that this stabilisation is accurate enough since the AMS Wildfire has been tested with positive results on an airplane [20, 21], which is less stable, than an airship. All other cameras, however will need dedicated gimbals to stabilise them. The challenge of designing an ADCS in general, but also for this design, is obtaining the required pointing stability.

POINTING ACCURACY

High pointing accuracy can be obtained with high-end Inertial Measurement Units (IMU) and a Global Navigation Satellite System (GNSS) receiver. These IMUs and GNSS receivers are implemented in a gimbal. Figure 5.3 gives the reader an idea of what an high-end gimbal systems looks like. [9] High-end gimbals can obtain pointing accuracies in the range of 1 - 5 arcseconds [36–38].

Figure 5.3: Helicopter-mounted gimbal for aerial surveillance

The misalignment error between the IMU and the lens is 2 arcseconds after very accurate placement [24]. Therefore, the total pointing accuracy that can be obtained is 3.03 arcseconds. The error in location due to the pointing accuracy can be calculated by means of simple geometric formulas. It is given by the tangent of the pointing accuracy, from the gyro-stabilised system, multiplied by the respective altitude as can be seen in Formula 5.3.1, where n_{0° is the actual location error in metres, H is the height in metres and e is the error imposed by the ADCS in degrees.

$$n_{0^\circ} = H \cdot tan(e) \tag{5.3.1}$$

If the distance is moved further from the centre point (which will be seen when looking vertically down from the airship) to the end of the FOV, then the error will be higher as well. This pointing

[7] https://www.youtube.com/watch?v=bZe5J8SVCYQ [cited 22 June 2017]
[8] https://www.anwb.nl/binaries/content/assets/anwb/pdf/verkeer/eurorap-tap-onderzoeken/provinciale-wegen/verkeersveiligheid-provinciale-wegen-2013-09-10.pdf [cited 14 June 2017]
[9] http://www.blueskyaerialfilming.com/delivery-gyro-stabilized-systems-c516/

accuracy is calculated with Formula 5.3.2, where E is the coverage length minus the length induced by the error in metre, θ_{rot} is the angle at which the camera is allowed to rotate, this is 60° from the origin.

$$E = H \cdot tan(\theta_{rotation} - e) \tag{5.3.2}$$

The actual location error n can be obtained by means of Formula 5.3.3, where L is the total coverage length in metres and n is the maximal location error when a 60° angle is used.

$$n_{60^\circ} = E - L \tag{5.3.3}$$

If $\theta_{rotation}$ is zero, then Formula 5.3.1 should be used to obtain the location error. In this case the maximal location error is used. After calculating this, for the most critical case, the maximal location error due to the pointing accuracy is 1.2 metres.

POINTING KNOWLEDGE

High pointing knowledge is important as it allows for accurate geo-referencing of images. Combined implementation of IMUs and GNSS receivers gives the best possible pointing knowledge [39]. The GNSS receiver is used to determine the camera's position; the IMU, its attitude. Together, the IMU and GNSS can figure out exactly where the camera line of sight is pointing. The total error for pointing knowledge is determined by compounding the IMU and GNSS receiver errors. As a result, both systems will be used, because knowing only the camera's attitude and not its position – or vice versa – would give too large an error.

Pointing knowledge is also required in order to re-point the camera. The camera is pointed by means of a stabilising system (gimbal), two GNSS receivers and two IMUs. The pointing accuracy of the gimbal is thus an output of the pointing knowledge and the ability of the ADCS to point in a certain direction. The pointing knowledge of the entire system can be obtained by combining the information of the ADCS with the attitude and location of the airship. Which explains the need for two IMUs and GNSS receivers: one of each for the camera, and one of each for the airship.

In conclusion, the pointing knowledge of the gimbal is twice the combined pointing knowledge of an IMU and a GNSS receiver. This achievable value is 3.03 times 2, which is 6.06 arcsec. The value obtained is considered accurate enough to determine which road the vehicle is on, thus the pointing knowledge requirement is met.

POINTING STABILITY

The pointing stability is calculated by using Equation 5.3.4:

$$\theta_{stability} = tan^{-1}\left(\frac{\eta \cdot GSD}{H}\right) \cdot \frac{1}{t_s} \tag{5.3.4}$$

where η is the fraction of a pixel by which the image is blurred. The maximum achievable pointing stability by the gimbal is 1.03 arcsec/s which will give an η of 0.0167. This means that the image is blurred for $\frac{1}{60}$ part of the image. Effectively, part of the light that is supposed to fall on one pixel of the sensor is falling on another. This will naturally have an adverse effect on the image quality. However, this effect is considered to be negligible, placing the analysis of this effect beyond the scope of this project. The 1.03 arcsec/s pointing stability exceeds what is required to distinguish the targets, but it gives a good indication of the gimbal's capabilities. GSD is the ground sampling distance in metres, H is the altitude in metres and t_s is the shutter time (= time to take a picture) of the camera in seconds. Earth's radius is neglected in this equation, because with a swath radius of 34 km the influence of the radius of the Earth is negligible. Specifications for the cameras are summarised in Table 5.4. The highest required pointing stability is for the CI and this value is 1.05 arcsec/s. The pointing stability that can be obtained by an high-end stabilising system is

1.03 arcsec/s. Stabilisation is also needed for the antenna. However, the dimensions for the antenna are minimal, therefore the mass of the ADCS that is needed is negligible and is thus not included.

Table 5.4: Camera stabilisation input parameters

	CI	Hyperion	IRIS
Req. pointing stability [arcsec/s]	1.05	5.84	2.75

MASS & POWER

The mass calculation of the stabiliser has been done by comparing multiple stabilisers from an high-end company, named Gyro-Stabilized Systems. The gimbals of this company are able to meet the requirements set by the cameras. Moreover, these gimbals are able to obtain the minimal required location error. Then the relation between the different values was obtained. This can be seen in Equation 5.3.5 with a coefficient of determination, R^2, of 0.904 with the volume in dm^3. The graph which represents this can be seen in Figure 5.4. In the text boxes the (code) names of the different systems with their respective volume and mass can be seen as well [10]. The line with the equation displays the expected mass with respect to the volume. Filling in the volume for both cameras will result in a weight for the ADCS for CI of 2.7 kg, for Hyperion 66.4 kg and IRIS will weigh 13.8 kg.

$$m_{ADCS} = 0.867 \cdot V - 0.5268 \tag{5.3.5}$$

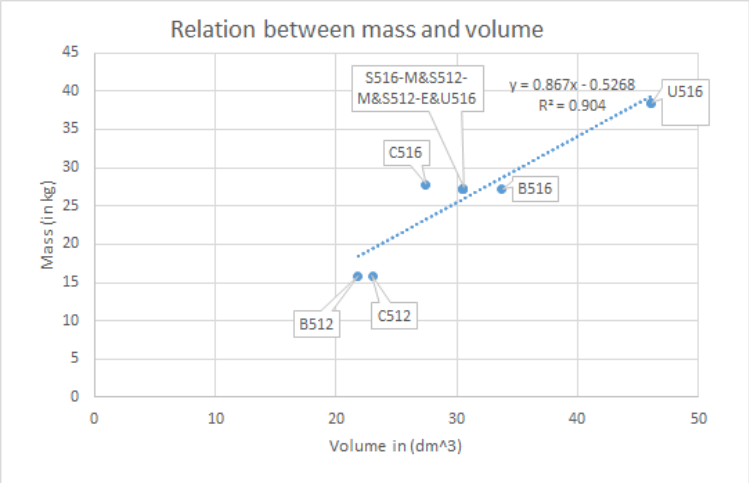

Figure 5.4: Relation between mass and volume for selected camera stabilisers

The power usage root-mean-square (rms), which is the effective value or average quadratic, is 140 Watts for one stabiliser. The maximum power usage is 420 Watts.[11] Which can be obtained by multiplying the maximum current, which is 5 A times the maximum voltage, which is 28 V [38].

ADCS OUTPUT VALUES

The pointing accuracy and the pointing knowledge is the same for all gimbals, this is shown in Table 5.5. The pointing stability and the maximum location error for all gimbal systems is also

[10] http://gyrostabilizedsystems.com/products-services/
[11] http://gyrostabilizedsystems.com/products-services/surveillance-series/s516-m/ [cited 15 June 2017]

shown in this table. As can be seen the maximum location error complies with the 2.75 meter requirement set earlier. The final values of the different ADCS systems in order to stabilise the different cameras will be displayed in Table 5.6. The total mass in kilograms, the total power rms in Watts and the maximum power in Watts is calculated and shown in the last row of this table. The ADCS weighs 36.6 % of the available payload which is clearly a problem. It appears that the ADCS will need to be custom-made. A requirement for the ADCS is namely that it should weigh not more than 70 kilograms. Therefore, this problem should be tackled. This can be done in two ways, where for both methods the weight of one of the gimbals can be reduced significantly, such that the requirement can be met. First of all, instead of using Hyperion a lighter spectrometer might be used, for example Tropolite. Lastly, the Hyperion should be integrated perfectly in the gimbal, in order to reduce weight.

Table 5.5: Achieved ADCS values

Definition	Value	Units
Pointing accuracy	3.03	arcsec
Pointing knowledge	6.06	arcsec
Pointing stability	1.03	arcsec/s
Maximum location error	2.35	m

Table 5.6: Mass and power for the different gimbals

ADCS for:	Mass (kg)	Power rms (W)	Maximum power (W)	Multiplicity
CI	2.7	140	420	4
Hyperion	66.4	140	420	1
IRIS	13.8	140	420	1
Total:	91.5	1120	2520	

5.4. PROPULSION, NAVIGATION, AND STATION KEEPING

Manoeuvrability of the Stratobus is required to keep it stationary or move it to a new location. In the stratosphere at a latitude of 52° wind speeds normally range from 10-20 m/s [2]. To maintain position with these winds the airship must be capable of achieving an airspeed of at least the wind speed. For the Thales Stratobus it is claimed to be operational at wind speeds of up to 25 m/s, as seen in Section 5.1. The required airspeed to move the airship for re-positioning and redundancy in the system depends on the number of airships in the system. Another airship capable of achieving air speeds of 25 m/s is the ESA-HALE concept [1]. Figure 5.5 gives a speed range for airships. This lower speed limit depends on the gust loads at the time in the stratosphere, whereas the upper speed limit is dictated by the drag generated by the airship.

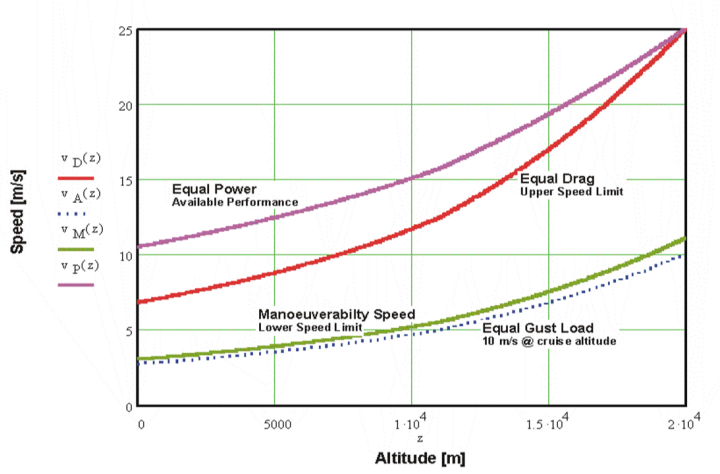

Figure 5.5: Overview of airship minimum and maximum speed limits [1]

5.4.1. PROPULSION

The most logical way for a propulsion system is using an electrical propulsion system, both from a sustainability standpoint and usability standpoint. The use of conventional air breathing propulsion systems like turboprop, turbofan, or turbojet cannot operate efficiently due to the lack of oxygen at these altitudes. In addition, they require fuel to burn which has to be taken on board. Therefore the airships will be equipped with electrical propellers.

For propellers there are two main groups: fixed or controllable pitch. The fixed propellers can be further divided in climb and cruise propellers. The climb propeller has, lower pitch which has less drag as a result. For cruise propellers, the reverse is true. Increasing aerodynamic performance of the propeller blades will result in a more efficient propeller. To obtain high efficiency, the propeller tip Mach number should not exceed 0.95-0.97. Instead of using control surfaces to control the airship's attitude, thrust vectoring is another possibility by using ducted fans [40]. The Stratobus airship uses an electrical double bladed propeller. Thales designed the propulsion system in a way to optimise its performance, therefore more details can be expected from Thales when the Stratobus gets closer to its launch date.

5.4.2. LIFTING GASSES

Airships are classified as lighter than air aircraft. They rely on a lifting gas which has to be lighter than air to create buoyancy. Two main gasses that can fulfil this are presented in this section together with their advantages or disadvantages. The Thales Stratobus uses hydrogen, however, the use of helium can also be explored. The lift is generated by buoyancy; gas in the balloon is less dense than the air in the atmosphere, causing the airship to rise. The balloon has a total volume of 50,000 m^3 as mentioned before in Table 5.3. Depending on which gas is used, the amount of lift can be calculated by knowing the lift generation of that gas per cubic metre.

HYDROGEN (H_2)

Molecular hydrogen is the lightest gas in the universe. It is approximately 14 times less dense than air. However, hydrogen is highly flammable, and because of its small size it diffuses through materials. Hydrogen is easy to create using electrolysis. Hydrogen is a sustainable lifting gas, since it can be created at the same rate as used. Since the air density at 20 km altitude is known using ISA calculations, it is possible to determine the lifting capability of hydrogen. For hydrogen this is 0.082 kg/m³.

HELIUM (HE)

Helium is the second lightest gas, only an effective 8% difference with hydrogen. A helium atom is twice as heavy as molecular hydrogen. It has as main advantage over hydrogen that is incombustible. Helium is much scarcer on Earth and therefore much more expensive than hydrogen. In addition, due to its small size it has the same diffusion problems as hydrogen. Until nuclear fusion is possible, helium is non-sustainable since it cannot be created. In a similar way as with hydrogen, the lifting capability can be calculated. For helium this is 0.076 kg/m³, which is lower than the lifting capability of hydrogen. Therefore for the same lift, more helium is required than hydrogen.

5.4.3. NAVIGATION AND STATION KEEPING

To perform observation tasks, it is crucial for the airship to know its location. After all, if the airship is at the wrong location there will be gaps in the coverage area. This section specifies the navigation and station keeping characteristics of the airship. Station keeping is key to maintain the yearly operational time without maintenance, to let the ground know the system functions as intended.

A straightforward method to determine the location and movements of the airship is by using GNSS receivers. Dual frequency GNSS receivers enable real-time positioning with centimetre level

accuracies. The use of dual frequency GNSS receivers is available for commercial use, but it is limited to professional applications due to price.[12]

An example is the OEM7720 GNSS receiver made by Novatel. It is capable of tracking all current and upcoming GNSS constellations. It is capable of providing horizontal position with accuracies around centimetre level, and is able to operate at -40 ° C.

The airship has a length of over 100 metres, so the attitude can be determined by placing one GNSS receiver at the nose and another one at the stern or just simply using an IMU and a GNSS receiver. If you know the position of each of them, you know their relative position and thus know the orientation of the airship. The GNSS can measure and determine where the airship is with an accuracy of around 0.01 metres. [13]

Since GNSS has such a high accuracy, it is a good design option to use the GNSS for the navigation system. The GNSS receivers could also be used for the pointing accuracy, as mentioned before, by comparing the relative position of the sensors at the other ends of the airship.

Stationkeeping means maintaining the position of the airship. The main factors disturbing the position of the airship are the stratospheric winds. The airship knows its position from the on board navigation system, and its attitude from the ADCS. The propulsion system provides the required thrust to maintain the required position. As seen in Section 5.4, the airship should be able to maintain its position with wind speeds of 25 m/s. The examples provided in that same section show that airship propulsion systems are capable of producing sufficient thrust levels to maintain position. The attitude of the airship is controlled by the propulsion system as well. The shape of the airship aligns it with the wind, making attitude control easier.

5.5. COMMAND AND DATA HANDLING

The data gathered from the Hyperion Camera, AMS Wildfire, IRIS and Colour Imager fitted in the Stratobus should be able to be stored in order to be sent down by the antenna (discussed in Section 5.6). This data is handled by the command and data subsystem. What is important to note is that the NSS produces vast amount of data that might be hard to be sent down. A solution to this is discussed in this section as well.

5.5.1. COMMAND AND DATA HANDLING ARCHITECTURE

The command and data handling system interacts with every other subsystem to make sure they fulfil their tasks. It is also the subsystem that receives input from the ground station (via the telecommunications subsystem) and processes that input. As the name suggests, the subsystem deals with the received data, by either storing it, or sending it to the communication subsystem, which in turn sends it back to the ground station. In this section the command and data handling system for the airships will be briefly explained, both what it consists of as well as an architecture of the interaction between the subsystems.

The processor is seen as the brain of a computer and could therefore be seen as the brain of the processes happening in the airship as well. The processor has four core functions: fetch, decode, execute and store. Processors are developing very fast and are becoming extremely powerful and capable of fulfilling their task. It could then be assumed that a processor could easily be found which fits the amount of processes it should be able to process on the airship, and as a result the processor would not be the limiting factor.

Besides the processor, a storage unit is needed to store obtained information. A storage unit is always needed on board of an airship. For instance, in case of communication problems with the ground station, it is important that the obtained data is saved on the unit such that it could be send to the ground station when the communication has been resolved. Storage unit are very well developed nowadays as well, that those discs will not be the limiting factor either: they can store a lot of data and are becoming smaller and smaller. Of course not all the data that is obtained by the

[12] http://www.gps.gov/systems/gps/performance/accuracy/ [Cited 7 June]
[13] https://www.novatel.com/assets/Documents/Papers/OEM7720-Product-Sheet.pdf [Cited 7 June]

optical system and the sensors is being sent to the ground station; it is first being manipulated, by compressing it and by removing parts of the data which are either redundant or which is irrelevant data. Which will be discussed in Section 5.5.2.

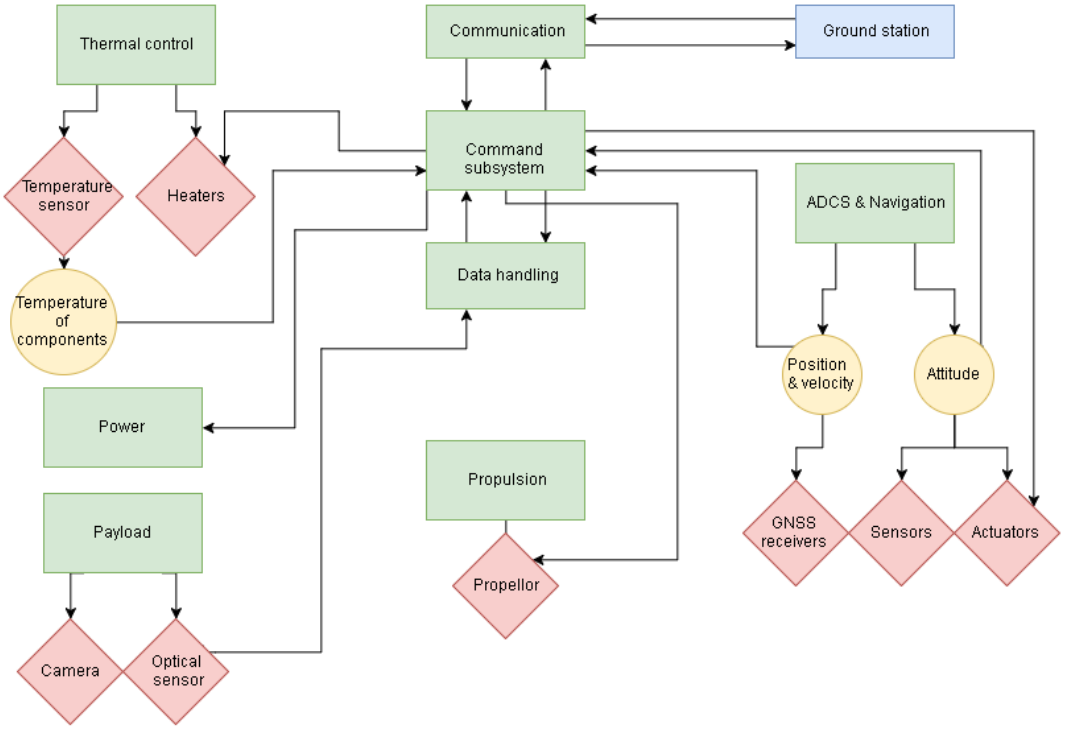

Figure 5.6: Architecture of the command and data handling system

To give an indication of what the command and data handling subsystem (especially the commanding part) interacts with, an architecture is presented in Figure 5.6. The green rectangle blocks represent the subsystems of the airship and the ground station is an element of the NSS. The diamond red blocks are the actual elements of the subsystem and the round yellow blocks are quantities that the subsystem has as output. Arrows to the 'command subsystem' block represent input values for the command subsystem to compare to a reference value. If the input value is different from a reference value by more than a certain margin, then the command system should activate the element that is responsible for getting the right value of that quantity again. That is why there are also arrows from the command block to certain actuators. Another thing that should be noted is the fact that this figure only shows the interaction of the command and data handling subsystem with the other subsystems, that is why there are no arrows from other subsystems to other subsystems.

5.5.2. DATA REDUCTION

The payload is expected to generate enormous clusters of hyperspectral data. This section describes the steps which must be taken to acquire, filter and process this data.

STEP 1: DATA ACQUISITION

Figure 5.7 shows how hyperspectral data is acquired and structured. Photometric data will be received from multiple spectral bands simultaneously. The different images are stacked to form a so-called hyperspectral cube. Thus, pixels are organised in a 3D array with dimensions $(i \times j \times k)$. Indices i and j relate to the along-track and cross-track directions; index k refers to the spectral band. Each pixel provides a measure of the luminous intensity I.

[14] http://www.hyspex.no/images/Kube.jpg [cited 15 June 2017]

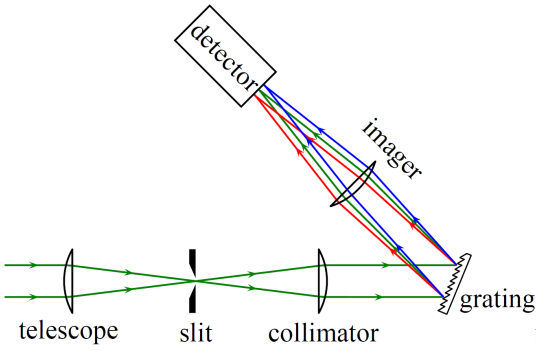

(a) Schematic representation of the hyperspectral imager [29]

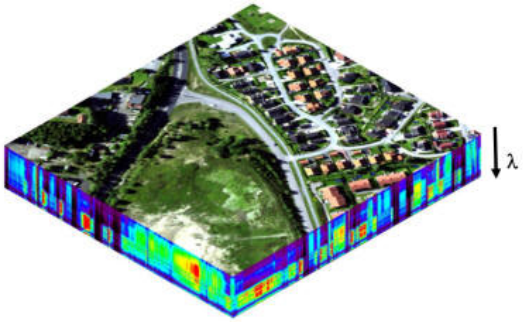

(b) Hyperspectral cube composed of spectral layers [14]

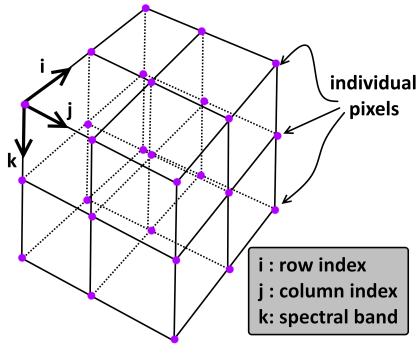

(c) 3D data structure

Figure 5.7: Hyperspectral data acquisition

STEP 2: PRE-PROCESSING

Pre-processing is an important step in the data mining process. During this step, irrelevant and redundant information is eliminated. This is achieved by:

- **Scanning within a demarcated region where objects of interest are expected to be located.** This is particularly relevant for moving targets. Based on previously calculated displacement vectors, a maximum likelihood prediction can be made as to where the target is located.
- **Reading out only the relevant spectral bands.** Spectral bands are selected based on pre-knowledge of spectral characteristics. E.g., fire detection requires only two spectral bands; smoke detection, four spectral bands [4]. Spectral bands for target recognition may depend on the particular colour composition of potential targets.
- **Performing good data checks.** All brightness temperatures (BTs) must be above 0K (a lower brightness temperature would be physically impossible).

All other data is flagged as obsolete and, henceforth, ignored by the data handling routines.

STEP 3: PROCESSING

The filtered data is fed forward through the data processing algorithms; see Figure 5.9 (next page).

The NSS will make extensive use of Hopfield neural networks for object recognition and tracking. A Hopfield neural network is shown in Figure 5.8. The unique advantages offered by neural networks stem from the fact that all the neurons are interconnected and outputs are fed back as inputs, creating a dynamic behaviour with all matches being performed simultaneously. The outputs of the network tend to converge to the global minimum energy solution – depending on the shape of the energy function which may of course contain local minima. Hopfield neural networks can be trained to recognise objects by matching particular features, given an energy function and

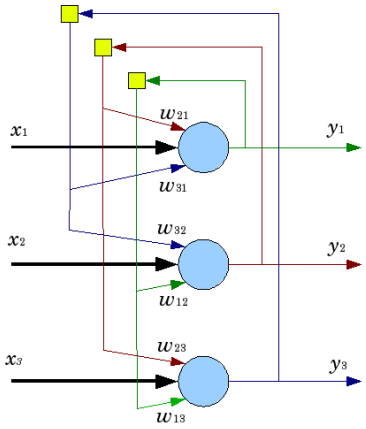

Figure 5.8: A Hopfield neural network

constraints [41–43]. Neural networks are unique in their flexibility and robustness. They can be made to solve virtually any optimisation problem while automatically satisfying constraints. Their superiority has been demonstrated in practice for cloud tracking applications [41].

To size the processor and data storage unit, it is estimated that the data influx from the imagers averages around 2 GB/s and peaks at 12 GB/s. To run the processing algorithms real-time, a 12 core processor is needed (assuming a data reduction of factor 10 or better).[15] 10 storage units with a capacity of 12 TB each would allow data to be stored for multiple days.[16]

STEP 4: POST-PROCESSING

Once all the important information has been extracted from the data, it is encrypted and modulated for down-link. Encryption techniques are commonly applied and well-documented, so they are not a limiting aspect to the software design. Current technology relies on the generation of an encryption key, which scrambles the data by means of 74xx and/or 74xxx logic gates.[17] Data can be recovered by unscrambling it; this requires that the same encryption scheme is used by the different components of the NSS. The disadvantage to traditional encryption methods is that they can be cracked – however, when using complex encryption keys such as the AES 256-bit key, the odds of this happening are slim. Side note: in the future, it is expected that breakthroughs in quantum communication will lead to absolutely secure transmission of secret messages (currently, TRL 1-2) [44].

STEP 5: MACHINE LEARNING

The last step is not directly part of Figure 5.9, however, it will make the system work faster and more efficiently: machine learning. Each target has distinct behaviour and with the data gathered, the system can use some cost functions to fine-tune its neural networks in order to better predict the target's location. Over time, this will make the system more efficient in tracking. Machine learning will take some time, since the system must have many data points to extrapolate the target's next location.

[15] https://www.intel.co.uk/content/www/uk/en/products/processors/xeon/e7-processors/e7-8870-v4.html [cited 20 June 2017]
[16] http://www.seagate.com/www-content/datasheets/pdfs/ent-cap-3-5-hdd-12tb-v7DS1925-2C-1704NL-nl_NL.pdf [cited 20 June 2017]
[17] https://electronicsmail.wordpress.com/2012/10/14/data-encryption-and-decryption-system-using-74xx-logic-gates/ [cited 14 June 2017]

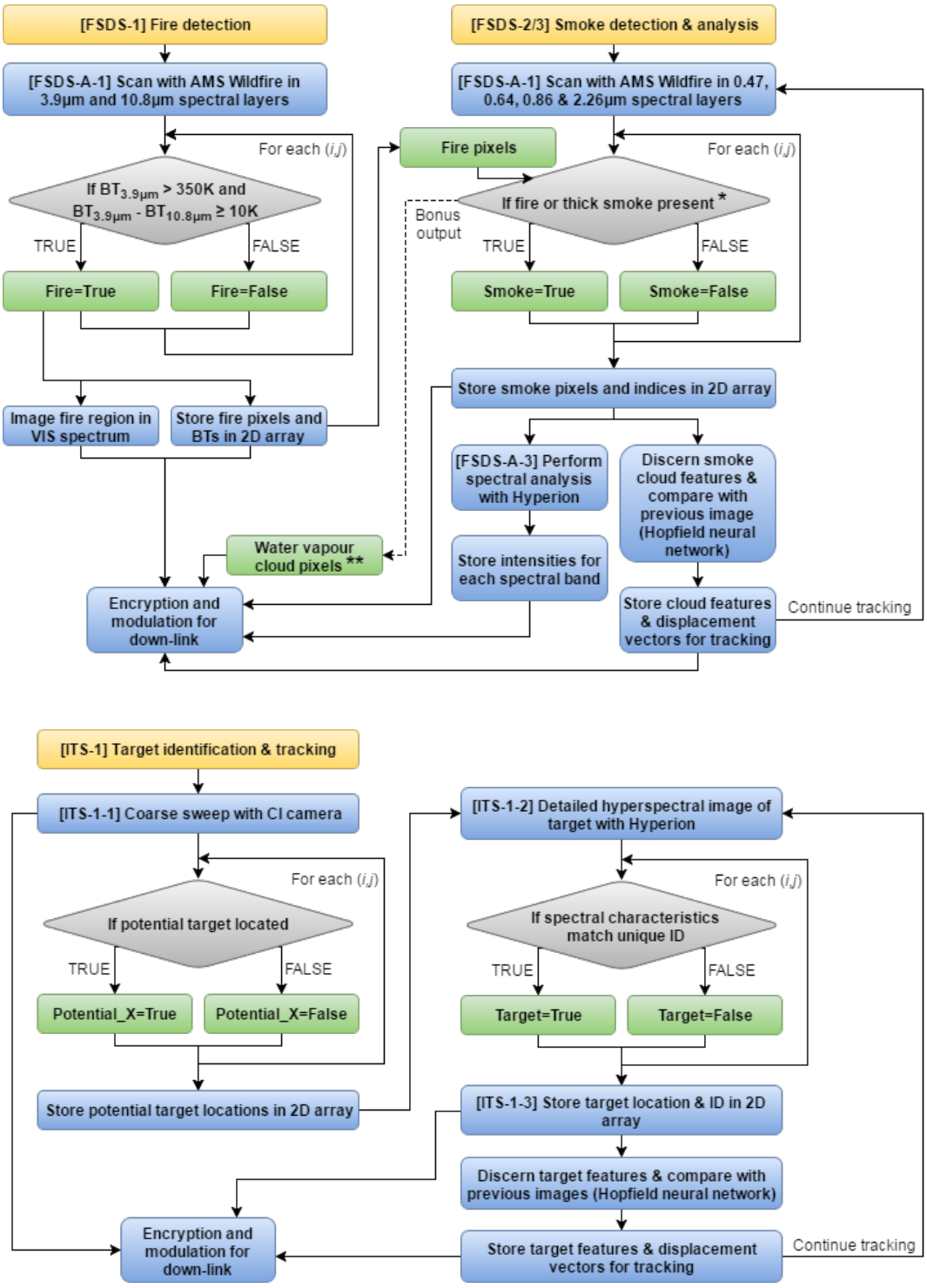

Figure 5.9: FSDS and ITS data processing algorithms

*For validated smoke detection algorithms, see [4]
**These same algorithms have the additional ability to recognise water vapour clouds

5.6. COMMUNICATIONS

Communications is an important subsystem for the Stratobus: it communicates with the ground segment and receives information on what it should do. In the previous report [2], it was found that it was most convenient to send data with frequencies corresponding to the X-band range. However, this band was mainly chosen for convenience for the CubeSats, and since those are not an option anymore, it may be better to send data in the K_a-Band. In this section, first the downlink communication between airship and ground segment will be determined and secondly, the uplink communication will be determined.

5.6.1. DOWNLINK

If a certain data rate is needed, the bandwidth should be adapted to that data rate, i.e. the bandwidth depends linearly on the data rate that is being used [2]. The K_a-band is larger than the X-band. Missions with a large data rate usually communicate in the K_a-band, since there is significantly more bandwidth available in that band than the X-band. One of the downsides of communicating with a higher frequency is the increase in losses (space loss, rain loss and zenith attenuation). However, increasing frequency will result in an increase in antenna gain and by increasing the transmitter power, the losses could be counteracted if the link does not close.

During the previous report, many formulas were presented for calculating the communication link. The only formula that will be repeated is the formula for signal to noise (SNR), as that is the most important one. The SNR can be calculated using Equation 5.6.1.

$$SNR = P + L_l + G_t + L_a + G_r + L_s + L_{pr} + L_r + 228.6 - 10 \cdot \log R - 10 \cdot \log T_s \tag{5.6.1}$$

P is the transmitter power in dBW, L_l is the loss of the transmitter, L_r is the loss of the receiver, G_t and G_r are the gains of the transmitter and receiver, respectively, L_a is the zenith attenuation, L_s is the space loss, L_{pr} is the antenna pointing loss, R is the data rate in bits/s and T_s is the system noise temperature. In order to have a successful communication, the SNR should be at least 7.4 dB to be successful. This includes the necessary 3 dB margin and a minimal SNR of 4.4 is needed as the BPSK and QPSK plus R-1/2 Vitterbi Decoding.

A tool was created to calculate the SNR directly. Most values were determined by the equations that are present in the MTR report, however, some values had to be assumed for some other parameters. The system noise temperature could be calculated using the equation present in the MTR, however the parameters that are present in the formula are antenna dependent first of all and they are mostly not provided. Therefore, the system noise temperature is estimated at 135 K plus the noise temperature caused by the rain attenuation and the antenna noise temperature. T_s had a value of 432 K with all the added noise features. The power the transmitter sends the signal at is only taken to be 2 W. The transmitter antenna has a diameter of 0.05 m and the receiver antenna has a diameter of 0.5 m. For the determination of the other parameters in the SNR equation, see the section on the link budget in the MTR. Using all these parameters it was found that the SNR is quite high: 18.3 dB. So it could be concluded that the link is not at all hard to close. It should be noted that the airships are relatively close compared to communicating with spacecraft which are at altitudes in the order of 300 km at least. The free space loss for airships is quite low and therefore a fairly small antenna (both receiver and transmitter) are sufficient to close the link. The operational frequency for the telecommunications is at 26.5 GHz (in the K_a-band) with a bandwidth of 10 MHz, which would allow for a data rate of about 200 Mbit/s. With this current SNR of 18.3 dB, it could be decided to take a cheaper modulation technique as well, which requires a higher SNR.

5.6.2. UPLINK & DOWNLINK FOR TELEMETRY

Apart from data that is send down, data should also be send upwards, like commands or information on the paint colours. The same holds for status updates that will be send down by a different antenna. This is called telemetry.

UPLINK TELEMETRY

For uplink telemetry, the UHF band will be used. With a frequency of 0.45 GHz the received SNR is 69.83 Db while the required SNR is 9.60 Db. The link budget for uplink therefore closes sufficiently. This antenna that will be used is omni directional antenna. These calculations have been performed during the mid-term phase of the report [2].

DOWNLINK TELEMETRY

The downlink telemetry system works the same the as uplink but of course the other way around. This was also discussed during the mid-term review. For Downlink telemetry the VHF-Band will be used with a signal strength of 54.18 dB [2]. Using this band and a dedicated omni directional antenna, the airship is able to communicate to the ground stations about its status.

5.7. THERMAL CONTROL

Thermal control is another subsystem which is of importance for the functioning of a system. The payloads found in Chapter 4 operate at a certain temperature or in a temperature range. The maximal temperature in the stratosphere is -40 °C and it could even reach lower than -65 °C. In Table 5.7, different operating temperatures of the used sensors are displayed. The temperature of these components should be kept at those temperatures as much as possible, so that the sensors work properly.

Table 5.7: Operating temperatures of the used sensors

Name	**Operation temperature [K]**
AMS wildfire	218-343
CMV50000 Colour imager	243-343
Hyperion	157
IRIS	233-323

Some antennas also need to be inside a certain temperature range for them to work properly. Therefore, their temperature should be controlled well.

There are different ways of controlling the temperature. The easiest way is to apply a coating. If it is desired that the object absorbs heat, the coating has to be made black, as that colour absorbs all the light and if the object needs to be kept at a low temperature, a white coating should be used. Another passive thermal control element is multi-layer insulation (MLI). It can be used for preventing heat loss and prevent the object from being heated. By putting the insulation on the object, the object will be thermally controlled.

Even though many passive thermal control methods exist, active control is also a possibility, and may even be more applicable in this case, as the airship is not entirely in space and still (compared to space) in significant atmosphere. Heating systems which are common are so called patch heater, which is basically an electrical resistance element between two sheets of flexible electrically insulating material. A maybe more obvious way to heat the object is by using heat pipes. On one side of the pipe there is a liquid substance, which evaporates by absorbing heat. It travels to the other side of the pipe where it releases its heat by condensing. The side at which the liquid evaporates should be placed next to a device that produces heat or a heating element should be added to make the liquid evaporate.

Cooling mechanisms should also be used, as some of the sensors operate at a really low temperature, lower than the temperature in the atmosphere at that height. One way of cooling could be to use a fan, however, a fan cannot reach that low temperature. A fan is more effective for a hot component to lose heat than cooling the component to a temperature lower than the surrounding temperature. To lower the temperature of a component to a temperature that is lower than the surrounding temperature, convection could be used. Convection is the movement of groups of molecules in a liquid or a gas. This method absorbs energy from the component using this liquid or gas substance, using advection and diffusion.

Besides all the aforementioned heating mechanisms, there are still a lot of other thermal control options left. The use of composites and diamond films for thermal control is still looked into, which could be a proper way of thermal control in the future as well. To make sure that sunlight does not shine into the aperture, the aperture should be covered from the Sun, which also results in the Sun not giving too much heat to the camera. This is necessary to make sure the camera is not blinded by the incoming sunlight. However, since the camera and sensor should operate at least at a temperature of -40°C, the optical system should be heated by one of the aforementioned methods, as it is not able to remain at a temperature higher than -40 on its own at that altitude. These methods have worked before, so it is guaranteed to work for the payload on the airship as well.

5.8. ELECTRICAL POWER SYSTEM

The Electrical Power System (EPS) is the subsystem that generates the power for the airship. The EPS is of major importance since without electricity nothing can operate. At an altitude of 20 km, there are no clouds above the airship, so harvesting solar energy is a very feasible option. The airships are equipped with solar panels at the top for energy generation during day. For energy generation during the night, a reversible fuel cell is used. During day, the solar cells power the reversible fuel cells to store power which can be used during the night, mostly for sending data.[1] The total payload available power is 5 kW on the 250 kg Thales stratobus.[2] This power is the same that has to be used by all other subsystems, except for the propulsion. The basic EPS architecture is presented in Figure 5.10a and 5.10b. As stated earlier, the fuel cell is reversed during day time to produce hydrogen which can be used during night time to produce electricity and water.

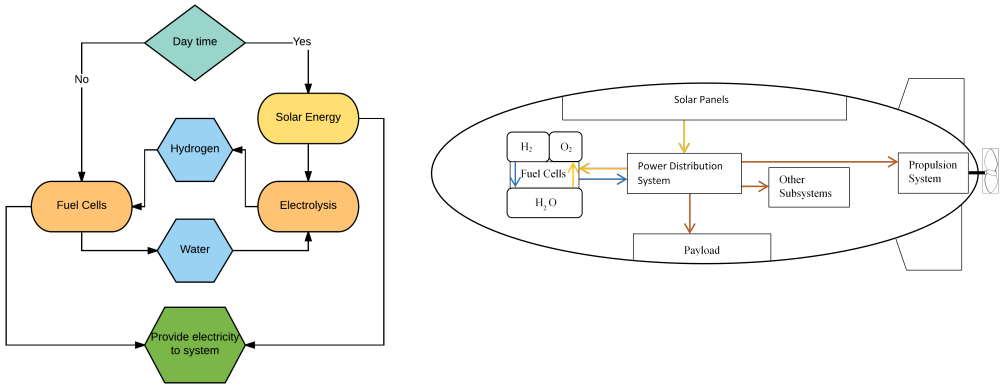

(a) EPS Functional Diagram

(b) EPS Architecture

Figure 5.10: Electrical power system overview

To see if the available electrical power is sufficient, a rough estimate of the power usage for the payload and subsystems is presented in the following section (section 5.9).

5.9. SUBSYSTEM INTEGRATION

Now that all subsystems have been sized, it is time to integrate the final product. The mass, power, and envelope budgets for the payload are shown in Table 5.8. These budgets have been updated weekly; Figure 5.11 shows how the mass budget evolved throughout the subsystem design process.

[1] https://www.thalesgroup.com/en/worldwide/space/news/space-qa-all-about-stratobus [cited 8 June 2017]
[2] https://www.thalesgroup.com/en/worldwide/space/news/whats-stratobus [Cited 8 June 2017]
[4] https://www.intel.co.uk/content/www/uk/en/products/processors/xeon/e7-processors/e7-8870-v4.html [cited 20 June 2017]
[4] http://www.seagate.com/www-content/datasheets/pdfs/ent-cap-3-5-hdd-12tb-v7DS1925-2C-1704NL-nl_NL.pdf [cited 20 June 2017]

Table 5.8: Budget calculations

Component	Count	Mass [kg]	Mass subtotal [kg]	Nominal power [W]	Peak power [W]	Power subtotal [W]	Dimensions [cm^3]	Volume subtotal [L]
CI	4	3	12	3	-	12	12x12x22	12.7
IRIS	1	35	35	0.75	-	0.75	34x34x66	76.3
Hyperion	1	49	49	51	-	51	39x75x66	193.1
AMS Wildfire	1	57	57	-	140	140	38x38x38	54.9
Processor	12[3]	0.1	1.2	140	-	1680	12x(5x5x1)	0.3
Data storage	10[4]	0.7	7	10	-	100	10x(5x5x1)	0.3
ADCS	1	**92→70**	70	1120	2520	1120	4x(20x20x30), 1x(40x40x70), 1x(40x80x70)	102.0
Wiring	1	10	10	93	-	93	0.5x0.5x10000	0.0
Cooling	1	-	-	750	1200	750	-	-
Totals:			**242**			**3950**		**440**

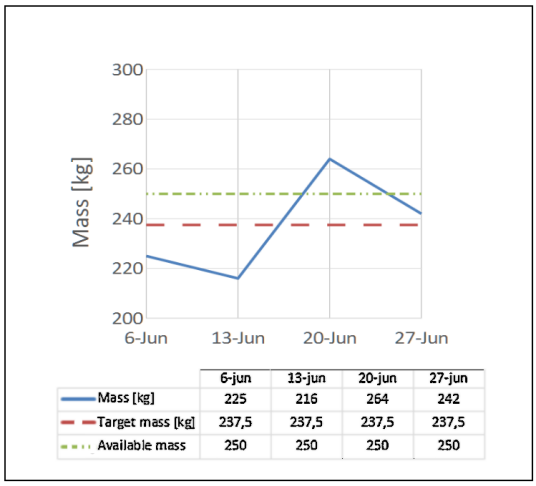

Figure 5.11: Evolution of mass budget over time

In this figure, a large increase in mass can be observed on June 20th, resulting directly from the ADCS design. To close the mass budget and leave some margin, the ADCS will need to be re-designed to a mass of at most 70 kg (currently 92 kg). This is left to the post DSE stage.

Luckily, the power budget closes with a large margin: only 3950W of the allowed 5000W will be used.

A sketch of the payload envelope, indicating estimated dimensions of the stabilised cameras, is shown in Figure 5.12. Tolerances are included to allow for flexibility in the integration of ADCS, camera mechatronics, wiring and cooling. The AMS Wildfire is drawn separately, as it can operate independently (it has its own thermal control and stabilisation). So, to save space, the AMS Wildfire is for now assumed to be installed outside of the payload bay. It is still unknown how much space is available for the payload.

The cost breakdown will be discussed later on, in Section 7.3.

5.10. RISKS ASSOCIATED WITH AIRSHIP PLATFORM

Airships are the main platform of the NSS and allow for constant, full coverage of the Netherlands. Their importance to the system is such that any risks associated with them have high levels of severity and so they must be mitigated as much as possible. The presence of winds of up to 20m/s in the stratosphere implies a serious risk for any of the airship's manoeuvrability. This creates the

[5] https://www.nasa.gov/sites/default/files/images/258234main_ED07-0210-3_full.jpg [cited 20 June 2017]

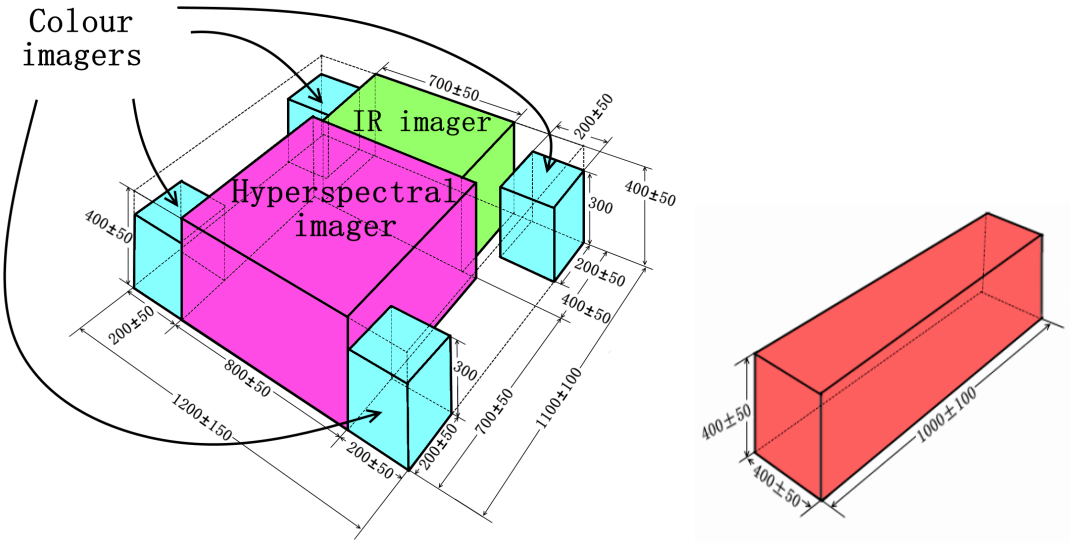

(a) ITS Payload

(b) FSDS payload[5]

Figure 5.12: Payload envelope (dimensions in mm)

need for a propulsion system in all airships that is able to provide at least this much velocity to the airship so that fixed positions can be held with ease. Another major risk related to the airships has to do with the use of hydrogen as a lifting gas. As mentioned before hydrogen is a highly flammable gas and so extra care needs to be given to ensure that the balloon does not ignite. This is achieved by ensuring proper separation between any electrical components and the balloon. In data processing tasks, the use of Hopfield neural networks for object recognition bears the risk that in the first stages of its usage the network might not be working at full efficiency since it needs to acquire data to develop properly. This is issue mitigated by extensive testing of the network and by double checking its outputs for the first few months until its reliability is at a high enough level. Finally, the threat of someone hacking the system is a very real one, which is the reason why AES 256-bit encryption is used to protect all the data being generated by the airships from any third parties.

5.11. CONCLUSION

The Thales Stratobus will be used for the NSS. The Stratobus has a payload of 250 kg with a power generation of 5 kW, which should be sufficient. A dedicated ADCS will provide stabilisation for the four colour imagers, the Hyperion and the IRIS imager. The main challenge is to limit the total weight of these stabilisers to 70 kg, as the first design iteration yielded a mass of 92 kg. On the Stratobus, an electric propulsion system is already present. It is capable of propelling the airship at a speed of 20 m/s, so the airship itself does not have to be designed. The lift is generated by the gasses inside the airship and different gasses can be used to fulfil this task. However, there is only one obvious option: hydrogen. Overall it will be cheaper than any of the other gasses as well as more efficient and environment friendly. Hydrogen can be produced on board by means of a fuel cell. For the navigation of the airship, it is best to use GNSS receivers because they are highly accurate, in the order of 0.01 m. The command and data handling system consists, among others, of a 12 core processor and a storage unit weighing roughly 7 kg. Nowadays, there is a wide variation of those items, also, they get better and more capable by the day, therefore they are not the limiting factor. The data that is generated should be reduced, because not all data is useful. Useful data is extracted from the generated data and is encrypted, to make sure it does not get in the wrong hands. For the communication subsystem, a SNR of 23.4 dB is used with a transmitter antenna diameter of 0.05 m and a receiver antenna diameter of 0.5 m. The required SNR is 7.7 dB, so 23.4 dB is quite high for a SNR, it is even possible to take a cheaper modulation technique which requires a larger SNR. It is most probable that the airship is going to need a heating system

inside the payload bay, as most optical elements (like sensors) operate at a temperature between -40 °to 71 °C. Heaters and coolers are already integrated in many flying objects, mostly spacecraft. Since thermal control has been applied to so many aerospace systems, it can be implemented on the airship as well. Figure 5.13 is a representation of what the airship will look like.

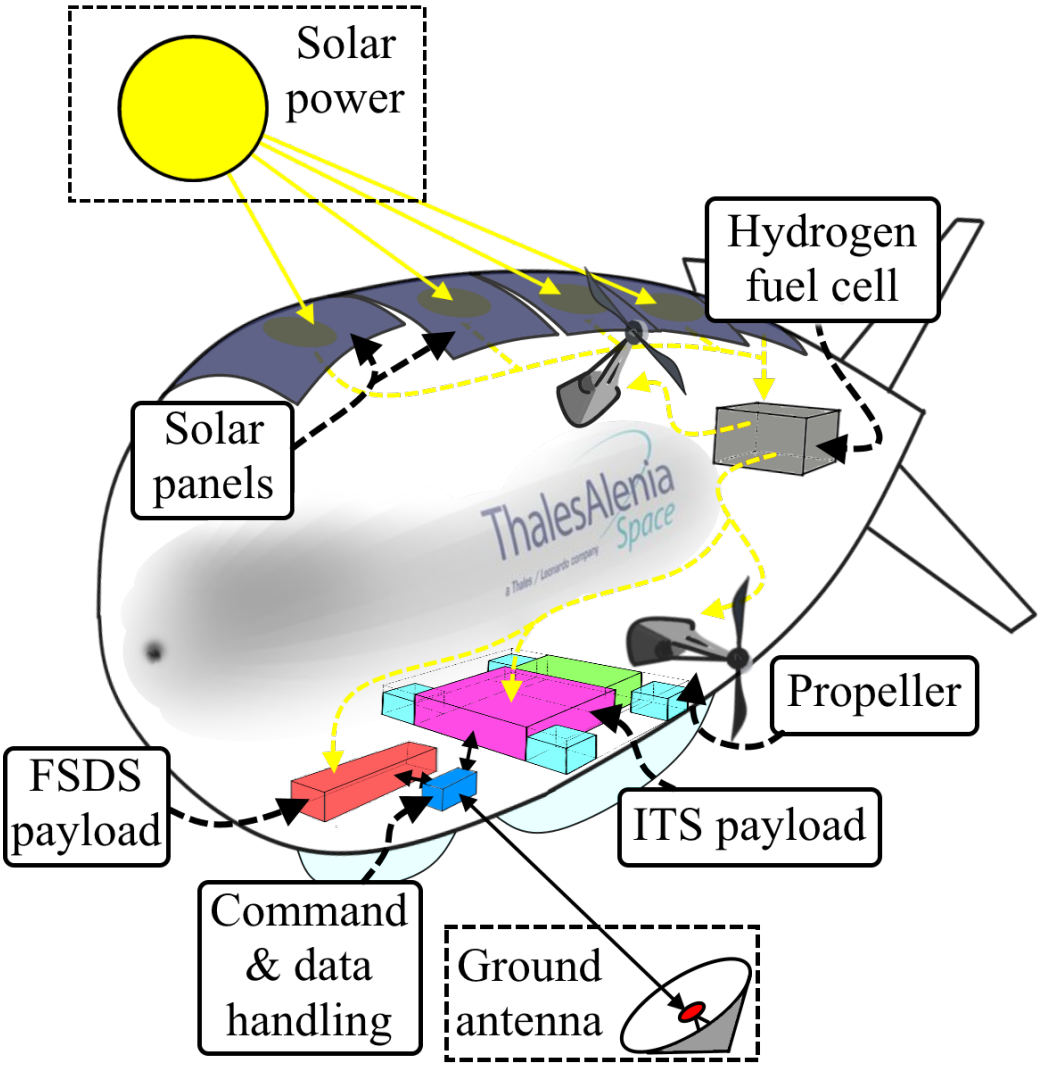

Figure 5.13: Representation of the airship with its subsystems

6 | Other System Elements

The previous chapter exclusively discussed stratospheric airships and its subsystems for the NSS. This chapter contains information on the other elements, namely mission control (Section 6.1), the ground station (Section 6.2), airship ground base (Section 6.3) and drones (Section 6.4).

6.1. Mission Control

Mission Control (MiCo) will function as the brain of the NSS. All project level decisions will be made here. MiCo can be housed inside an office building, preferably in a central location. The main requirements for such a building are as follows. First off, there must be enough office space for government employees and contractors; not to mention facilities such as conference rooms and other peripherals. Notably, a heavy-duty data centre will likely take up quite some space. Secondly, the building must be highly secured, as much of the information within its walls will be sensitive if not confidential.

Development of the MiCo centre is left for the post DSE phase. The main aspect to be decided on, is the location of the mission control centre. There are two strong candidates:

1. **Near the airship ground base in the middle of the Netherlands.**
   Based on a cost estimation performed in the MTR phase, the NSS will employ more contractors than government employees to maintain the system, as most of the labour costs will go towards maintaining and upgrading the airships. To tailor to these contractors, there is a strong push to locate mission control near the maintenance site at the airship ground base. Moreover, since the nominal operations centre around the airships, it would be convenient from an operations point of view to make mission-critical decisions in close proximity of the airship base.

2. **Near VenJ in Den Haag.**
   Since the ministry of Security and Justice will be the chief stakeholder and user of the NSS, there exists a similarly strong push to locate MiCo in Den Haag. As the stakeholder and user, VenJ will have final authority over mission-critical decisions. In these decisions, they might choose to involve other government bodies. As Den Haag is the political centre of the Netherlands, this location would facilitate intra- and intergovernmental cooperation.

VenJ should decide for themselves which of these two locations best serve their needs. If VenJ is looking for a good cooperation with contractors and smooth operations, it would be wise for them to lay the foundations for a mission control centre near the airship base. If, on the other hand, VenJ is more focused on cooperation between national and international government organs to help develop the NSS, they should opt for Den Haag instead.

6.2. Ground Station

The number of ground stations is influenced by the distance at which a ground station can still make contact with an airship. Theoretically it would be possible to have a single ground station cover the entire Netherlands. This however is hard to achieve due to the relative low altitude of the airships which would require a very small elevation angle (the angle between the signal path and the horizon). Having a very small elevation angle is prone to obstructions and has to travel a longer path through the atmosphere and potentially rain clouds. A typical minimum elevation angle is 10°, substantial information is present regarding atmospheric and rain attenuation, and thus will be used to determine the range of one ground station [45]. The radius of one ground station was found to be 110 km, but will be underestimated to be 100 km to be on the save side. Looking at Figure 6.1 it can be seen that two ground stations (indicated with the green circles) are

able to cover the whole Netherlands. The location of the two ground stations are in the North of the province Flevoland and in the South of North Brabant near Tilburg.

Figure 6.1: Position of ground stations with a radius of 100 km

The number of ground antennas is also something to be determined. It might be obvious to use one ground antenna per airship, however the number could be reduced by receiving signals from several airships on one antenna. This would require these airships to transmit in different bandwidths to discern the signals and thus more bandwidth has to be allocated. Additionally, one antenna can only up-link to one airship at the time, thus not all airships can be instructed at the same time. Finally, for an antenna to receive multiple signals at the same time these sources, should lie in the beam width of the antenna. This is a hard requirement to meet, as the data transfer frequency selected is very high causing the beam width to be very small and subsequently makes it virtually impossible to have multiple sources within the view cone of one antenna. Thus for each airship a ground antenna would be required, which has a diameter of one metre as determined in Section 5.6. Each of the ground stations should also have one redundant antenna in case of maintenance or breakdown of one of the others. Thus the ground station in Flevoland and North Brabant would require 8 and 9 antennas respectively.

6.3. AIRSHIP GROUND BASE

The airship ground base is where the airship will come annually to have its maintenance or when an emergency occurs. It requires three main components which are displayed below. Then the base size will be discussed and lastly two possible locations will be discussed.

1. **Portable mooring mast**
   A mooring mast is a structure that holds the airship in place when it is docking. To be able to transport the airship back in the hangar and the other way around, a portable mooring mast needs to be designed. An example of a portable mooring mast used by the Goodyear blimps can be found in Figure 6.2b.

2. **Hangar**
   The hangar is where the balloon is stored when it needs servicing. This hanger must be larger than the airship in order to store it.

3. **Launch pad**
   The launch pad is the area where the mooring mast is driven to, to launch the airship. The launch pad shall at least have the radius to accommodate the airship is every direction of wind.

BASE SIZE

The only airship hangar built after the second world war is the hangar built for Cargolifter CL 160 by Cargolifter AG.[1] This hangar is 360 m long, 210 m wide and 107 m high. Sadly, it was never put in good use since the company went bankrupt. The hangar that houses the Stratobus can be a lot smaller since the Stratobus is smaller. As can be found in Table 5.3, the length of the Stratobus is 115 meters and at its widest point has a diameter of 34 meters. Using these dimensions and the fact that space for two airships might be needed in case of emergency of 1 airship when another one is already in maintenance, two options exist for the hangar dimensions; see Table 6.1.

Table 6.1: Hangar options

1 big hangar			**2 separate hangars**		
Width [m]	Height [m]	Length [m]	Width [m]	Height [m]	Length [m]
90	45	135	45	45	135

To maintain the airships and move them around in the hangar, the dimensions of the hangar are at least 15 % bigger than the airship. In a further design stage the feasibility of the big hangar should be investigated and a trade-off should be done between the two.

Next to the hangar, the base of the airships is also composed of a launch pad. From literature, it is known that the airship base might look something like Figure 6.2.

(a) Example of an airship maintenance base [2]

(b) Mooring mast Goodyear

Figure 6.2: Impression of the airship ground base

In this configuration it can be seen that both hangars are connected to the launch pad from where the airships will go airborne. The mooring mast is centred in the middle of the circle. This launch pad will have a radius that is longer than the airship, for instance 130 meters. The total area needed for the maintenance base will be in the order of 0.5 to 1 square kilometre.

BASE LOCATION

The location of the base should be centrally located in the Netherlands to be easily accessible for all airships. Naturally, a maintenance base in the middle of The Netherlands has to be chosen. The city of Amersfoort is considered to be in the middle of the Netherlands. A deactive military base is near Amersfoort called 'Vliegbasis Soesterberg', the terrain next to this Air Force Base might be used as maintenance base. Another option would be using the south west of Flevoland. The two options are displayed in Figure 6.3. The base will not be chosen in this stage of the project though. This will be done in a later stage of the project.

[1] http://www.aerospace-technology.com/projects/cargolifter/ [cited 16 June 2017]

[2] http://gizmodo.com/these-massive-wooden-hangars-once-housed-wwii-airships-1604793645 [cited 14 June 2017]

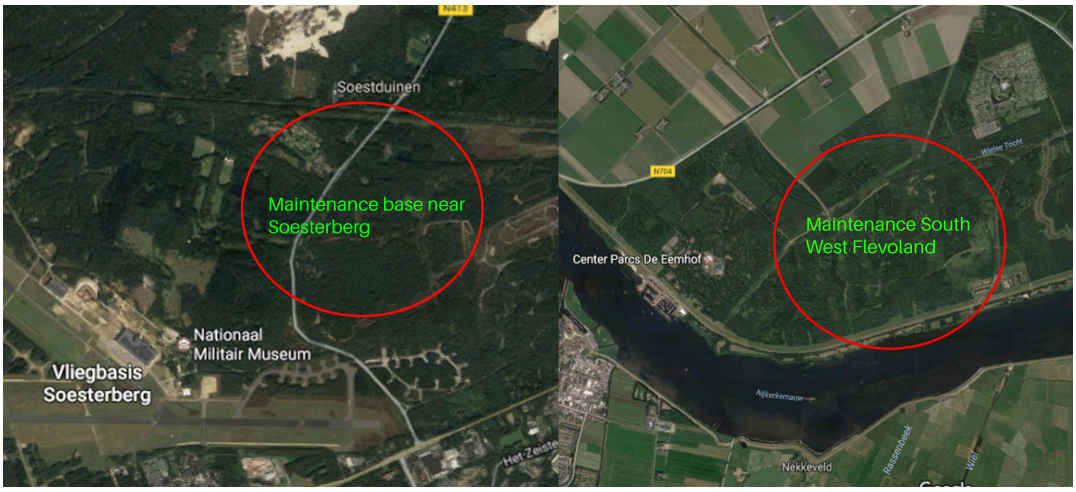

Figure 6.3: Proposed maintenance base locations

6.4. DRONES

Because drones operate below the clouds, they can be used to substitute the airships during cloudy conditions. This section deals with the selection of drones for the NSS. The selection process starts with setting requirements for the drone. The next step is to compare detection methods and select sensors. Subsequently, some drone platforms are considered. In the end, a trade-off is made.

6.4.1. REQUIREMENTS

There are several drones on the market that are able to analyse smoke clouds to determine the toxins in the clouds. With regards to FSDS functionality, the drone must fulfil the following requirements:

- **Arrive at a fire or gas leak in under 10 minutes.** The goal is to improve on the response time which can be achieved with current methods. This is a key requirement, because the drone has no added value if its response speed falls short.
- **Operate beyond visual line of sight.** This requirement stems from the fact that a drone will reach the scene faster by air than ground transport. Rather than being taken to the scene by car, the drone must fly to the scene on its own. Thus it will need to traverse considerable distances, causing it to go beyond visual line of sight.
- **Measure concentrations of substances which lead to acute toxicity.** Acute toxicity is defined as the adverse effects of a substance that result either from a single exposure or from multiple exposures in a short period of time (typically less than 24 hours).
- **Estimate size of smoke or gas clouds.** This information is crucial when coordinating an emergency response, as it gives an indication of the affected area.
- **Determine direction of movement of smoke or gas clouds.** This helps response teams figure out where the cloud will be in X amount of time.
- **Loiter in the affected area for 15-30 minutes.** This should be sufficient time to acquire data about the affected zone.
- **Downlink location and observation data to ground station.**

Drones can also be used for close-proximity tracking of certain high priority targets. This is especially relevant on cloudy days, when the airships cannot perform their tasks. ITS functionality sets the following requirements on the drones:

- **Reach target within 10 minutes.** Here, the reasoning is that the NSS should improve on current capabilities of emergency response teams. For drones to be useful during pursuits and bust operations, they must arrive to the scene ASAP.
- **Operate beyond visual line of sight.** Rather than being taken to the scene by car, the drone must fly to the scene on its own. Thus it will need to traverse considerable distances, causing it to go beyond visual line of sight.
- **Loiter near target for 30 minutes.** In case the target must be tracked for a longer period of time, this may cause the drone to run out of power. If this happens, another drone will fly in and take over.
- **Take visual and IR images of target.** This will allow day and night operations.
- **Be stealthy.** The suspect being tracked must not become aware of the fact.
- **Downlink location and observation data to ground station.**

6.4.2. SENSOR SELECTION

This part deals with sensor selection for the drones. First, the most obvious choices: visual and IR cameras for day and night operations, GNSS for location and velocity determination, transmitters and receivers for communication. It is assumed that most drones have these sensors already built in; if necessary, payload capability can be allocated to carry additional sensors. Moreover, it is expected that the drones will require dedicated sensors for smoke and gas analysis. Three types of devices for the analysis of smoke and gas are considered here: electrochemical sensors, lasers, and hyperspectral cameras. Their pros and cons are summarised in Table 6.2.

Table 6.2: Pros and cons of smoke and gas analysis sensors

Sensor type	Pros	Cons
Electrochemical	Relatively inexpensive	- Limited number of target substances - 2-3 hr warm up time before use - Cross-sensitivities with extraneous chemicals
Laser absorption spectrometry	- Very little cross-sensitivity - Good tunability - Long lifetime	Optical interference near lower detection threshold
Hyperspectral	- Detailed spectral analysis of object - Possibility to recognise target markings	- High complexity - Needs development

An electrochemical sensor measures the concentration of a particular substance using an electrochemical cell. An electrochemical cell is a device capable of either generating electrical energy from chemical reactions or facilitating chemical reactions through the introduction of electrical energy. When a chemical reaction takes place, one can relate the voltage change to a concentration of the particular substance which the sensor is designed to detect.

Scentroid is a company which builds sensors for electrochemical analysis that can be carried by a drone. The drone has live monitoring of gasses and is also able to determine the temperature in plumes. Together with GNSS, the drone can make a 3D map of the gasses contained by the cloud.[3]

[3] http://scentroid.com/scentroid-sampling-drone/ [cited 14 June 2017]

The main advantage to electrochemical sensors is that they are relatively inexpensive. Scentroid offered us a quote for the 5 sensors listed in Table 6.3 – $9239, which includes on-board data handling, GPS, controller, mount to install sensor on drone, and a portable ground station; shipping and handling are also included.[4] On the downside, each chemical substance requires its own dedicated sensor to be detected, which severely limits the number of substances which can be detected by a single drone. Moreover, some sensors need to be powered on 2-3 hours (!) before they can begin measurements. This would pose a very strict constraint on operations. Another disadvantage to this measurement technique lies in cross-sensitivities: due to uncertainties which are inherent to chemical activity, the sensor may be sensitive to extraneous chemical compounds [46]. As a result, the detector may over- or underestimate toxin concentrations. This is a problem, as it may cause emergency response teams to over- or underestimate hazards.

Table 6.3: Scentroid electrochemical sensor specs

Sensor ID	Target gas species	Health effect	Sensor life [years]	Warm up time [min]	Response time [sec]
CM2	Carbon monoxide	- Mild exposure: lightheadedness, confusion, headache. - Large exposure: toxicity of the central nervous system and heart, and death	2	45	25
HCL1	Hydrogen chloride	- Inhalation: coughing, choking, inflammation of the nose, throat, and upper respiratory tract, and in severe cases, pulmonary edema, circulatory system failure, and death. - Skin contact: redness, pain, and severe skin burns. - Eye contact: severe burns to the eye and permanent eye damage.	1	120	200
HCY1	Hydrogen cyanide	Cyanide ion halts cellular respiration	1	120	120
HS2	Hydrogen sulfide	Everything – mostly nervous system	2	180	55
PD2	VOCs (e.g. isobutylene)	Release in air may cause asphyxiation	5	5	3

Alternatively, laser pulses can be used to analyse the chemical composition of substances – a technique known as laser absorption spectrometry (LAS) [47, 48]. This requires instrumentation to emit laser pulses with specific wavelengths and thereafter detect the reflected light. The received signal is then compared to reference signals to figure out the chemical make-up of the substance.

The advantage of using lasers is that there is very little cross-sensitivity with other gas species, which significantly reduces the occurrence of false alarms. Due to their good tunability and long lifetime (> 10,000 hours), most practical laser-based absorption spectroscopy is today performed by distributed feedback diode lasers emitting in the 760 nm – 16 μm range. This gives rise to systems that can run unattended for thousands of hours, with minimal maintenance.

A drawback to the LAS method is that there can be quite a large influence of optical noise, particularly at lower concentrations of the target substance. However, the larger the concentration compared to the detection threshold, the smaller the noise and the more reliable the reading of the device. This means that there is less of a risk of underestimating the concentration, so the problem of optical noise is only a minor issue.

Hyperspectral imagers have been discussed already for the stratospheric airship. Their advantage is that they can image objects in a whole range of wavelengths, allowing them to discern reflectance spectra and characterise the chemical composition of substances. Another advantage is that they would be able to recognise PC and QD target markings. A drawback to hyper-

[4] B. Bakhtari [personal communication, 14 June 2017]

spectral imagers is that they tend to be highly complex – arguably more than necessary for close-proximity drone applications. Moreover, hyperspectral cameras developed for drones are typically tailored for agricultural applications, so they would need development to better suit the NSS purposes.

6.4.3. AVAILABLE PLATFORMS

Below follows an overview of the current drone market available for the ITS or FSDS. Basic specifications are tabulated in Table 6.4. Response radii are based on 10 minutes' deployment time. The required number of drones assumes a 20% overlap in coverage areas.

TU Twente in cooperation with Saxion developed a drone to analyse composition of gas and smoke clouds in order to determine whether clouds hold toxins. This drone is currently used by RIVM and the Dutch Fire Department. No more information is known regarding the specifications of the drone. The only thing that is known about the drone, is that the drone works.

The AR100 is a quadcopter drone that has been developed by BAM, Federal Institute of Materials Research and Testing, and AirRobot GmbH & Co. The producer has developed an algorithm to estimate the size and expandature of the smoke cloud using video data, flight control data, GPS and measurements data from the gas sensors. The drone houses an on-board camera and gas sensors to analyse the gas clouds. The drone has been validated and tested in gas clouds produced by volcanoes.

The GasFinder2-UAV is a fixed wing UAV built by the company Boreal. The UAV houses both a camera for close observation (ground resolution 5- 10 m) and a gas detector relying on tunable diode laser absorption spectrometry. The data is sent back to the ground station using an antenna. The drone is delivered with a ground station and catapult system to launch it. The drone lands on a soft surface. Its maximum speed is 51 m/s.[1]

DJI is a company which developed the Matrice and Spreading Wings Series for industrial applications. The Matrice 600 Pro and Spreading Wings S1000+ have payload capacities which exceed that of most drones, at 6 and 11 kg respectively. Unfortunately, the battery life of these drones strongly limits their endurance.[2]

Aerialtronics offers a drone with in-built autonomy and adaptable payload options, including visual and IR imaging (2- and 3-axis gimbals included) as well as a sniffer/VOC monitor to detect hazardous materials. With an endurance of 30 minutes and a payload capacity of 2.9 kg, Aerialtronics's Altura Zenith ATX8 outperforms most drones currently on the market.[3]

The Aeryon Skyranger is well-suited for military and government applications. It offers 50 minutes of flight time up to 450 meters altitude (at which altitude it will be unnoticeable to the human eye and ear), with dual EO/IR high resolution cameras, advanced autonomy and network pairing for secure data transmission.[4]

Draganfly is preparing to bring a new drone to the market in 2017, the Tango2, which will carry battery packs bringing its endurance to an impressive 4 hours, with the ability to fly a wide range of modular payload systems. For now, however, only limited specifications are available.[5]

So far, only commercial drones were considered. For completeness, a military option is included as well. The Dutch Ministry of Defence is currently awaiting the delivery of MQ-9 Reaper drones. Although they are far more expensive than commercial solutions, with a unit cost of $17 million, these drones are worth considering for the NSS. Due to their high flight speed, any location in the Netherlands can be reached within 10 minutes using only 3 of these drones. Note that a system with fewer elements is per definition less complex. Add to that, an endurance of 14 hours would allow them to survey a host of targets for extended periods of time.

[1] http://www.boreal-laser.com/products/uav-based-gas-detector/ [cited 12 June 2017]
[2] http://store.dji.com/shop/industrial?from=menu_products [cited 12 June 2017]
[3] https://www.aerialtronics.com/altura-zenith-engels/payload-performance/ [cited 12 June 2017]
[4] https://www.aeryon.com/wpp/wp-content/files/brochures/Aeryon-SkyRanger-Brochure.pdf [cited 12 June 2017]
[5] https://www.draganfly.com/products/tango2/overview [cited 13 June 2017]

Table 6.4: Drone specifications

Drones	Endurance with payload [min]	Payload capacity [kg]	Max flight speed [m/s]	Estimated airborne response radius [km]	Estimated number of drones needed
AR100	30	0.2	-	-	-
GasFinder2-UAV	600 <TBC>	0.5	51	30.8	18
DJI Matrice 600 Pro	16	6	18	10.8	142
DJI S1000+	15	11	29	17.4	55
Altura Zenith ATX8	30	2.9	20	12	115
Aeryon SkyRanger	50	-	25	15	74
Draganfly Tango2	240	1.5	-	-	-
MQ-9 Reaper	840	1700	134	80.3	3

6.4.4. TRADE-OFF

A trade-off is performed based on the basic specifications given in Table 6.4. Right off the bat, some drones can be crossed out. Both DJI drones are eliminated as their endurance is insufficient. The Altura Zenith ATX8 is eliminated because its limited flight speed drives the number of drones to an unreasonable value. The AR100 is eliminated due to its limited endurance and the fact that its flight speed is unknown.

The Tango2 is not on the market yet, but the 4 hour endurance and 1.5 kg payload capacity seem promising. Its specifications should be looked into as soon as they become available.

The Reaper has such great capabilities that in fact it seems overqualified for the mission. A recommended approach would be to cooperate with the Ministry of Defense and request they keep a few of their drones on stand-by for tracking high priority targets.

The two drones which were deemed most suitable are the GasFinder2 and the Aeryon Skyranger (Figure 6.4). The GasFinder2 meets all requirements for FSDS. It is an off-the-shelf, fully integrated solution for chemical analysis, designed for industrial applications. 18 of these drones are needed. The sensor specifications look promising,[6,7] particularly when considering the advantages of the laser detection method (as discussed earlier). The Aeryon Skyranger meets all requirements for ITS. It already has built-in visual and IR cameras with good specifications and it was designed for surveillance missions.[8] 74 of these drones are needed.

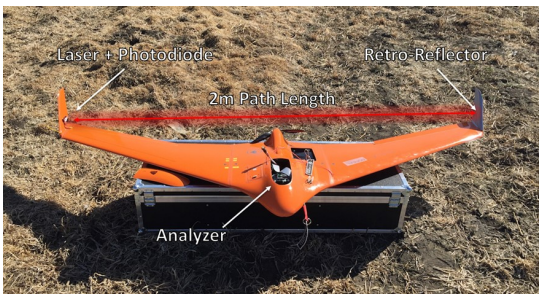

(a) Boreal GasFinder2-UAV (Edmonton, Alberta, Canada)

(b) Aeryon Skyranger (Waterloo, Ontario, Canada)

Figure 6.4: Selected drones

[6] http://www.boreal-laser.com/info-center/ [cited 21 June 2017]
[7] http://www.boreal-laser.com/products/uav-based-gas-detector/specifications/ [cited 21 June 2017]
[8] https://www.aeryon.com/wpp/wp-content/files/brochures/Aeryon-SkyRanger-Brochure.pdf [cited 21 June 2017]

6.5. ASSOCIATED RISKS

In this chapter additional elements of the NSS have been designed and discussed. These are an integral part of the system and naturally they also carry risks associated with them that might negatively affect the system. The ground stations are the bases where all data is gathered, all elements are controlled and all communications go through. For this reason it is vital to ensure that these stations are well protected and guarded from third parties. This will help reduce the risk of one of them being seized or destroyed, and thus affecting the system. Also power outages are not admissible in a system like NSS and so emergency power sources should be given to the stations to ensure the system can proceed with operations smoothly in case they occur. In the NSS, drones are used as short-term, high manoeuvrability platforms that can operate in case it is cloudy. For FSDS their main task is chemical analysis of smoke or gas which is usually done through electrochemical detection and carries inherent risks associated with it, like cross sensitivity in the analysis. This is tackled by using laser detection instead which greatly reduces this risk. Regarding ITS operations, one of the requirements was that the drones used should be stealthy and silent. It is expected that it will be virtually unnoticeable due to its 450 m service ceiling. However, if necessary, modifications could be made to the original design of the Aeryon Skyranger that would help reduce its visibility and noise created by the propellers.

6.6. CONCLUSION

From this chapter the following conclusions can be drawn. Firstly, mission control of the NSS will be located either near the airship ground base in the middle of the Netherlands, or near VenJ in Den Haag. VenJ must determine which of these two locations serves their needs best. Furthermore, there will be two ground stations to handle all the data. These ground stations will have multiple antennas, each pointing to a dedicated airship. The ground stations shall be highly secured to prevent individuals from dismantling activities of the NSS. The ground stations also need to have back-up power sources. Moreover, an airship ground base is needed, which consists of a mooring mast, two hangars and a launch pad. The ground base will be located in the centre of the Netherlands, such that it is easily accessible for all airships. As for the drones, they will be used as a back-up when it is cloudy or nighttime. The Boreal GasFinder2-UAV will be used in order to perform chemical analysis where it will have an endurance of 600 minutes (TBC). The Aeryon Skyranger drone will be used in order to identify and track targets. It has a loiter time of 50 minutes. Both drones are specifically designed for performing their respective tasks.

7 | System Description

The system description contains all system elements and describes their interaction. First a basic overview of the entire system will be given. Afterwards the observation strategy will be determined using a trade-off. At the end of this chapter couple of sections follow on system properties like cost, risk and sustainability.

7.1. System Breakdown

For the NSS, airships and drones will be used, as has been determined in the MTR [2]. In Figure 7.1 the system description of the NSS can be found. The figure shows that mission operations control everything, either directly or indirectly through the ground station. The ground station is the element that processes data, distributes it to relevant parties and sends commands to the airships. Maintenance is the location where airships and drones go to whenever there is something wrong with them or whenever they go for their periodic check-up.

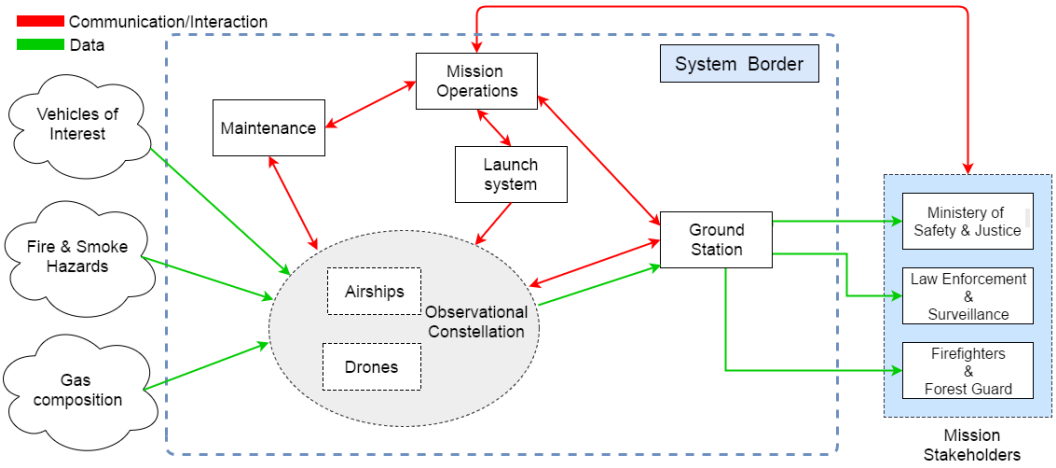

Figure 7.1: System description of the NSS

In the figure, one sees that there is a communication and interaction link between the stakeholders and the mission operations. If one of the stakeholders wants to change one of the requirements of the system or just wants the system to cover a different area, they should communicate it to the mission operations which will make sure that the system does what it needs to do. In Chapter 8, a more detailed description of the entire system will be given, especially how the system operates as a whole.

7.2. Number of Airships

When deciding on the amount of airships for the NSS, it must be assessed whether the entire Netherlands will be covered for the 100% constantly, or within a certain response time. Five different trade-off criteria were chosen:

Coverage The amount of coverage as a percentage of the Netherlands's surface area – which increases with the number of airships. This is an important criteria, as the total area covered should be as large as possible.

Response time The amount of time it takes for an airship to move to a target that is outside the FOV. This decreases with increasing number of airships.

Redundancy Meaning the ability for the NSS to operate efficiently in case of an airship failure without adding another element to the system.

Costs Related to the number of airships as well as the operational costs and maintenance costs.

Overlap The area that is covered by two or more different airships. Overlap is inefficient, as there is no direct use in covering the same area twice. A higher overlap, however, does indicates a higher redundancy, because when one airship fails some of its area is still covered by other airships.

To weigh the previously mentioned criteria the same trade-off method as described in the MTR will be used: the Analytic Hierarchy Process [2]. This resulted in the relative weights as seen in Table 7.1.

Table 7.1: Weights of the trade-off criteria

Criteria	Weight
Response time	8%
Redundancy	15%
Coverage	41%
Cost	31%
Overlap	5%

Using the previously obtained trade-off criteria and weights, the following three approaches will be evaluated.

Stationary A stationary system consists of airships that are stationary during nominal operations. Only during exceptional conditions the airships are relocated to another position nearby their nominal position. This type of operation will have 100 % coverage.

Medium manoeuvrability A system classified as medium manoeuvrability has a nominal position from which the airships are allowed to deviate to reach ground area uncovered by the system. The airships will remain within a certain distance of their nominal position. As a rule, the maximum response time for the system has been set at 5 minutes in this case.

High manoeuvrability A high manoeuvrability system is allowed to deviate further from its nominal position, covering more ground. Airships used in this option must provide higher thrust levels to increase their airspeed to reach the uncovered grounds. This classification has a maximum response time of 10 minutes.

The coverage percentage and overlap will be evaluated based on the number of airships and the coverage radius of a single airship, which was determined to be 34 km as determined in Section 3.4. It was found that number of airships required for stationary, high manoeuvrability and medium manoeuvrability are 15, 11 and 13 respectively. Costs are directly linked to the total number of airships required. Although the cost of a single airship might go down when multiple are bought, this will not be taken into account as the price of an airship itself is still unclear, let alone bulk discount. The number of airships also influences redundancy. Table 7.2 presents the results from the trade-off. Therefrom it can be seen that the best scoring operational mode is the stationary mode. It was found that movable airships do not significantly reduce the required airships, decreasing its potential advantage on cost over the stationary case. With respect to the requirements, the stationary case fulfils them best as well.

Table 7.2: System operational procedure trade-off table

System operations		Criteria											
		Response time		Redundancy		Coverage		Cost		Overlap		Final Score
Operation modes	Stationary	8%	Excellent	15%	Excellent	41%	Excellent	31%	Good	5%	Good	
		10	0 minutes	***10***	Most redundant	***10***	100% coverage	***6***	15 units	***4,8***	21%	***8,5***
	Medium Manoeuvrability	8%	Good	15%	Good	41%	Good	31%	Good	5%	Good	
		5	5 minutes	***5***	Moderately redundant	***9,5***	90% coverage, 96% reachable	***8***	13 units	***6,6***	15%	***7,9***
	High Manoeuvrability	8%	Acceptable	15%	Acceptable	41%	Acceptable	31%	Good	5%	Good	
		0	10 minutes	***0***	Least redundant	***8,5***	80% coverage, 90% reachable	***10***	11 units	***10***	10%	***7,1***

Excellent: exceeds requirements	Acceptable: correctable deficiencies
Good: meets requirements	Unacceptable: major deficiencies

It can be concluded that there is a need for 15 airships in operation at all times to achieve near 100 % coverage. However since the airships need to be maintained every year an additional airship is required such that during maintenance of one airship there will still be 15 operational. The 16th ship can potentially be used in case of an emergency. Figure 7.2 shows the proposed distribution for the 15 airships.

Here the blue circles represent the field of view of each of the airships. Intersecting FOV is represented with a darker shade of blue. The nominal position for each airship is represented with a blue dot inside the FOV circle. Each FOV area has a diameter of 68 km, covering close to 3650 km² of surface area. It is important to note the difficulty in achieving 100% full coverage due to the irregular shape of the Netherlands. For this same reason it is inevitable to have areas of redundancy where two or more fields of view intersect. The airship distribution shown before tries to achieve maximum coverage possible using the least amount of airships, while keeping the redundant zones located in high density areas. This resulted in a final number of 15 airships covering 99% of the Netherlands' area at all times. To achieve the full 100% coverage more airships are needed which will have a large overlap with the 15 proposed airships, i.e.: the added airships will have a large redundancy but low efficiency. Therefore using more airships than 15 at a time is not considered cost effective.

7.3. COST BREAKDOWN

A cost estimation has to be made to estimate the total costs of the project. It has been decided that 15 airships are used with two ground stations and one airship on the ground to substitute with the one that has to undergo maintenance. Here the cost of one airship will be estimated using Table 7.3. Afterwards, the cost of different other elements will be estimated, such as the ground station itself.

7.3.1. COST OF AIRSHIP

In Table 7.3, the cost estimation for the Hale-D20 is given with its own values for the different components of the airship as well as the specific costs for those components. For the NSS, the Thales Stratobus will be used, which has a length of 115 m and a maximum diameter of 34 m, as mentioned before. Since no explicit values are known for any of the components/properties in the figure for the Stratobus, they have to be estimated. The envelope is estimated by an ellipse, which

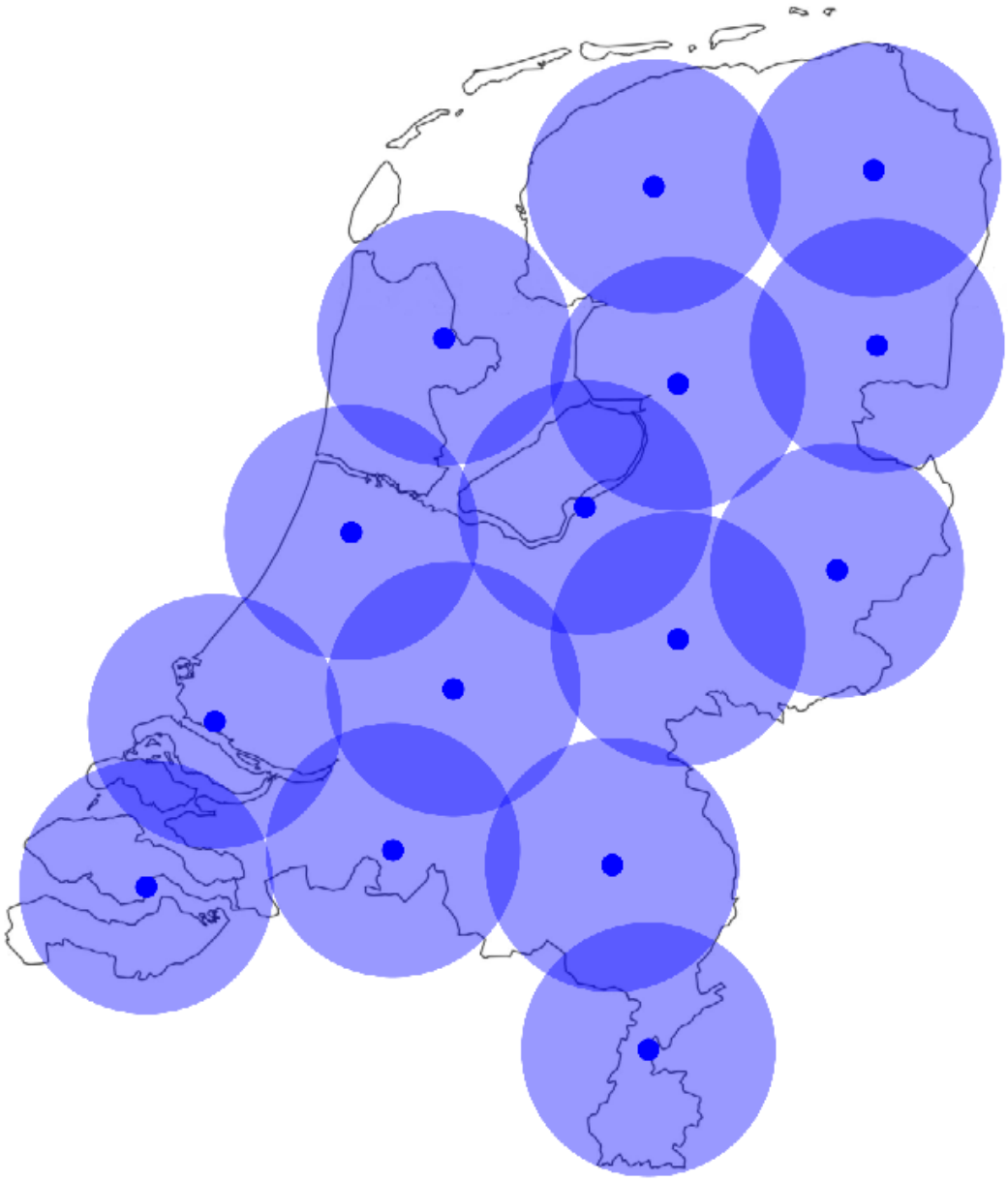

Figure 7.2: Proposed stationary airship distribution

goes to the points (x, y) = (-115/2, 0), (0, 17) and (115/2, 0), see Figure 7.3.

The formula for an ellipse is given in Equation 7.3.1.

$$\frac{x^2}{a^2} + \frac{y^2}{b^2} = 1 \tag{7.3.1}$$

Here a and b are the value for the semi-major axis and the semi-minor axis, respectively. In case of the Stratobus, the values for a and b will be 57.5 and 17, respectively. In Figure 7.3, the function is also mirrored around the x-axis. By now turning the graph around the x-axis, the area of the envelope can be calculated. For this, Equation 7.3.2 is used.

$$\int_{x_1}^{x_2} 2\pi f(x)\sqrt{1+\left(f'(x)\right)^2}\,dx \tag{7.3.2}$$

where $f(x)$ is the function, $f'(x)$ is the first derivative of the function and x_1 and x_2 are the lower

Table 7.3: Typical costs for a Lindstrand D20 airship

ITEM	VALUE	UNIT COST	TOTAL
Envelope	20,000m²	$250/ m²	**$5 million**
Fins	1,000kg	$1000/ kg	**$1 million**
Flight Controls	Unit	-	**$1.5 million**
Propulsion	46kW	$50,000/ kW	**$2.3 million**
Solar Array	300kW	$10,000/ kW	**$3 million**
Fuel Cell	150kW	$30,000/kW	**$4.5 million**
Electrolyser	180kW	$15,000/ kW	**$2.7 million**
		SUB TOTAL	**$20 million**
Flight Operations	Package		
System Integration	Package		**$2 million**
Ground Support	Package		
Programme Management	Package		
		GRAND TOTAL	**$22 million**

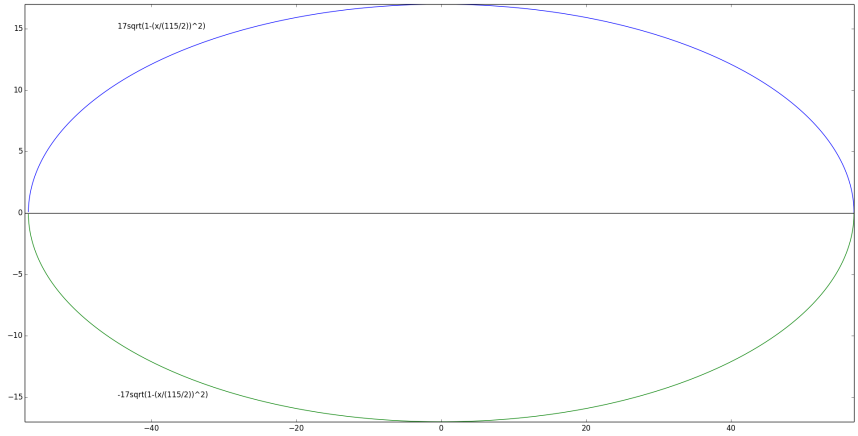

Figure 7.3: Assumed curve of the airship

and upper limit respectively. Here x_1 and x_2 are taken to be -115/2 and 115/2, respectively. It is then found that the envelope is 9985 m^2. Now the other components have to be estimated in size. In Table 7.3, flight controls is assumed to be €1.5M in total. For the Stratobus, it is assumed that this is also approximately €1.5M as it is assumed to be independent on the size or mass of the airship. The same holds for the flight operations, system integration, ground segment and programme management, which will be assumed to cost €2M. However, contingencies are added to have a feeling of how much the cost could vary from the calculated value. For the envelope, a contingency of 5% is taken, as this is approximated very well. The components that cost €2M in total (last four in the table) have a contingency of 50%. This is quite large, but still it is done, because the NSS is a very complex system with a lot of ground antennas. Since the system operates at a high level of difficulty, the on board computers need a lot of coding and therefore programme management could cost more than is estimated right now. Therefore a contingency of 50% is chosen for these four components. The flight controls have a contingency of 10% as well. The rest of all the components have a contingency 10% as well, since it is assumed that these components are very much related to the mass of the airship itself. The rest of the components will also be estimated using mass ratios: the mass of the Stratobus and the Hale-D20 is known, therefore a mass ratio can be calculated and this one will be multiplied by the value given in the figure. In Table 7.4 a

clear overview is found of the different components with its costs as well as the contingency that is used. On the bottom, an estimation of the cost for a single airship is shown.

Table 7.4: Cost estimation for the Stratobus

Component	Value	Price	Contingency	Cost [M$]	Contingency [M$]
Envelope	9985	$\$250/m^2$	5 %	2.5	0.125
Flight controls	Unit	$1.5M	10 %	1.5	0.15
Fins	501 kg	$1,000/kg	10 %	0.5	0.05
Propulsion	23.05 kW	$50,000/kW	10 %	1.15	0.115
Solar Array	150 kW	$10,000/kW	10 %	1.5	0.15
Fuel cell	75 kW	$30,000/kW	10 %	2.25	0.225
Electrolyser	90 kW	$15,000/kW	10 %	1.35	0.135
Flight operations	-	Unit	50%	2	1
System integration					
Ground segment					
Programme management					
Total				12.75	1.95

The cost estimation for a single Stratobus airship is approximated at €11.45M, with a contingency of almost €1.8M. Besides the airship, a lot of other elements are also needed for the system to operate, such as a ground station, where part of the receiver antennas are located, a mission control location and the launch and maintenance location as well.

7.3.2. COST OF MAINTENANCE BASE

The maintenance base will consists of a launch pad, two hangars (90x45x135 m) and two portable mooring masts as explained in Section 6.3. Using the most recent construction of a hangar (360x 210x107 m) for airships by Cargolifter AG in 2002, a cost estimation can be performed for the hangar of the Stratobus. The hangar of Cargolifter cost 110 million dollars in 2002 and was supposedle a factory, office and maintenance base.[1] Using an inflation of the 35.92 % throughout the period 2002-2017, assuming the same costs per cubic meter and a dollar-euro exchange rate of 0.895, the following calculation can be performed to calculate the costs of the hangar:[2]

$$\text{Cost Hangar (euros)} = \frac{\text{Volume NSS}}{\text{Volume Cargolifter}} \cdot \text{inflation} \cdot \text{Cost Cargolifter Hangar} \cdot \text{exchange rate} \tag{7.3.3}$$

Using Equation 7.3.3 the hangar costs will be €8.7 million. Asphalt is also needed for the launch pad of the balloon. Using €20 per square meters asphalt and 130 meter radius, the launch pad will cost about €1 million.

In order to transport the airship to its hangar, a portable mooring mast should be bought or designed. The Goodyear Blimp uses a Mack Granite as a portable mooring mast, however no information is given about its costs.[3] It is estimated that two trucks will be needed and they will cost 1 million euro each.

To finalise the costs of the maintenance base, Table 7.5 has been composed displaying the different elements and the total costs. It must be said that these costs are just for the first elements of the maintenance base and more costs will be added during the next phase of the project.

[1] https://www.forbes.com/forbes/2002/0429/042.html [cited 12 June 2017]
[2] http://www.in2013dollars.com/2002-dollars-in-2017 [cited 12 June 2017]
[3] http://www.overdriveonline.com/photos-modified-mack-granite-mast-truck-moors-new-goodyear-blimp/[cited 12 June 2017]

Table 7.5: Cost estimation of the maintenance base

Element	**Costs (M€)**
Hangar	8.7
Portable mooring mast	2
Asphalt	1
Total	11.7

7.3.3. CONTROL ELEMENTS

The control element consists of several parts:

1. **Ground Station**
   This part ensures communication between ground and airship is performed.
2. **Mission control**
   From here, commands for the airships are determined and transferred to the ground stations.
3. **Workforce**
   The crew is responsible for operating the airships and deciding where the drone are going to be used.

Determining the cost of each individual part is necessary to get an idea how each part is related in the control element. The ground station and mission control centre, also known as ground element, can be estimated by multiplying the cost of a satellite (in this case an airship) and a certain constant, in this case 0.066. NSS would need two antenna ground stations and one mission control centre. The mission control centre would preferably at the hangar base. The relation is proposed by SMAD and can be found in equation 7.3.4 [45].

$$\text{Cost ground element} = \text{Cost airship} \cdot 0.066 \tag{7.3.4}$$

Filling in 12.75 million euros results in a single ground station and mission control that woulds cost 841500 euros. Two ground stations and a single mission control centre would be estimated at 1.7 million euros.

The mission control centre and maintenance base need to be operated by people in order to have a working system. It is assumed that 100 contractors are used for maintenance and operability and that 50 people of the ministry work directly with NSS. Next to that, assuming that they have 20 vacation days, earn 50 euros an hour on average and work 8 hours a week, the total cost to run NSS one year is 13.7 million euros. In Table 7.6, a small summary can be found.

Table 7.6: Cost estimation of the control element

Element	**Costs (M€)**
Ground & mission	1.7
Workforce	13.7

7.3.4. COST OF DRONES

Cost estimation of the drones has to be done as well. In Chapter 6 it is discussed which drones are going to be used and how many of each. The conclusion was drawn that the GasFinder20-UAV will be used for the FSDS whenever the airships are unable to see anything (at night and when it is cloudy) and the Aeryon Skyranger will be used for the ITS, of which 18 and 74 are needed, respectively.

It is hard to find the cost of such drones, since most companies simply do not show the costs on their website. One has to call the company, either to ask for that information or one has to show interest in the product and has to be already wanting to buy such a drone. Therefore, a rough

estimation has to be done. It was found that the DJI Matrice 600 Pro costs around €5,000. [4] In order to come up with a relatively accurate estimation, the different parameters of each drone has to be compared such that a cost estimation of the other drones could be done. As can be seen in Table 6.4, the DJI Matrice 600 Pro drone has an endurance of only 16 mins and the GasFinder2-UAV has an endurance of 600 mins. However, the Matrice can carry a payload which is 12 times as large. The GasFinder2 could reach higher speeds then again. That is why the GasFinder2 has to be more expensive than the Matrice 600 Pro. The same holds for the Aeryon SkyRanger: it should also be more expensive than the Matrice 600 Pro due to the same reasons.

Up to this moment, not many UAV cost estimation methods are present, therefore it will be done using ratios of the different specifications the drones have. It will be assumed that the cost relates linearly to endurance, payload capacity, flight speed and response radius, which are the specifications present in Table 6.4. When comparing the Matrice 600 Pro with one of the other drones, the ratios of these specifications are multiplied by each other and also multiplied by the cost. This way a rough estimate of the drone is obtained. The cost estimations for the GasFinder2 and the Aeryon SkyRanger can be found in Table 7.7.

Table 7.7: Cost estimation of the drones

Unit	**Cost [k€]**	**Contingency [%]**	**Total cost [M€]**
GasFinder2	112	10	1.98 ± 0.2
Aeryon Skyranger	27	10	1.98 ± 0.2

In the table it is found that the GasFinder2 UAV is estimated to cost approximately €112,000 and the Aeryon SkyRanger will be €27,000. In the table one could also see that there is contingency added, this is to account for made errors during the calculation, because not all parameters relate linearly to the cost of the drone. The total cost plus contingency can be found in the last column.

7.3.5. COST OF THE PAYLOAD

The cost of the payload is also an important contributor to the total costs. The payload consist of 4 different cameras of which 3 need an ADCS system, which is quite costly. The payload has 4 different colour imagers, such that each colour imager only has to scan one quadrant of the total FOV of one airship, which makes it more likely to meet the time constraint. The ADCS system for one of these cameras costs $180,000. The Hyperion camera needs an ADCS system that costs $300,000 and IRIS's ADCS system will cost $200,000. The cost of the camera in itself is hard to find, but it is assumed that the price of an IMAX camera should be close to the Hyperion and the other type of cameras that are on the payload bay. An IMAX camera costs $500,000.[5] To get to the same order of magnitude for the cost of the camera, it is assumed that the camera itself, without stabilisation, costs the same as the ADCS, with a contingency of 40%. In Table 7.8 the cost of the camera itself can be found.

Table 7.8: Cost estimation of the camera apertures

Camera	**Cost [$]**
CI	180,000
Hyperion	300,000
IRIS	200,000

In Table 7.9, the estimated cost of the cameras can be found, including the ADCS and contingencies which are added, since not much is found about either of these cameras.

[4] https://www.kamera-express.nl/product/122067692/dji-matrice-600-m600-/?channable=e13909.MTIyMDY3Njky&gclid=CjwKEAjwsqjKBRDtwOSjs6GTgmASJACRbI3fHhxI1Ev6guUGUcWzvDA7_uvozDRTp6WO2fpaHC-_ChoChkXw_wcB [cited 21 June 2017]

[5] https://www.premiumbeat.com/blog/you-cant-afford-this-expensive-hollywood-camera-gear/ [cited 22 June 2017]

Table 7.9: Cost estimation of the payload

Camera	ADCS cost	Unit Cost [$]	Count	Contingency	Total cost [k$]
CI	180,000	180,000	4	40 %	1440 ± 288
Hyperion	300,000	300,000	1	40 %	600 ± 120
IRIS	200,000	200,000	1	40 %	400 ± 80
AMS	-			40 %	600 ± 120
Total	-				3040 ± 608

Note that the contingencies in Table 7.9 only apply to the camera itself, without the ADCS. The price of the ADCS is known with a high certainty, so no contingency is added here. The price of the AMS wildfire is not known, therefore it is assumed that the cost of this camera is approximately equal to most expensive camera for the ITS. Then, the payload is going to cost a total of €2.7M per airship.

7.3.6. CONCLUSION COST BREAKDOWN

The costs found for NSS can best be displayed in a table. From Table 7.10, it can be seen that a fully working National Safety System would cost 270 million euros to have the system for the first five years and 13.7 million euros every year to have a competent workforce. The first 5 years is chosen since to much is known about airships for Thales have refused give that information.

Table 7.10: Cost breakdown summary

Element	Costs (M €)
16 Airship	184 ± 46
Maintenance Base	11.7 ± 2.9
Ground element	1.7 ± 0.4
Drones	4.9 ± 1.3
Payload	43.2 ± 10.8
Development	25 ± 6.3
Subtotal	270 ± 68
Workforce yearly	13.7 ± 3.5

7.4. NSS SUSTAINABILITY

An important aspect of the NSS is sustainability. With the Paris climate agreement sustainable engineering becomes even more important if mankind wants to reach the goals posed there. The NSS is no exception, especially as a governmental service. Sustainability does not only mean looking after the environment, but looking after society and economics as well. The first thing that comes to mind when thinking about sustainability, is the environmental aspect of it. The NSS has been designed to take environmental sustainability into account. Several decisions that have been made during the NSS design directly influence environmental sustainability.

One of these decisions is the choice to use hydrogen as a lifting gas instead of helium. Although helium is incombustible, it is also much scarcer on Earth. Additionally, helium is created naturally at very slow rates classifying it as a non-renewable resource. When helium escapes it flies to the highest parts of the atmosphere where it is blown away by the solar winds. Hydrogen can be created by steam reforming natural gas or by electrolysis of water. Electrolysis can be considered a renewable and sustainable method of generating hydrogen [49]. Although hydrogen is highly flammable, its use poses no environmental risks. Since it can be created at the same rate as it is used, hydrogen is renewable. The hydrogen that is used in the balloon to generate lift has as added advantage that it can be used to generate electricity by using fuel cells during the night. If helium would have been used, dedicated batteries would be required.

The energy generation onboard of the airships is done by solar cells during daytime and the fuel cells during the night. The use of an electrical propulsion system is the most obvious and most

sustainable choice. The energy for the propulsion is generated in a sustainable way. A more in depth discussion on the propulsion system was found in Section 5.4.

To reduce the environmental effect of the NSS care should be taken to create all parts as close to the Netherlands as possible. The further it has to travel to reach the Netherlands, to more energy is required during transport and the more greenhouse gasses are produced. Since many parts of the NSS come from different countries like Canada, France, and the US efforts should be made to reduce transport cost and emissions. Globally the CO_2 emissions of the transport sector were 22.9% in 2007, so reducing the distance elements have to travel will reduce the environmental impact of the NSS [50].

The decision to track targets using quantum dots poses potential risks to human health and the environment. To create these quantum dots, heavy metals like cadmium are used [51]. Humans can breathe cadmium containing particles or ingest it with their food and drinks. Some crops, like wheat, can accumulate cadmium from polluted soil. Accidental acute intake of cadmium is rare, but has clear symptoms. When exposed in lower doses for long amounts of time health effects are less easy to identify. When manufacturing cadmium compounds in the twentieth century, workers were contaminated by the inhaled cadmium increasing the likelihood of lung cancer. The role of cadmium as a co-carcinogen is generally acknowledged as it is supported by biochemical data [52]. This should be taken into account for the systems effect on health and the environment. Quantum dots are being developed without cadmium that should mitigate the risks related to cadmium based quantum dots.[6]

The FSDS and ITS payloads of the NSS enable the monitoring of the Netherlands, resulting in the early detection of fire and smoke and tracking of criminal suspects. This has the potential to decrease the effect of fires and criminal misuse, like dumping garbage from drug labs, on the environment. A reduce in crime rate will also have a positive effect on society and the economy.

[6] http://www.nanocotechnologies.com/what-we-do/products/cadmium-free-quantum-dots [Cited 23 June 2017]

8 | Operations

Now that a complete description of the payload and platform has been given, it is time to show how all the elements of the NSS will function and interact with each other as a complete system. This will be shown in the nominal operations section where several flow charts will guide through each step of the system's functions. Unfortunately sometimes (or most of the times) circumstances are not exactly as predicted and the system needs to be ready to deal with them. The numerous risks that the NSS might face are tackled in the back-up plan section where another flow chart will show how the procedures of different elements when faced with unexpected circumstances. This is followed up by a discussion on the maintenance required for the system and in the end, the overall risks and the risk mitigation strategy used in the design of the NSS are shown.

8.1. Nominal Operations

Nominal operations for the entire NSS are presented in this section. The nominal operation plan covers all elements present in the NSS. Nominal operations are considered when it is cloudy and nigh-time too. Non-nominal, also known as back-up plan, is considered when onf of the systems fail. In this section there are two subsections which will delve more into operations of each element, these will be presented by operational goal (FSDS and ITS). However, before considering the specific operations of each of these segments the function of the system as a whole will be discussed.

The primary operational mode involves airships and drones. Airships have obvious limitations, such as being obstructed by clouds or having limited operational capabilities during night which justifies the need for drones. Therefore, it is important to consider which element fulfils which task during specific conditions, this is presented in Table 8.1 and also includes the the task number which represents a block within the functional flow diagram presented in Figure 8.1.

The functional flow diagram of the entire NSS system, as seen in Figure 8.1, shows that the entire system has been subdivided into five main system operations as indicated with SYS-X. The system will first check whether it has contact with all system elements, and when there is a discrepancy appropriate action should be taken (SYS-1). This will be discussed together with non-nominal, or so called back-up operations (SYS-2) in Section 8.2. If both the contact and status reports are correct, the nominal operations will be initiated. This will first start by checking which system will perform which task depending on the presence of clouds or nighttime. These are separated by function, being FSDS (SYS-3) and ITS (SYS-4), and will be discussed in Sections 8.1.1 and 8.1.2 respectively. The final system element is concerned with the gathering of all data and then distributing it to the relevant stakeholders (SYS-5).

Table 8.1: Nominal operations per system element

	FSDS / SYS-3			**ITS / SYS-4**
	Fire detection	**Smoke tracking**	**Chemical analysis**	**Target tracking**
Daylight	Airship / FSDS-1	Airship / FSDS-3	Airships / FSDS-2	Airships / ITS-1
Night	Airship / FSDS-1	Drone / FSDS-5	Drone / FSDS-4	Airships / ITS-2 (Only high priority)
Overcast	None	Drones / FSDS-5	Drone / FSDS-4	Drone / ITS-3 (Only high priority)

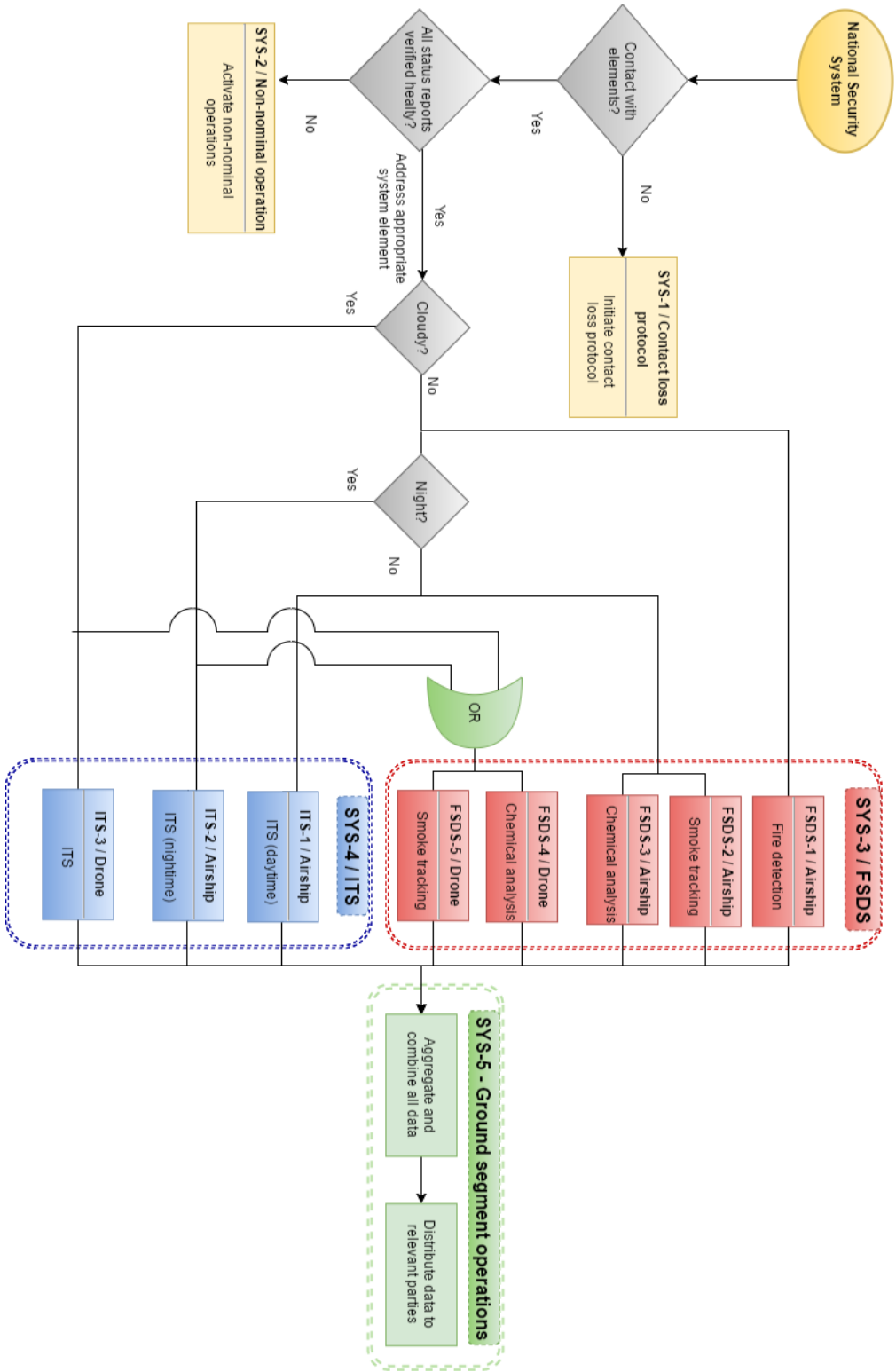

Figure 8.1: Nominal NSS operations flow diagram

8.1.1. FSDS PROCEDURES

This section discusses the nominal FSDS operational procedures, or SYS-3. Cloudy weather conditions and night time make operations more difficult. Since both of these aforementioned conditions happen quite often in the Netherlands the nominal FSDS operations have to cope with their occurrences. The decision of which element will be activated has been made previously by the overall system. This section will delve more into the operations of each separate element. Figure 8.2 shows the operational flow diagram for each element, they are separated in the same 5 main tasks as indicated in the overall system flow diagram and have a specific name indicated with FSDS-X and refer back to Figure 8.1 within SYS-3. First the FSDS procedure for the airship will be discussed after which the drone operation will be discussed, these are indicated with FSDS-A or FSDS-D meaning airship and drone operations respectively.

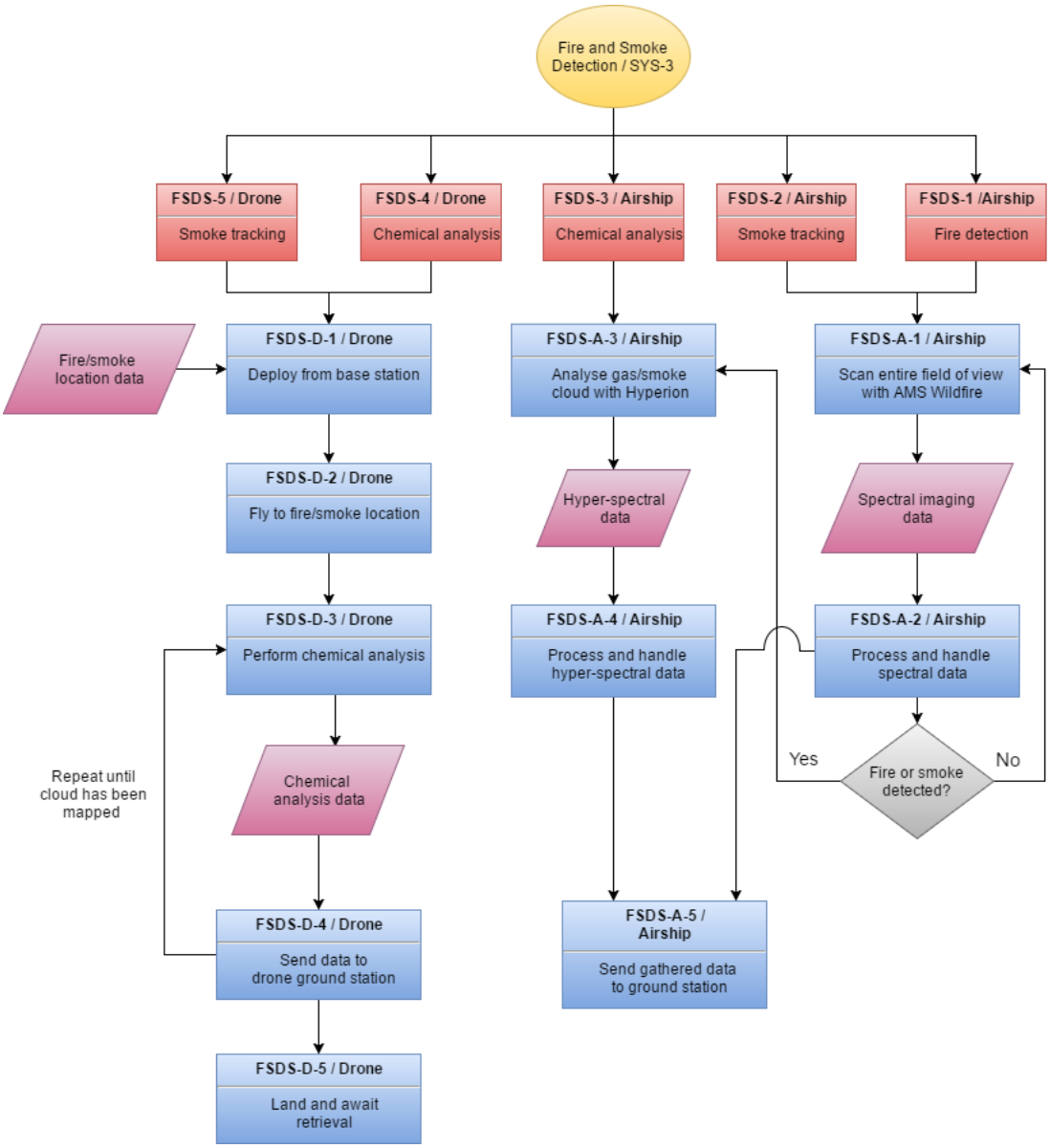

Figure 8.2: Nominal FSDS operational flow diagram (SYS-3)

One can see from the figure that for the airship both the smoke tracking and fire detection require the same procedure. Both these procedures use the same equipment, being the AMS Wildfire. However these two are separated as inputs since the fire detection is still possible during night, but the smoke tracking and chemical analysis are limited and thus will be done by means of the

drone (FSDS-4/5). Once the airship has identified fire, it will give instructions to perform chemical analysis on it. This function is handled by the airship itself (FSDS-3) during the day, and during night by a drone which will also map the cloud (FSDS-4/5). All three airship operations end in sending data to the ground station, which will be further handled by the ground segment (SYS-5). The system can use the data from the airships combined with wind speed data to predict the spread of the smoke or gas cloud. These predictions are done on the ground by computer programs and will be updated with the latest information from the airships.

The drone operations (FSDS-4/5), much like the airship operations, are also combined as they are being performed through the same procedures. As indicated by Figure 8.1 the FSDS drone will be used when it's either cloudy or night. Once the drone gets a signal, either straight from the fire department or from the airship, it will be deployed from the base station. When it arrives at the location it will determine the composition and the size of the cloud which will be directly sent to the fire department. After this it will land and await for pick up by the fire department.

8.1.2. ITS PROCEDURES

This section elaborates upon the nominal ITS operations. Similar to the FSDS, cloudy weather and night time make the operations of the system harder. These conditions are present in the nominal ITS operation plan, and are discussed after the clear skies condition.

The nominal ITS operation is described in a flow diagram in Figure 8.3 and describes SYS-4 in detail. For a target to be tracked it should first be marked by the stakeholder (ITS-S-1). Applying panchromatic paint is more difficult than painting the target with quantum dots. Quantum dots could just be sprayed on a car, whereas the panchromatic paint has to be painted manually and it therefore has to be made sure that there is no changes in paint thickness on the roof, neither should there be a difference in colour. The colour and location of the target should be provided to the system (ITS-S-2). This would allow the system to confirm that the target can be detected and compare the given mark with the actual measurements such that its unique identifier can be recognised, although this confirmation would not be required and could be done at a later stage. When it is not cloudy or night, the system scans the area for potential targets (ITS-1-1). It does this using the CI and identifies the potential targets based on the input colours. Once it has identified the potential targets, the system will check whether a potential target is actually a marked target (ITS-1-2). This will be done using the CHSI, or Hyperion, which is able to identify the mark, be it QDs or PC. If a potential target is not marked, it will look at the next potential target. If the target is marked, it will update and store the location of the marked object (ITS-1-3). By means of data processing the velocity and direction of the target can be inferred. By knowing where it is, which direction it is travelling and its speed, the area required to be searched for the upcoming update will be smaller (ITS-1-4). Once the data has been processed it will be sent down to the ground station (ITS-A-1) and from there distributed to relevant parties (SYS-5).

When operating the ITS at night, different tactics have to be applied. QDs and PC require light to detect them, which is insufficiently available at night. Therefore, both the panchromatic and quantum dot detection mechanisms do not work. The colour imager also has limited use during night operations, thus an additional imager is put on the airship which is dedicated to nighttime operations (ITS-2). This imager images in the MWIR allowing it to see at night. Only an individual target can be tracked. Then if you know where your target was, you can see it move in the MWIR image knowing where the target is going. This camera can be manually controlled so a target can be followed with more ease, although limiting the number of targets tracked at any given time.

During overcast weather conditions the airships cannot perform the ITS tasks. To make sure target tracking is not halted, drones are integrated in the ITS operational system. The ITS drones are capable of tracking a single target per drone. The drones will do this only when a high priority target has to be tracked during cloudy weather conditions or night conditions if the airships cannot fulfil the tracking on their own (ITS-3). With drone operations, there comes a higher risk of the target detecting that it is tracked than when solely using airships. These drones are equipped with a visible light and TIR camera to track targets during day and night. If a target has to be tracked using a drone, then this procedure has to be initiated manually. A human operator controls the drone

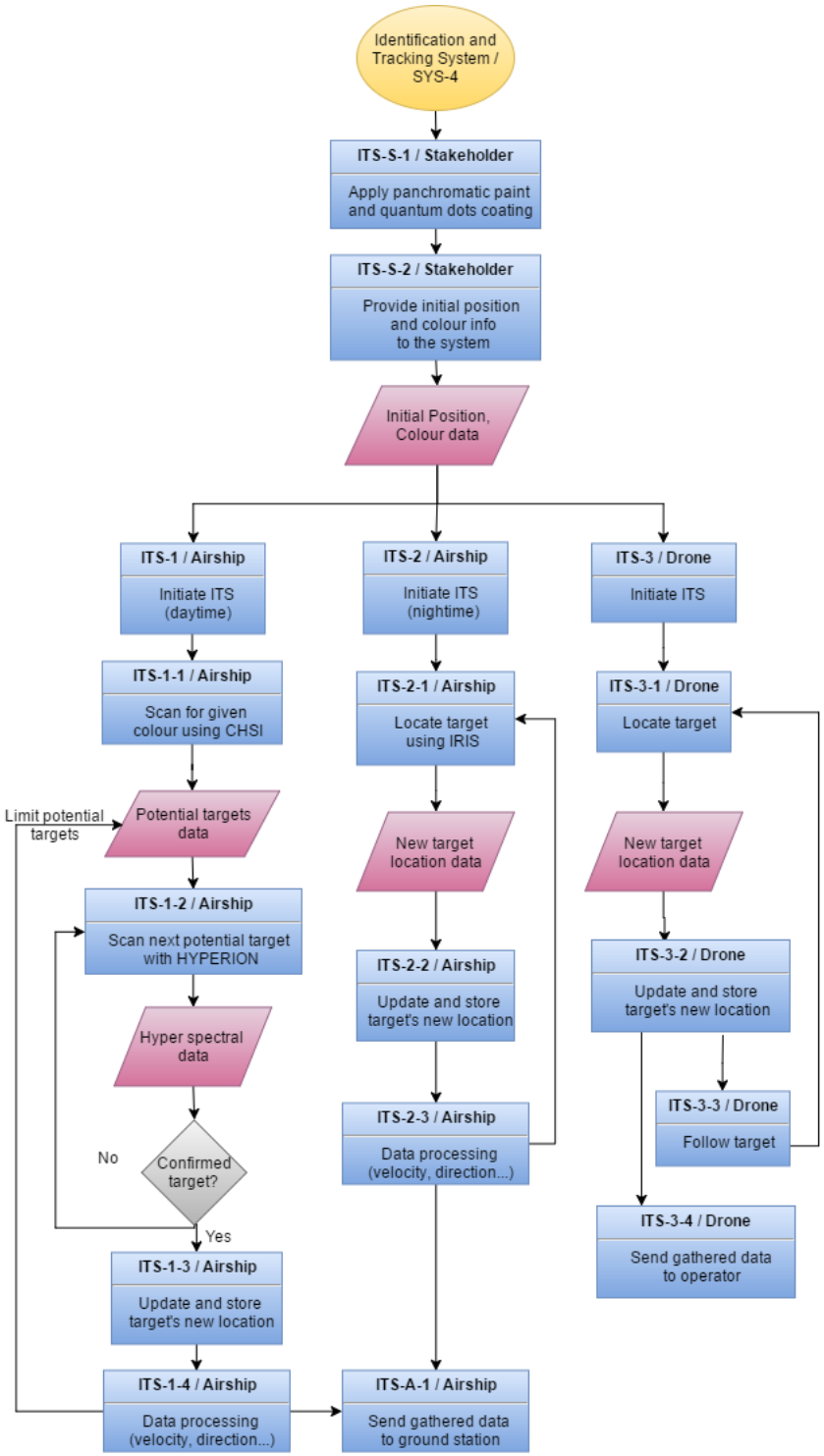

Figure 8.3: Nominal ITS operational flow diagram (SYS-4)

when it is tracking its target. After operations, it will return to its base which can be at a police station.

Since the airship cannot perform any ITS task when it is overcast it can perform a data dump, sending large amounts of data to the ground station.

8.1.3. GROUND OPERATIONS

The ground operations cover the final segment (SYS-5), as shown in Figure 8.1. The ground stations (see Section 6.2) play an important role in the ground operations as well. These elements receive data from the airships and send commands to the airship. Figure 7.1 shows the system description. The ground station receives information and sends this information to institutes and departments that want to receive this information. These are the fire department, the ministry of Security and Justice and law enforcement departments such as the police. In Section 6.1 mission control is discussed, which is the location at which important decisions are made. Signals are sent from mission control to the ground station, which in turn sends the commands to the airships. Data transmission can be done 24/7. All data collected by the airship is saved on board before it is sent down. Once the ground station receives the data, the data on the airship is overwritten to reduce the total required storage capacity. The way these commands are send are as follows. If it is a command for a specified airship, it is first send to the ground station which controls the airship which relays it to the airship. In case of a manual override the operator has to indicate in which area it wants to look, then the system automatically connects the manual controller with the airship in that area. If a target that is being tracked leaves the line of sight of the airship, the system will automatically switch to an airship that has a sight line on the target. If the target leaves the entire system FOV by entering an area uncovered by the system, the system relays this information to the operator.

8.2. BACK-UP OPERATION PLAN

In a system like the NSS there is a great deal of issues that might arise and compromise its normal functioning. Since it is impossible to predict these occurrences, it is important to have a system able to operate regardless of these events, either by introducing redundancies or being prepared for said occurrences. The back-up operation plan comes into play whenever some unexpected instances occur, whether it is the loss of an airship, malfunction or loss of contact with any of the NSS elements. This section will deal with the mitigation strategies for such risks and with the standard procedures of the system in case it is not able to procced with nominal operations.

Figure 8.4 shows the procedure the system takes if one of its elements is not able to proceed with nominal operations. Both airships and drones are able to generate status reports for their subsystems that are used to assess their performance and if they even are operational. If the reports come with any anomalies a 'safe mode' is activated for that element (F.S.2-A for airships and F.S.2-D for drones). The airship will start by checking whether it is in its correct position since this is of major importance for the system (during nominal operations the airship is constantly being tracked by the ground station but in case of a communications malfunction this needs to be checked by the airship itself). In case of a negative output the propulsion system is activated (F.S.2-A-P.1) and the airship tried to relocate to its correct position (F.S.2-A-P.2). It does this continuously for two hours and in case the target position has not been reached the airship assumes that is being drifted away by strong wings and tries to minimise the drift (F.S.2-A -P.4) and also sends health reports to the ground station (F.S.2-A-P.5). If this process goes on for longer than 12 hours the airship automatically initiates descent for maintenance (F.S.2-A-P.5). The procedures for drones are relatively simple because it can always be substituted by a new one. The drone sends its 'unhealthy' report to the ground station (F.S.2-D.1) and returns to the deployment centre(F.S.2-D.2). The ground station can then send a a new drone to perform the desired operations.

CONTACT LOSS

Contact loss with one of the NSS elements can be almost as severe as losing that element. Not communicating with one of the airships means that no data is being received from it, which is pretty much the same as not having the airship, in terms of performance. Therefore, it is vital to ensure that the system reacts properly in case of loss of communication with any of its elements. One of the main reasons that might lead to such occurrence is antenna pointing accuracy. In case either the ground station or the airship have their antennas not pointing exactly at each other the link might not close, resulting in contact loss. To tackle this, measures on both sides need to be taken. The ground station should have registered the last location of the airship and do

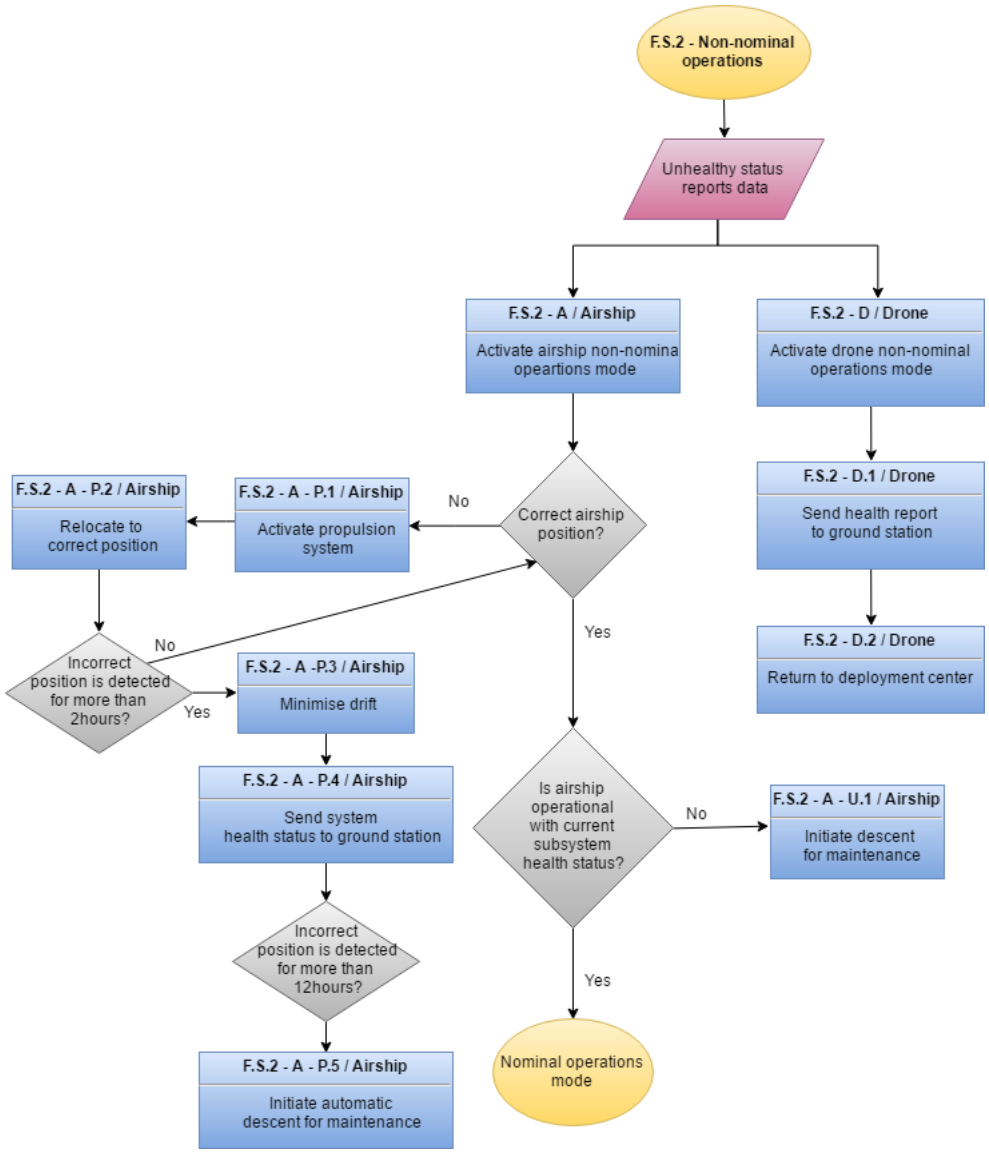

Figure 8.4: Non-nominal operations flowchart

minor adjustments to the antenna so as to try to regain connection (SYS-1-GS-1). This is done with a specific algorithm that extrapolates the most probable locations of the airship based on their location history. A similar algorithm is applied on the airship computer, so that the on-board antenna immediately attempts to regain contact with the ground station.

Another important thing to consider is that upon losing contact, the airship might still be acquiring data which is not being sent. This data cannot be lost and so the on board computer should be aware immediately start storing all the data gathered while communications are down.(SYS-1-A-2) Upon re-connection this data can then be sent back to the ground station.

It is decided that if the airship does not have contact with the ground station for more than 24 hours, the airship should automatically initiate the procedure to descend for maintenance. Of course, before sending the airship down, it should be checked whether the ground station antenna is not the one causing the contact loss, as the ground station antenna can fail as well. This could be checked in two different ways: the current ground station antenna could try to communicate with another airship by turning its pointing angle (same holds for that airship) or the redundant antenna on the ground could try to contact the airship. If it is found that the ground antenna worked, then the airship should be brought down.

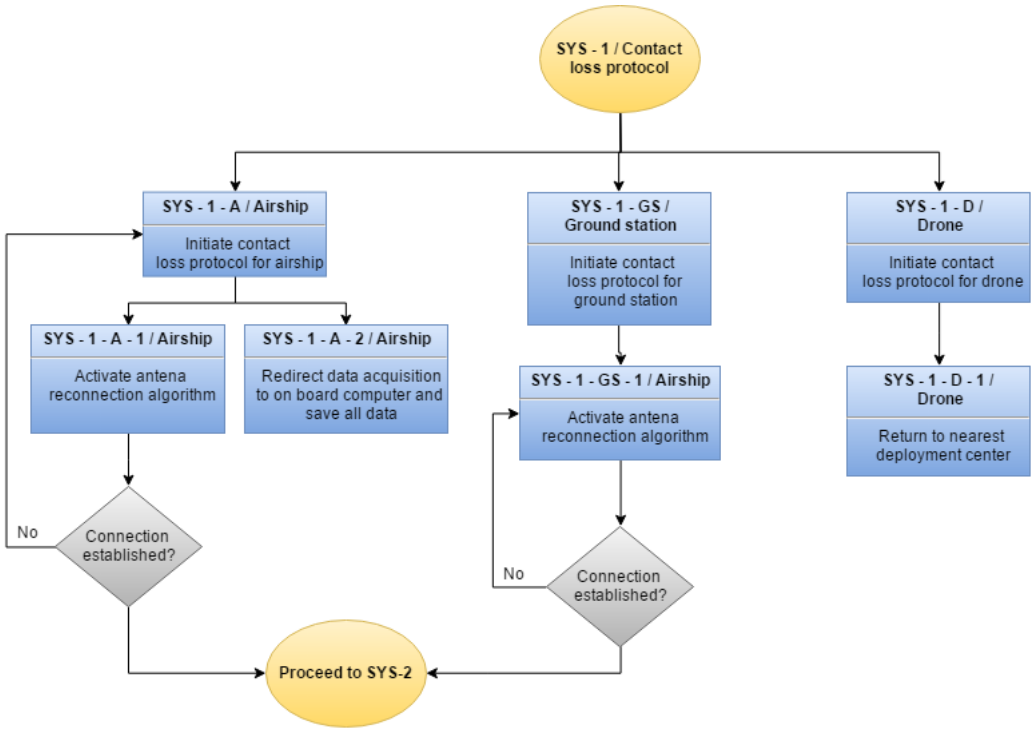

Figure 8.5: Contact loss protocol flowchart

AIRSHIP LOSS

One of the biggest risks threatening the system is the possibility of losing one of the NSS airships. This would have a major impact in the operations performed by the NSS since the system would lose track of part of the field of view. This would be even more serious if the said area was located in a high-density zone like Amsterdam or Den Haag. There are two major ways of counteracting this risk: redistribution and redeployment.

Once the loss of an element is confirmed, the instantaneous response of the system is to redistribute the airships. The ground station will have an integrated distribution algorithm that will take into account which airship has been lost, its location and the current location of current targets and fires to determine the best possible distribution for the other airships. The main idea is to achieve maximum coverage possible with the available airships, minimise the loss in coverage and maintain it in high density areas.

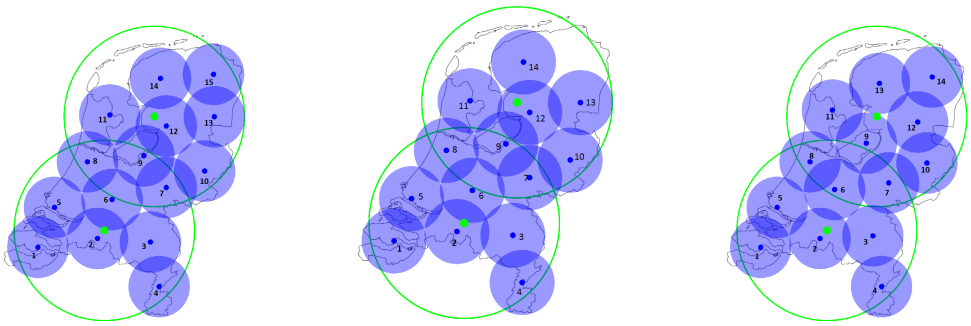

(a) Original NSS airship positions

(b) NSS loses airship number 15

(c) In-built algorithm redistributes airships to minimze performance loss

Figure 8.6: Loss of an airship in a low density area

In Figure 8.6 an example of this process is given. The first subfigure shows the complete NSS with all airships operational. In the second subfigure the system realises that an airship is missing and reacts, initiating the redistribution process. Since airship number 15 is located in a relatively low density area, the focus is on making covering the gap that is left by the ship without creating new gaps in high density areas like Amsterdam, Den Haag and Rotterdam. The airships closest to the newly formed gap will approach it, and the closer the airship is to the gap the more it will change its position to help 'cover' the new gap. Behind such an algorithm it absolutely vital to have a map with a realistic distribution of 'high risk' and 'low risk' areas that is reliable and combines the potential risks of fires and specific targets that are currently being tracked.

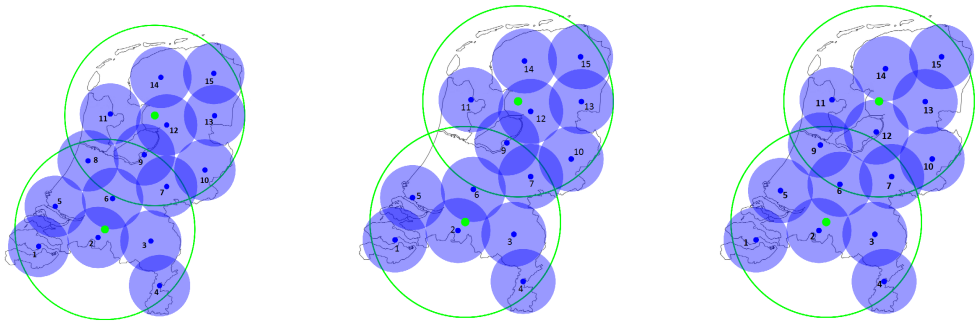

(a) Original NSS airship positions

(b) NSS loses airship number 8

(c) In-built algorithm redistributes airships to minimise performance loss

Figure 8.7: Loss of an airship in a high density area

Figure 8.7 shows the reaction of the system if airship 8 goes missing. In this situation the algorithm prioritises covering the gap in the high density area. It achieves so by clustering all nearby airships to said gap and adjusting the position of airships in low density area so that most coverage is lost in those zones.

The strategy proposed in the previous section is a great way of dealing with airship loss on the short term. However there is a reason why the NSS was designed to have as many elements as it does, and being one element short will have an impact on the system performance in the long term. This means that eventually it will be necessary to deploy a new airship if the original one is destroyed, captured or damaged beyond repair. It has been announced that production is planned to reach levels of 15 units a year,[1] meaning that upon ordering, a new airship for the NSS could be ready within 12 months. An event that would 'eliminate' one of the NSS elements is very unlikely, so it is safe to assume that it is rather hard for such to occur in a time line of one year. Another important factor to take in is the fact that the airships should descend for maintenance at least once a year, and since the system is composed of 15 airships in total it is easy to see that there will be one descending approximately every 3 weeks. Since there should be 15 airships operational at all times, it logically follows that there will always be an extra one in maintenance. In case on of the airships is lost, the one currently in maintenance could almost immediately be deployed and substitute the one that was lost, restoring the system to its full operational performance. This would increase the time margin for the NSS to contact Thales and order a new airship. It could even be arranged with Thales that under such conditions the company would be able to produce and provide an airship much faster than their usual production time.

8.3. AIRSHIP MAINTENANCE

First the procedures for take-off and landing are discussed and secondly the maintenance procedures are explained. The maintenance procedures also elaborate on the safe handling of hydrogen.

[1] http://www.janes.com/article/68513/stratobus-demonstrator-set-for-2018-launch[cited 13 June 2017]

8.3.1. AIRSHIP TAKE-OFF AND LANDING PROCEDURE

Take-off and landing are two critical stages within the flight of an airship. Both will be briefly discussed.

Take-off of airships, and blimps alike, requires propulsion. However, since the Thales Stratobus uses hydrogen as lifting gas, hydrogen will be produced in order to take-off.[2] The take-off of the Stratobus is defined as follows:

The process of getting from the ground level where it is stored to a stable cruise altitude.

The sequence of events during airship deployment can be found in Figure 8.8.

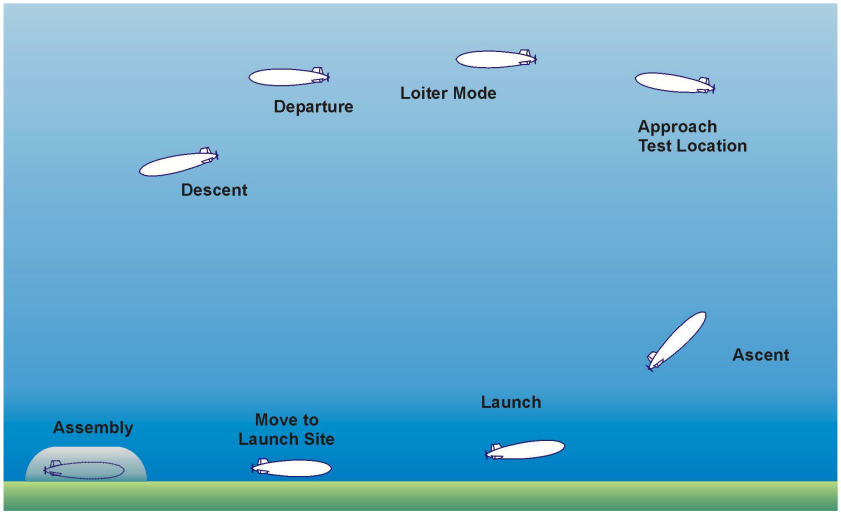

Figure 8.8: Illustrations take-off and landing airship [1]

Using the elements presented in Section 6.3 a flow chart can be made for the take-off process. It is assumed that the airship is already built and needs to inflate inside the hangar under a controlled environment. The flow chart can be found in Figure 8.9.

The airship lands for maintenance. This will happen every year if the system operates nominally, but these may occur more often in case of unexpected failures. Landing procedure is defined as follows:

The process of getting the airship from its dedicated position at 20 km altitude to the hangar where it will undergo maintenance.

The elements defining the take-off of the Stratobus also define the landing. Using these elements a flow chart which defines landing operations can be produced which can be found in Figure 8.10.

8.3.2. MAINTENANCE PROCEDURE

The Thales Stratobus needs annual servicing and a complete overhaul after 5 years. To accommodate this, a maintenance cycle needs to be developed. With 15 airships and annual servicing required, a single airship has the ability to be maintained 24 days. It is assumed that travelling the maintenance base and back to its initial position requires 2 days. The largest distance that has to be covered by a single airship is about 150 kilometers which would be from Limburg to a location proposed in Section 7.3.2. It is known that when normal 20 m/s winds are encountered, a ground

[2] http://spacenews.com/thales-alenia-space-stratobus-eyes-contract-in-2017-kuka-band-frequency-ok-in-2019/ [cited 13 June 2017]

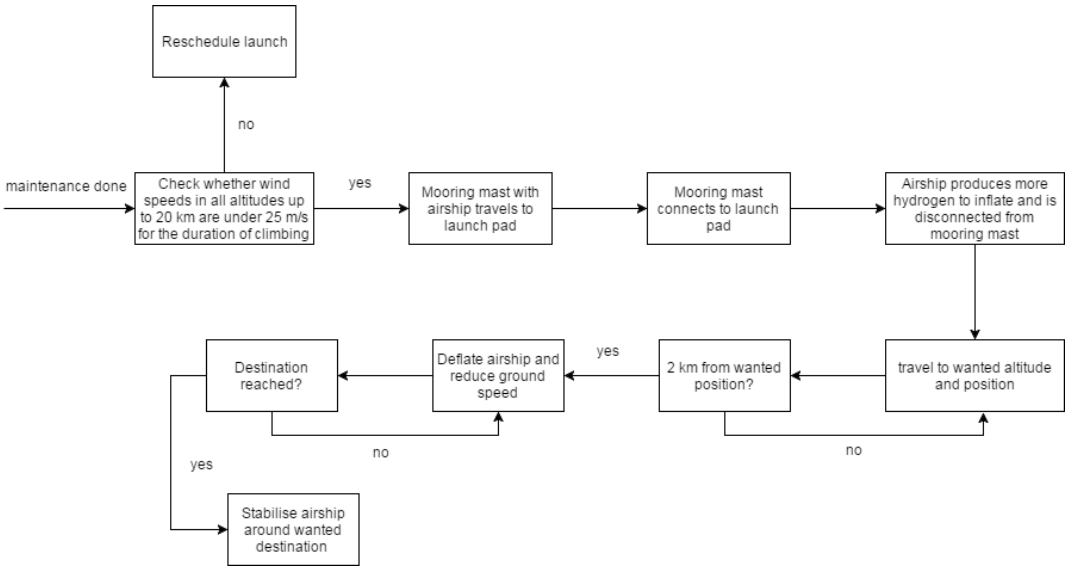

Figure 8.9: Airship take-off flowchart

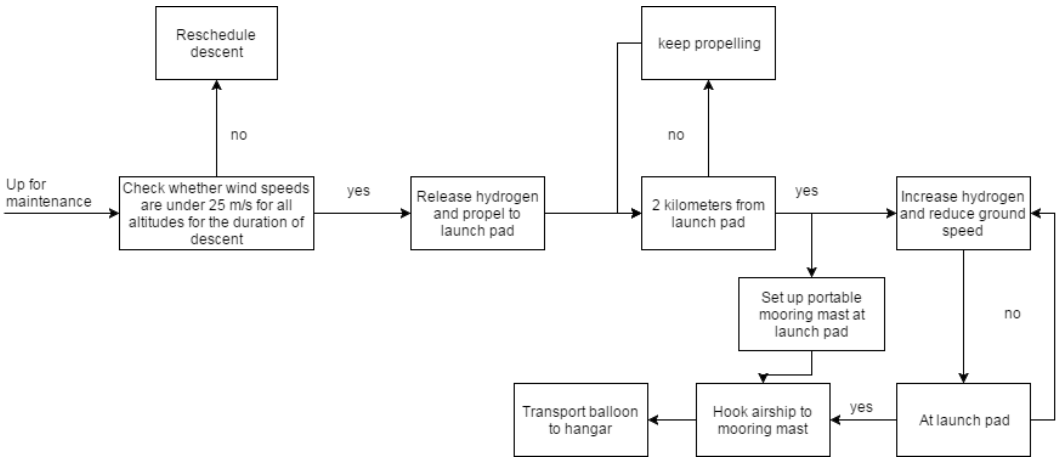

Figure 8.10: Airship landing flowchart

speed of 5 m/s can be achieved. At most travelling will cost 8 hours and 20 minutes to maintenance base and back to its designated area which validates the assumption that travelling will cost 2 days. This implies that one airship needs to be available to be able to cover the Netherlands. This procedure will results in the following flow chart found in Figure 8.11. However, sometimes winds can reach 30 m/s, rendering stationkeeping impossible. This situation only lasts for 1-2 weeks yearly.

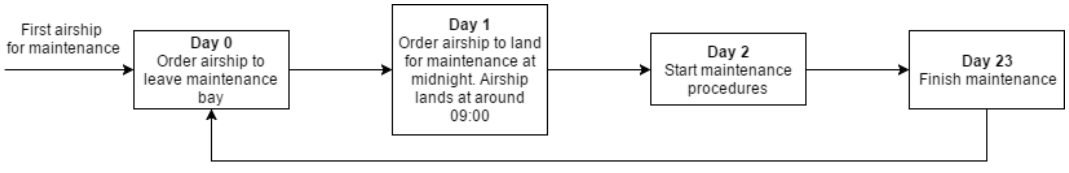

Figure 8.11: Airship maintenance cycle

Regarding the complete overhaul, an estimate of time and amount of airships which will not be present above the Netherlands, should be discussed with Thales.

During the maintenance cycle, the personnel and facilities are exposed to the hazards of hydrogen. The most famous disaster regarding airships and hydrogen, is the zeppelin Hindenburg. This airship exploded due to a hydrogen leak and spark caused by static electricity on the skin of the air-

ship. [3] This shows that working with large amounts of hydrogen and airship can be extremely dangerous if not done properly. Therefore a good understanding of hydrogen as a lifting gas should be achieved and a manual should be made on how to handle the airship during maintenance, takeoff and landing.

As explained in Section 5.4.2 hydrogen is highly reactant when in contact with oxygen and a spark is present. However this is also true for all other flammable substances. Hydrogen diffuses rapidly in the air, dilutes quickly into a non-flammable concentration and will go to the roof of building. The hangar should therefore be well ventilated since hydrogen might be escaping through little cracks in the fabric of the hydrogen compartment. Since no spark may be present if a hydrogen leak occurs, all electrically charged tool should be turned of immediately. Also the pressure in the hydrogen compartments must be watched during take-off and landing to see if no hydrogen is abnormally escaping. If this is the case, the objects that touch the Stratobus must not conduct electricity. Otherwise a hydrogen and oxygen reaction might happen. Lastly, during maintenance special attention must be paid that the compartments holding hydrogen are not ruptured, releasing the hydrogen. Detailed maintenance procedures and handling of hydrogen on the ground will be provided by Thales Alenia Space upon delivery of the airship [53].

8.4. RISK MANAGEMENT AND MITIGATION

Any engineering project carries several risks associated with it. This is even more true for a project involving national security, since people's safety is at risk and there is no room for failure. So far, the risks of each part of this project have been subtley introduced in the respective chapters. In this section a small discussion about the various risks that came up during the design of the NSS risks will be presented and the mitigation strategies used for each. This will be shown in a risk table and two risk matrices for before and after mitigation.

Being a system of systems, it comes naturally that the NSS is mostly faced with operational kind of risks, when compared to the technical ones. This does not imply that the technical risks are negligible, but since most of the technology utilised in the design has a relatively high TRL and has been used in previous missions, it is safe to assume that they do not pose as high of a risk as the operational ones do.

Most of the technical risks were discussed in their respective sections and were found to be related to the payload and detection methods. For example, when using PC for detection, it was found that the applied coating could potentially be visible when under certain light conditions, meaning that it could eventually be detected. The same applies for the QD detection method, which when looked at under an IR camera, could also be detected by targets. The fact that both these detection methods can be noticed is the main reason for the proposed design involving the two of them. In the odd chance that one of them gets detected and the target somehow manages to remove it, there is the option of applying the other method and prolong the time span in which the target is trackable. When looking at chemical analysis performed by drone, the risk of cross sensitivity associated with electrochemical analysis lead to the design choice of applying laser chemical analysis, where this phenomenon is much less likely to occur.

In Chapter 8, the nominal operations section was followed up by a back-up plan section. Here, the major operational risks that threaten the NSS were introduced and mitigation strategies for each were proposed. Naturally, one of the biggest threats to the system was the loss of an airship. As discussed before, losing one of the main NSS elements would have a major negative impact on the functioning of the system, since a big part of the coverage would be lost. This is even more true if the missing airship was located in high-density areas like Amsterdam or Rotterdam. Two main strategies were proposed to tackle this: redistribution, which involved an in-built algorithm that would redistribute the airships in such way as to minimise coverage losses, especially in the high-density areas. Redeployment, which consisted in the redeplotment of a 16th airship that would be in one of the hangars in maintenance while the other 15 are operational. If one of the 15 operational airships went missing this could be deployed to 'buy time' to the NSS and give the possibility of ordering a new airship without losing performance in the meantime. Another major

[3] http://www.airships.net/hindenburg/disaster/ [cited 15 June 2017]

operational risk was the possibility of loss of contact with any of the elements, which could be almost as severe as losing that element. The proposed mitigation for this involved a 'contact loss protocol' which activated a redirection algorithm to the antennas in both the ground station and the airship. The airship would also immediately start saving any unsent data to ensure that none of it is lost due to loss of contact.

For the sake of brevity, not all risks involving the NSS are discussed here. The risk matrices before and after mitigation are given in Table 8.2 and Table 8.3. All the risks, together with the respective mitigation strategies can be found in Table 8.4 and Table 8.5.

Table 8.2: Risk matrix before mitigation

		Severity				
		Negligible (1)	Mariginal (2)	Serious (3)	Very serious (4)	Critical (5)
Likelihood	Frequent (5)			Ops-4,Ops-5	Pay-1	
	Moderate (4)		AS-1,AS-5,	Pay-5,Drone-1	Ops-3,Ops-6,Ops-7,Com-3,Pay-4	Com-1
	Occasional (3)			Com-2,Pay-8	Ops-9,Pay-2,Pay-3,Pay-6,Pay-7,Drone-2,Drone-3,Drone-4	AS-2,AS-3,AS-6,Ops-1,Ops-2,Com-4
	Remote (2)			Com-5,	AS-4	Ops-8,
	Unlikely (1)					

Table 8.3: Risk matrix after mitigation

		Severity				
		Negligible (1)	Mariginal (2)	Serious (3)	Very serious (4)	Critical (5)
Likelihood	Frequent (5)	AS-5,Ops-4,Com-2		Pay-1		
	Moderate (4)	AS-1	Ops-5,Ops-6,Ops-7			
	Occasional (3)	Pay-7	AS-6	Ops-8,Pay-2		
	Remote (2)	AS-3,Drone-3	AS-2,Ops-1,Ops-3,Com-1,Pay-3,Drone-1	Com-4,Com-5,Pay-5	Ops-9,Com-3	
	Unlikely (1)	Pay-8			Pay-4,Pay-6,Drone-2,Drone-4	AS-4,Ops-2

From Table 8.2 to Table 8.3 there is a clear change in the severity and likelihood of most risks. There is no particular preference in strategy, meaning that likelihood and severity were both reduced with the same frequency. This implies that mitigation strategies involved both the addition of redundancies and also risk prevention through testing, simulation and using high TRL technologies. It is interesting to note that one of the risks with less mitigation was Pay-1, the risk associated with the inability of the payload to identify targets during night time. This was tackled with the addition of an IR camera that is able to visualise targets at night (although not identify them). This mitigation slightly decreased the severity of the risk but still shows that this is one of the system's weakest points. The same can be said for Pay-2 which is the inability of performing neither FSDS or ITS in the presence of clouds. Again, this risk had a major influence in the design and was mitigated through the introduction of drones as 'emergency' system elements.

The proposed mitigation strategies tried to reduce the risks associated with the NSS as much as possible. This process drove the design to the extent of making it a fully redundant system, capable of coping with unexpected circumstances and rebounding in case something bad happened to it, whether it is an airship loss, bad weather or a simple loss in communication. The system as it is presented right now is fully capable of resisting to any of these occurrences and is a system worth of engaging the task of protecting and ensuring the national safety of the Netherlands.

Table 8.4: Risk table (1/2)

Index	Cat.	Cause	Event	Consequence	Severity	Likelihood	Risk Priority		Mitigation	Sev. after mitigation	Lik. after mitigation	Risk Priority after mitigation	
Airship element risks													
AS-1	Balloon	Weather is very severe	Airship just finished maintenance and is ready for take-off	Airship cannot take off	2	4	8	Review	Perform the maintenance at a slightly higher frequency than advised, providing with contingency time in case of a storm	1	4	4	Risk acceptable
AS-2	Balloon	Airships require yearly maintenance	NSS needs to be operational 24/7	Maintenance implies there is a airship down at all times	5	3	15	High priority	Introduce a 16th airship that will introduce a rotation in the maintenance routine	2	2	4	Risk acceptable
AS-3	Balloon	Unknown cause	Airship ascends to an altitude higher than the optimal	Pressure difference causes unbearable loads effectively causing the aiships structure to fail	5	3	15	High priority	On-board computer has constant awareness over the balloon's height and autonomously controls it to remain under a certain value	1	2	2	Risk acceptable
AS-4	Balloon	Unknown cause	Balloon crashes	Debry falls on to a populated area	5	2	10	Review	Extensive testing, simulation and analysis of all subsystems and the airship as a whole	5	1	5	Risk acceptable
AS-5	Balloon	Stresses are too high in some components	Material failure of structure	Payload is at risk of falling	2	4	8	Review	Use known materials for this type of application, test it before in fatigue mode	1	5	5	Risk acceptable
AS-6	Balloon	Flammable gas is used for lifting	Spark ignites gas	Airship is burnt down	5	3	15	High priority	Ensure proper separation between balloon and all electronic circuits. No landing or take off during storms	2	3	6	Risk acceptable
Operational risks													
Ops-1	Operations	Unknown cause	NSS airship is lost	Area covered by the lost NSS airship is not under surveillance anymore	5	3	15	High priority	Redistribution: inbuilt algorithm redistributes airships in the most efficient way possible; Redeployment: additional airship on maintenance is always ready to substitute an airship that has been lost	2	2	4	Risk acceptable
Ops-2	Operations	Detection methods are detectable	Criminals become aware of detection method	Criminals take measures against said detection method	5	3	15	High priority	Two distinct detection methods are introduced	5	1	5	Risk acceptable
Ops-3	Operations	Unknown cause	Contact with an airship is lost for over 24h	Data is not transfered from said airship to ground station	4	4	16	Not permissible	On board computer automatically initiates the descent procedure to put the airship in maintenance	2	2	4	Risk acceptable
Ops-4	Operations	Circular fields of view and irregular shape of the Netherlands do not mach	Almost impossible to achieve 100% coverage with an ok number of balloons	100% coverage requirement not met	3	5	15	High priority	Distribution was performed so as to attain at elast 99% coverage. Additional set-ups are recommended for this distribution in case 100% coverage is really needed. The lack of coverage occurs in low density areas	1	5	5	Risk acceptable
Ops-5	Operations	Winds of up to 30-35 m/s can be expected in the stratosphere	Propulsion system is unable to make the airship move around in such winds	Airship manuverability is severly hindered and unpredictable	3	5	15	High priority	The selected distribution and design was chosen in such way that the airships are stationary and their movment is minimal	2	4	8	Review
Ops-6	Operations	Unknown cause	One of the airships' subsystems is damaged/malfunction	Subsystem failure may cause severe failure of airship element	4	4	16	Not permissible	On board computer is able to create health reports for each of the subsystems and communicate them to the ground station. The ground station is able to process any changes that may be occuring in the subsystems and might be able to predict failures	2	4	8	Review
Ops-7	Operations	Winds over 30-35m/s occur in the stratosphere	The propulsion system cannot keep up with how strong the winds are	The airship begins to drift from its intended position	4	4	16	Not permissible	The computer has an inbuilt feature that is activated after X time outside of its inteded position. If it occurs it will use the propulsion system in such way to minimze de drift.	2	4	8	Review
Ops-8	Operations	Ground station is siezed	Third party is able to take control over the ground station	Thirdy party takes over control of the NSS	5	2	10	Review	Have proper security in the ground station zones, possibility of transfering full power from one ground station to another	3	3	9	Review
Ops-9	Operations	Thunderstorm occurs in the ground stations area	Thunder strikes ground station	Electrical system affected by lightning	4	3	12	High priority	Use a lightning conductor to protect the ground station	4	1	4	Risk acceptable

Table 8.5: Risk table (2/2)

Communication risks														
Com-1	Communications	Unknown cause	Contact with an airship is lost	Data is not transfered from said airship to ground station	5	4	20	Not permissible	Airship in-built algorithm starts saving all gathered and not sent data in dedicated storage, also onboard antenna and ground station antenna are moved around so as to reconnect	2	2	4	Risk acceptable
Com-2	Communications	Unknown cause	Contact with a sniffer drone is lost	Sniffer drone's task is not completed on time or target is lost	3	3	9	Review	Immediate redployment of another drone in the area and heading to last known location	1	5	5	Risk acceptable
Com-3	Communications	Communications require high pointing precision	Stability on the airship its hard to achieve	Link cannot be closed	4	4	16	Not permissible	Use a very accurate pointing mechanism for the antenna, test it extensively	4	2	8	Review
Com-4	Communications	Third party tries to hack system	System is hacked	Sensible information is leaked	5	3	15	High priority	High levels of encryptation should help reduce the possibility of hacking and sensible information leaking	3	2	6	Risk acceptable
Com-5	Communications	Dedicated frequency for network communications is required	The ust of this frequency can potentially be disproved	Communications are made impossible	3	2	6	Risk acceptable	No real mitigation can occur, just redesign	3	2	6	Risk acceptable
Payload risks														
Pay-1	Payload	At night there is no radiation coming from targets	ITS payload cannot locate targets	ITS cannot be performed during the night	4	5	20	Not permissible	An additional IR camera is added that is able to track moving veichles (without knowing their ID). This can help the system keep up with the tracking	3	5	15	High priority
Pay-2	Payload	Clouds block almost all useful radiation	Radiation cannot reach airship payload	ITS and FSDS cannot be performed if it is very cloudy	4	3	12	High priority	This is a major risk of the project for which there isn't a clear mitigation strategy. The presence of clouds will effectively constitute a 'hole' in the data created by the NSS. This can be extrapolated with maps to predict how the rest of the data might look. The use of drones for night time ITS is suggested	3	3	9	Review
Pay-3	Payload	Use of the 3.9 micron band for fire detection makes the system highly sensitive to fire presence	A big number of fires are caught byt the FSDS operations	A big number of fires is actually a false fire alarm, due to the bands high sensitivity	4	3	12	High priority	Use of 10.8 band helps to reduce this phenomenon. The 10.8 bands acts as a 'check' to distinguish fire from non fire pixels	2	2	4	Risk acceptable
Pay-4	Payload	The payload design is based on optics	A lot assumptions and approximations are being used to perform the calculations	The assumptions and approximations might lead to results that are either questionable or different from reality	4	4	16	Not permissible	Real life testing, analysis and simulation is required so that the numbers and the design are confirmed to be realistic	4	1	4	Risk acceptable
Pay-5	Payload	Spatial resolution requires a very small GSD	Having a low GSD implies that the required stability is very big	Platform is unable to achieve the desired stability values	3	4	12	High priority	Lowering the GSD to acceptable values, such that the system can still perform its tasks, helps lower the stability requirement	3	2	6	Risk acceptable
Pay-6	Payload	Design is being made on the basis of physical limitations	It might be necessary to develop new cameras for it	Necessary camera for the design might require a veyr high level of precision to be developed and the project might be delayed	4	3	12	High priority	During the design phase try to use as high of a TR for the instruments as possible	4	1	4	Risk acceptable
Pay-7	Payload	Clouds block almost all useful radiation	Radiation cannot reach airship payload	Chemical analysis cannot be performed	4	3	12	High priority	The use of sniffer drones is a solution to this problem. These drones will be deployed whenever it is cloudy and will be able to reach the fire location relatively quickly	1	3	3	Risk acceptable
Pay-8	Payload	Several targets need to be tracked at the same time	Camera capable of imaging QD and PC needs to me moved around a lot	Mechanical wear off can occur, and high precision system needs to move a heavy payload	3	3	9	Review	Introduce a color imager able to detect potential targets and thus reduce the required manouverability	1	1	1	Risk acceptable
Drone element risks														
Drone-1	Drone	Chemical chromatographic analysis is not 100% reliable	Cross sensitivity in gas analysis	Some gas detections might be false	3	4	12	High priority	Depending on the specs of the instrument used it is possible to predict what kind of gases might be associated with false detection. Using laser detection could eliminate this risk	2	2	4	Risk acceptable
Drone-2	Drone	Drone chemical analysis operations location is unexpected and might be anywhere in the country	Drones might not be able to reach the desired location fast enough	Chemical analysis quickness not sufficient for the fire department	4	3	12	High priority	Use high endurance drones and distribute them throughout the Netherlands taking into account how fast they are. Minimize response time for any location	4	1	4	Risk acceptable
Drone-3	Drone	Drone sensors have warm up time	Usually there will be high pressure on how fast the drone can perform the chemical analysis	The warm up time might make the drone take too long and severly hinder its response time	4	3	12	High priority	Selecting drones with low warm up times and connecting them directly to the ground station so that warm up initiates as soon as possible	1	2	2	Risk acceptable
Drone-4	Drone	Drones need to be used for ITS when it is cloudy	Low clouds will require drones to fly flow	Drones might be spotted by targets	4	3	12	High priority	Drone pilot needs to be extra careful when low clouds are present, fly in a stealth formation	4	1	4	Risk acceptable

9 | Development

In this chapter further developments for the NSS are discussed. This is done by looking at technological improvements in the future that can improve the operational aspects of the NSS. A market analysis shows the potential of the airship platforms and opportunities for the NSS to fulfil additional tasks. Next, developments in the field of detection methods are discussed. This flows directly into the development of new payloads to perform the missions of the NSS at even higher quality. Afterwards, the development of the airship platform is elaborated upon. New technological advancements on the airship platform could increase productivity of the system. Finally, future system developments are discussed.

9.1. Market Analysis

To inform oneself about the possibilities of the market and opportunities which might arise along the way, it is important that a project performs a market analysis. The market where NSS is in, is the High Altitude Platform (HAP) market which is composed of airships, high flying UAVs and aerostats. Firstly, the size and potential growth is discussed. Subsequently, the trends are elaborated upon. Lastly, the opportunities for the system are discussed.

9.1.1. Size & Growth

The current market of HAPs was estimated at 2.7 billion euros in 2015 with an annual growth of 11% which can be found in Figure 9.1 [54]. According to this estimate the market would be at 4.35 million euros in 2020. The program director of the Thales Stratobus believes that the market of stratospheric airships will hit about 1000 million dollars by 2020 with an annual growth of 12% percent a year.[1] From both these statements one can determine that the stratospheric airship market is 22.7% of the the total HAP market and is growing fast too.

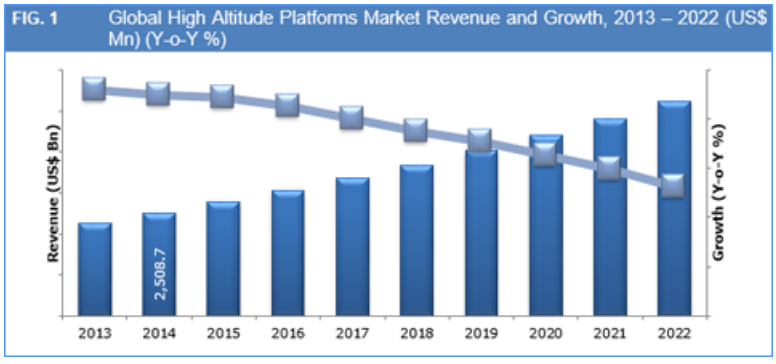

Figure 9.1: Market HAPs [54]

Key players having a major share in the HAP market are companies like TCOM L.P, ILC Dover, Isreal Aerospace, Raytheon, Lindstrand, Aerostar International, Northrop Grumman, Lockheed Martin, Airbus Defence&Space and Thales. Not all these companies are developing stratospheric airships though. The majority of the companies, like TCOM and Isreal Aerospace are developing aerostats. However, these companies could pivot to become competitors.

[1] https://www.thalesgroup.com/en/worldwide/space/news/whats-stratobus [cited 13 June 2017]

9.1.2. TECHNOLOGY TRENDS

Due to the long flight that HAPS have to perform, an increase in solar panels can be seen which are often used as the main source of energy. For night time use of the a HAP, batteries are needed. These can come in the form of lithium, RFC or – as is the case for Thales Stratobus – in the form of hydrogen [35].

Further technology trends might be coming from China, who did a large scale test on their stratospheric airship called Yuangmeng. According to the Chinese, this airship reached an altitude of 20 kilometres with ease and it was there for 48 hours.[2]

From Section 5.2.1, it can be seen that the development of stratospheric airships is at a quite low technology readiness level and it comes with high risks. This is evident from the crashes that have occurred in the past 15 years.

Concluding, technological development in the field of HAPs and especially stratospheric airships will occur in next couple of years when looking at the expected size and growth of the market.

9.1.3. OPPORTUNITIES FOR NSS

The sensors and camera that are fitted for ITS, FSDS and gas analysis can also be used for other purposes if used correctly. Three different cameras have been fitted, which in their own respect can perform a diverse set of other tasks.

The AMS wildfire images in the infrared and visible light. Some of the wavelengths that are on the camera can be used for other purposes too. This imager is able to perform meteorological measurements if appropriate algorithms are implemented in the system. The visible light and infrared sensors on the camera are able to know the position and altitude of clouds.[3] This information can be used by the KNMI to have an own dedicated system that monotirs weather realtime. Other uses of the camera would be tracking currents near the coast and monitoring the tides.

The second of the three cameras is the regular colour imager. With a ground sampling distance of 0.32 metres, this camera is able to observe objects of small size. This camera could be used for monitoring big crowds and following cars in a chase that is now performed by police helicopters. Since the airships are also operating above the IJselmeer and coastlines, it could also be used for missions when it is not cloudy.

The Hyperion camera is a hyper-spectral camera having a ground sampling distance of 0.85 metres and 220 available spectral bands to image in. Using these, the camera is able to detect the composition of certain gases and their respective parts per million. This makes it able measure and analyse the gas emissions of, for example, factories. Next to that, the camera is able to detect algae and specific chemicals in the water.[4]

9.2. DETECTION METHOD DEVELOPMENT

The detection methods proposed earlier are not yet fully developed and thus will require additional research to successfully be implemented. This will be discussed in this chapter.

9.2.1. QUANTUM DOTS

As briefly mentioned in Section 3.2.1 the technology concerning QDs is relatively new. It is already possible to engineer QDs which emit at very specific wavelengths. However, as of yet, no transparent sprays exist which implement QDs. Luckily, there is research being conducted on transparent QD paint, which would function as solar panels [11, 12]. This is considerably more complicated as it is required to conduct electricity and form some sort of circuit. The application of QDs which is proposed in this report, would not require a circuit, and is therefore considerably easier to be

[2] http://thediplomat.com/2015/10/is-this-chinas-newest-tool-to-thwart-us-military-power/ [cited 15 June 2017]
[3] http://www.theweatherprediction.com/habyhints2/512/ [cited 20 June 2017]
[4] https://www.nasa.gov/vision/earth/lookingatearth/great_lakes_algae.html

developed. Additionally, it is already known from the MTR that QDs can be made soluble and potentially integrated into spray paints. However, these do not yet exist and thus should be developed. Within the Netherlands there are many institutions which are working on quantum effects on nano scale such as QDs, these include Steele Lab from the TU Delft, TNO and NWO. These would be institution worth contacting for further investigation regarding the feasibility of a QD marking including both the detection and transparent coating.

9.2.2. PANCHROMATIC COATING

Until now there have been very few, if any, practical applications of metamerism, besides the occasional unintentional manufacturing mistake. The attention that has been dedicated towards metamerism, has so far mainly been to avoid it from happening. Therefore, the main uncertainty with the application of panchromatic coating is the intentional engineerability of metamerism for such products. In order to figure this out, dedicated research with access to the necessary data about car reflectance should be done, and with subsequent experiments to make an attempt at manufacturing coatings with the desired properties. As was mentioned in Chapter 3, all the spectral properties can be expressed mathematically, so targeted research would not be complicated, particularly with the aid of more accurate tools for colour calculations and representations. Potentially companies such as Akzo Nobel can assist in such research.

Additionally, the imager that was selected in Section 4.2.2 meets the optics requirements, but has a relatively low spectral resolution. Part of the reason that this camera was chosen over (e.g.) TNO's TROPOLITE, is due to the fact that the latter does not meet certain requirements with regards to the optics, and not all the required information was made public about this imager. However, the optics can be resized, as this is the least complicated part of a camera to design. Using this camera would enable more accurate imaging of deviations in the spectral reflectance of panchromatic coatings, therefore increasing the possibilities when engineering panchromatic coatings. It is for these reasons that it would be of tremendous benefit to the NSS if this imager would be optimised for the system's mission. TNO and specialised optics companies such as Cosine can help to perform research and design new optical systems.

9.3. EXTENDED FOV

One of the limiting factors is the maximum achievable FOV, this thus makes it worthwhile to investigate whether it is possible to enlarge this, and subsequently lowering the required amount of airships. First the possibilities for FSDS will be presented after which ITS possibilities will be discussed for both the PC and the QD solution.

9.3.1. EXTENDED FOV FOR FSDS

The FSDS FOV presented in Section 3.4.2 was determined under the presumption that the final set-up would provide full coverage, meaning that there will always be an airship covering the adjacent area outside of the FOV of a single airship. This meant that the FOV was limited to the maximum coverage area for the ITS detection method. However, if one disregards the ITS operations, the potential FOV for FSDS is much larger than the previously set 34 km. To give an indication on what is possible Figure 9.2 shows a picture taken from a weather balloon at an altitude of 29 km. The image was taken over the UK somewhere in between Boley Hill and Hadlow. The image shows easily distinguishable landmarks, such as the Isle of Wight that can be seen at the right end of the picture. When looking past Roffa the bear, the French coastal line can be seen which is indicated with an orange line. Although the coast itself is hard to discern, clouds at that distance would still be easily visible due to their size and elevation. The distance from where the picture is taken to, the French coast is about 150 km. Scaling this distance linearly with the relative altitude of the airship would yield a FOV radius of 100 km. This is the same distance a ground station would be able to reach and thus just two airships would be enough to cover the entire Netherlands, for a visual representation refer back to Figure 6.1.

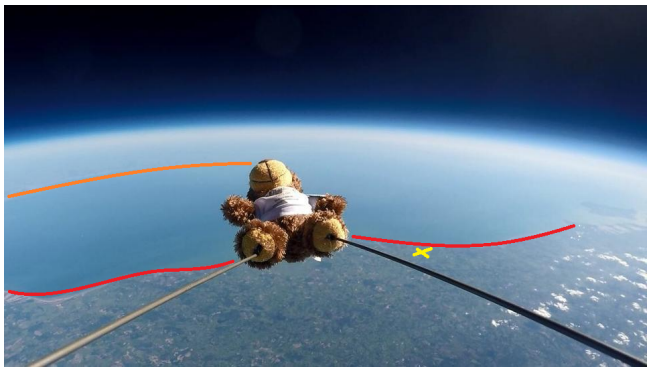

Figure 9.2: Roffa the bear at an altitude of 29 km [5]

However, as the range increases the cloud images would get more skewed, and thus it would be harder to infer the area that the cloud is covering. At least three airships equipped with an FSDS imager would be preferred, as having three allows for triangulation between their coverage area. Increasing the range would mean the spatial resolution of the AMS Wildfire would decrease below the required spatial resolution of 100 metres. If one accounts for AMS Wildfire spatial resolution to stay within the required spatial resolution, a maximum FOV with radius of 88 km was found. The triangulation can still be done beyond this range, however, at least one airship should be within the 88 km range of the cloud to accurately determine its size within the set requirement of 100 metres. This is depicted in Figure 9.3 and shows that 95% of the Netherlands is covered and the majority of the area is able to be triangulated. If the distance of 150 km could be achieved, a single airship would already be enough to cover 95 % of the Netherlands, however as previously mentioned it would make the clouds even more skewed, triangulation would be impossible, and a different FSDS imager should be selected, as the AMS Wildfire would no longer suffice.

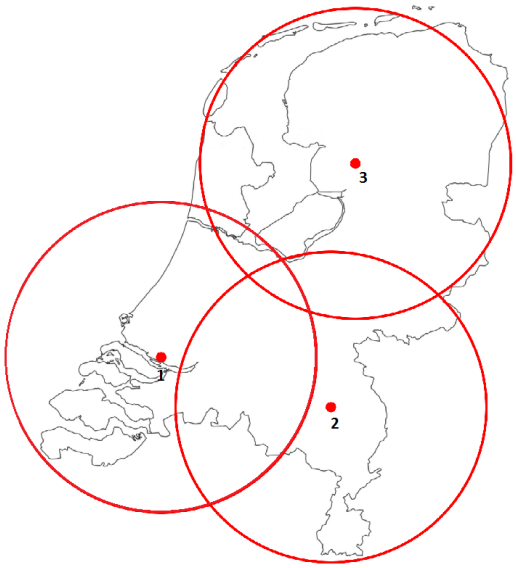

Figure 9.3: FSDS with three airships having a viewing radius of 88 km

9.3.2. EXTENDED FOV FOR PANCHROMATIC COATING

The PC solution requires good visibility to be properly identified. Figure 9.2 already showed that the French coastal line is hard to discern, however the UK coastal line, as indicated with the red line, is still very clear. Following the line towards the right the visibility decreases and past

[5] http://www.hindustantimes.com/world-news/roffa-the-teddy-bear-reaches-space-after-tied-to-balloon-by-kids-in-uk/story-FQPJpRzjIfrd5JsHVybFOK.html [cited 22 June 2017]

Brighton, indicated with the yellow cross, the image gets vague. The distance to Brighton is about 70 km. This gives an elevation angle from the ground of about 22.5°. Although it might seem arbitrary to determine the maximum FOV in such a way, it is however supported by the maximum observer angle in astronomy [55, 56] . This is depicted in Figure 9.4 and it shows that after a 70° zenith angle the deviation angle increases significantly. This is due to temperature gradient becoming the dominating factor, and can no longer be corrected for. Therefore the minimum elevation angle is typically set at 20°. Recalculating the maximum FOV for a elevation angle of 22.5° yields a maximum radius of 48 km. This would drastically reduce the amount of required airships, however it also has some glaring limitations. The optics would require larger apertures. Some calculations were made using the same procedure as in Section 4.2 and showed that the CI aperture size roughly doubled, which has some drastic consequences for the mass budget, because mass does not simply scale linearly with aperture. Additionally, obstructions become an even bigger problem. If having an average house at the edge of the FOV with a height of 9 metres and a car height of 1.6 metres will make the car only visible if it is at least 18 metres behind the building, whereas the proposed system requires it to be 'only' 12 metres behind a building. Not to mention that small clusters of trees would have an even larger impact. This means that the increase of FOV can only be applied in areas with lower average building heights, an example of such a setup is depicted in Figure 9.5 and shows that it requires only 10 airships to achieve 90% coverage. It should be noted that although this is theoretically possible, having an elevation angle of 30° as proposed in this report is already optimistic.

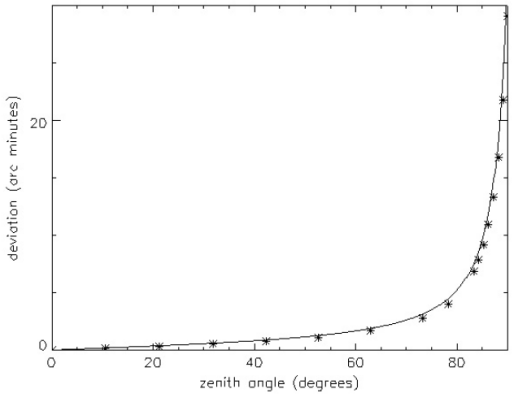

Figure 9.4: Deviation angle versus zenith angle (the angle w.r.t. ground normal) [56]

9.3.3. EXTENDED FOV FOR QUANTUM DOTS

A major disadvantage to the QDs solution, when compared to the PC solution, is the limited achievable FOV. This is due to the radiance pattern of QDs, although further research should be conducted whether this fully limits detection, or if detection at larger angles is still possible. As previously mentioned in Section 3.4.1 the majority of the radiance is emitted within 45° of the normal. This limits the ability to detect the signal when it is at a larger angle. The section also already motioned that there is considerable research being done to different radiance patterns achieved by specific structures. Figure 9.6 shows the radiance pattern of a QD mounted on the apex of a pyramidal structure [16]. Such a radiance pattern would be beneficial for the application within this system. If a QD radiates more of its energy at a larger angle, this would potentially enlarge the achievable FOV. It can also be seen that the radiation upwards diminishes significantly, this is however not a major problem as the distance to the object is smaller when it is directly beneath the platform. It is more preferable to have a larger power emitted at larger angles, since both the distance and the perceived size of the object are smaller when it is at a larger angle. The emitting pattern presented is mounted on a physical pyramidal structure, this obviously presents problems for the application within this system, as these will not be present on regular cars. Using chemical reactions when the spray is applied, structures could potentially be realised, however these have not been developed yet and should be further investigate and the same institutions as mentioned in Section 9.2.1 should be approached. However if this is possible it would allow for a considerable

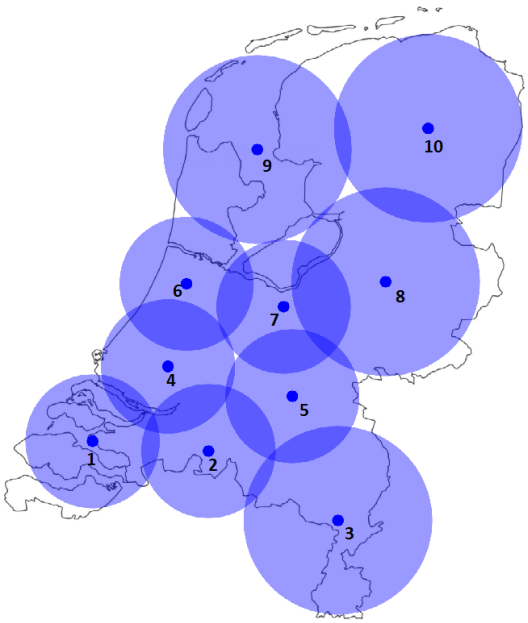

Figure 9.5: Example distribution of airships with increased ITS FOV [56]

larger FOV. As can be seen from Figure 9.6 it would emit its energy well beyond 60° of its normal, this would give a slightly larger or closely comparable FOV with respect to regular PC solution. This means that the required amount of airships would be around 15, as was determined for the PC solution.

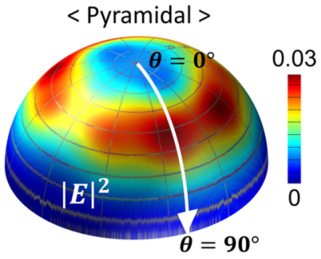

Figure 9.6: Radiance pattern of pyramidal mounted QD [16]

9.4. PAYLOAD DEVELOPMENT

In this section the steps to be taken are explained in order to have a working payload(bay) that will fulfil all set requirements on both target tracking, gas analysis and FSDS. The imagers found in Chapter 4 are the ones that can be fitted on the airship, however, it may not be possible to acquire theses cameras. The Hyperion camera was for instance a camera that is made as a one time project which is fitted upon a NASA satellite. This camera was not destined for mass production which the NSS needs. The Hyperion camera only shows that the technology has already been developed and has been used on working platforms. The same holds for the AMS Wildfire. For the colour imager and infrared imager the requirements and rough outline have been set. Experienced parties in the field of hyperspectral imaging, companies like Cosine and TNO Space, must be contacted to discuss the possibilities of creating and re-creating the imagers. A Dutch company would boost the space economy. Next to this it is important that a second opinion is involved during the selection of a company that further designs the imagers. Preferably this would be someone from the TU Delft or TNO Space. The company chosen to produce and or design the imagers must be able to do this in a set amount of time. The total timeline of design to production can be found in Chapter 12.

9.5. AIRSHIP DEVELOPMENT

In Chapter 7 the manoeuvrability of airships was discussed as it was a major factor in the choice of a set-up for the NSS. It is also true that high levels of manoeuvrability are hard to achieve with the current technology, leaving the airships with just enough propulsion power to be able to station keep in the wake of winds up to 25 m/s. This was one of the major reasons that led to a stationary airship design and imposed a minimum of 15 airships for full coverage of the Netherlands. In this section, the possibilities of an airship with an improved propulsion system are discussed.

The design options discussed in Chapter 7 considered only airships with manoeuvrability of at most 5 m/s when strong winds are present (~20 m/s). It is safe to assume that further research would be able to improve this to levels of 20 or even 30 m/s. Airships with this much manoeuvrability would change the possible set-ups of the whole system because full coverage would no longer be essential. If each airship can relocate itself relatively quickly, there is a big chance that an optimised system would use a distribution algorithm that would use the field of view and manoeuvrability of each airship to maximise coverage area.

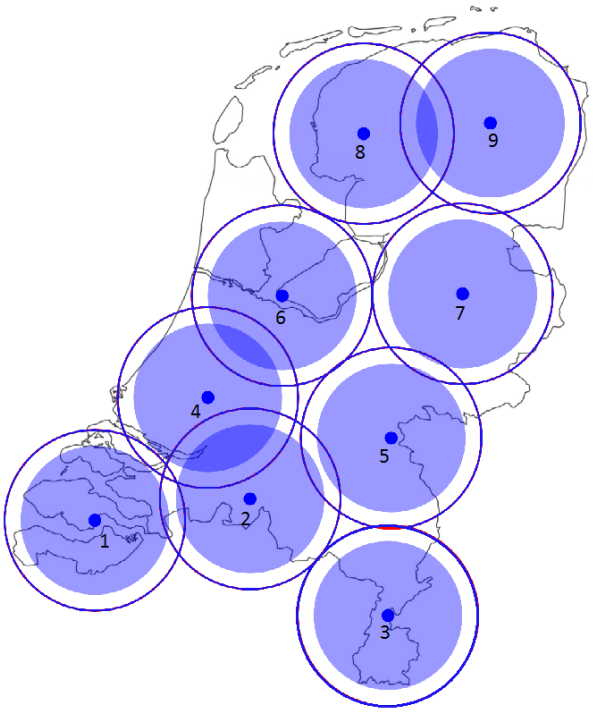

Figure 9.7: Proposed distribution for a system of highly manoeuvrable airships

Figure 9.7 illustrates the potential of such a system of improved airships. It shows a high coverage distribution of the NSS for airships capable of reaching speeds up to 25 m/s. The inner circles represent the field of view of 34 km, same as the standard NSS design, and the outer circles represent the achievable field of view within 5 mins. This configuration would achieve 75% constant coverage and close to 95% coverage withing 5 mins. If an optimisation algorithm is applied this could go as low as 95% coverage within 4 mins. The point of this illustration is to show just how much manoeuvrability can influence the set-up of a system like the NSS. By investing in the development of an improved propulsion system and aerodynamic structure for the airships (which was not Thales's main concern when designing the airship), it should be possible to reach these high manoeuvrability levels. A decrease of 5 airships from the original set-up, like presented, obviously leads to a massive reduction of costs associated with the system, while still fulfilling most of its requirements.

9.6. SYSTEM SIZE AND PERFORMANCE

At this point the team's vision of the NSS has been proposed and described thoroughly. However, like in any other engineering area there is always room for improvement or change, more so in terms of top level system properties. In this section the effect of the number of airships and their mobility will be discussed, with the purpose of clarifying how this system can be scaled up or down and what its limitations are in a number of different set ups.

PERFORMANCE VERSUS QUANTITY

Creating a system that can visually cover most of the Netherlands is not necessarily a complicated task. Obtaining full coverage however is an entirely different task, much harder to achieve. The main reason for this is related to the shape of the Netherlands which is completely irregular, hence hard to fill entirely with perfect circles. This is quite well represented in the next graph, where the increase in coverage area is given as a function of the number of airships.

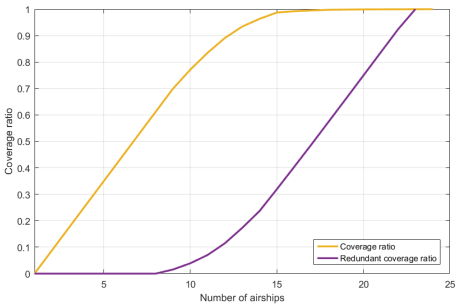

Figure 9.8: Coverage ratio as a function of number of airships

The previous graph in Figure 9.8 shows a concept that can be understood very intuitively. The first few airships that compose the NSS are placed in areas where there field of view is 100% efficient, meaning that it has no overlap with other fields of view or doesn't fall outside of the countries borders. For this reason the first 6 airships contribute with a linear increase to the coverage area. Once the main areas of the Netherlands are covered overlap begins to occur (redundant coverage), as the new airships try to fill in smaller and smaller areas that are still not covered. Overlap increases with each new airship, to the point that after the 12^{th}, increase in coverage area becomes minimal.

A direct conclusion that is taken from this is that the more airships the system already has, the less 'efficient' adding another one will be, meaning that the costs per coverage area will increase. This concept makes room for some interesting possibilities regarding the set-up of the whole system. The proposed design tries to accomplish the 'full coverage' requirement with the least amount of airships as possible. According to the previous conclusions if such requirement was loosened this would lead to a massive reduction in costs at the expense of very little performance. An example of this can be shown through the use of a high crime rate map.

In a (hypothetical) situation where the NSS' focus is on criminal activity only, it would be possible to optimise the system's set up for this purpose. Figure 9.9 shows a crime map on the left, where the red colour represents areas of high crime rate and green colour the opposite. As it is expected areas of higher crime rate tend to be associated with high population density areas like Amsterdam, Den Haag and Rotterdam. On the right the proposed set-up for a crime optimised NSS, where the amount of airships is minimised and their efficiency maximised. Adding additional airships to this system would be possible although highly inefficient and expensive. With 8 airships one can achieve high levels of coverage of areas of interest at a much cheaper cost. The same logic can be applied to the NSS with FSDS and ITS operations. Through research and investigation it could be possible to create a map of fire-related high risk areas and zones of maximum criminal

[6] http://www.ad.nl/binnenland/ad-misdaadmeter-2015-de-ranglijst-en-alle-cijfers~a6cb0742/ [cited 26 June 2017]

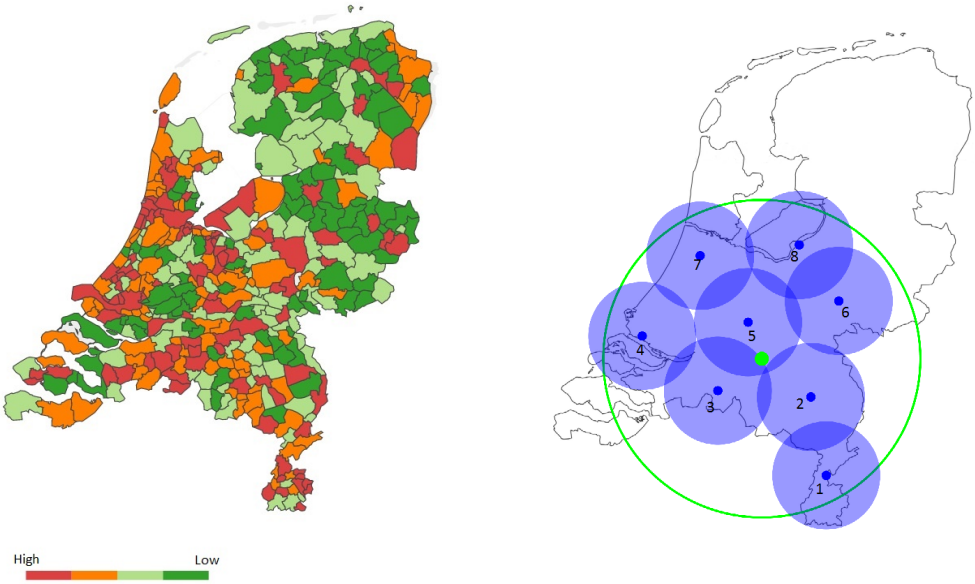

(a) Netherlands crime rate per zone[6] (b) Proposed set-up based on crime map

Figure 9.9: Netherlands crime map and proposed NSS set-up

activity that could then be used to optimise the NSS, and through this, massively reduce the costs of the whole project. This section did not intend to propose another airship set-up in any way, but simply to show how flexible the design of a system like the NSS can be when requirements like 'total coverage' are changed and optimised to best serve the customer's needs.

9.7. FSDS CUBESAT SOLUTION

There is one major alternative solution to the system that has been designed in this report. Up until the MTR, the possibility of only making use of CubeSats was still on the table. However, due to the highly stringent requirements posed by the ITS on the system as a whole, the only appropriate platform became a stratospheric airship. Since the FSDS-oriented payload could easily be placed n the airships as well, it would not make sense to design an all-new platform for that equipment. In this section, the feasibility and advantages are laid out of only performing the FSDS mission with the use of a CubeSat constellation. First of all, the use of satellites would be more in line with the VenJ's innovation programme for satellite applications. Moreover, this approach would also be supported by targets and goals that had been set by the Dutch government for the period of 2014-2020. In the *Nota Ruimtevaartbeleid 2016*[57], the government has presented some goals to the parliament (Tweede Kamer), regarding the advancement of the Dutch space industry. They acknowledge the tremendous advantages it brings to society as a whole, and the fact that the sector will significantly gain in importance in the upcoming years around the globe. Precisely how and why has been elaborated upon in the Market Analysis Chapter of the Baseline Review [58], as well as other general advantages of deciding to use CubeSats on a national level. Additionally, unlike the airships, the CubeSats could be designed in the Netherlands, should home-made products be preferred by the customers.

These are, however, not the only advantages of using CubeSats for FSDS. Another would be the financial advantage; the constellation would need 32 units to meet the requirements, each having a reliability of 50% over a 2 year span, therefore requiring 80 CubeSats over 5 years time. The costs associated with this would be 20 million; being cheaper than two airships. The resulting cost would be far lower than the possibilities laid out elsewhere in this report. Moreover, the TRL for such a system is higher than that for an airship, as this consists of more proven technology. As had been indicated in the MTR, it would be possible to design a 3U CubeSat consisting of a 1U bus which is already flight-proven, therefore having a TRL of 9[2]. The remaining 2U would

also suffice for the payload. The preferred choice for the payload would be the Arctic-1, which has already been designed under the supervision of dr. ir. J.M. (Hans) Kuiper, but still awaits development.

All in all, this CubeSat constellation would be a very promising system, and also more feasible than what is currently proposed. This would be at the cost of neglecting the ITS, but there are a number of significant advantages in doing so.

9.8. CONCLUSION

System costs can be reduced by developing the system by either improving the detection method, extending the FOV, changing the system size or the airship manoeuvrability, which was discussed in the previous sections. In this section the final conclusions regarding system level developments will be discussed. Table 9.1 will show the how different system set-ups have different costs associated. In this table several criteria are shown with purpose of better characterising the strengths and weaknesses of each of the configurations. Feasibility is given on a scale from one to five, the original configuration having a score of five, corresponding to the most feasible design. Lack of feasibility implies that there is a need for further research or just technology development. Constant coverage, given as a percentage, is the area that can be covered constantly with a temporal resolution of at most 1 minute. The cost of the total system is shown in the last column and naturally, it decreases linearly with a decrease in number of airships. The configurations that can be found in the table are described below:

1. **Original configuration**
   The original configuration is the concept that has been presented as a solution in this report.

2. **Extended ITS FOV configuration**
   This configuration will use the potential extended ITS FOV for both the PC and QD solution as discussed in Sections 9.3.2 and 9.3.3 respectively.

3. **Manoeuvrable configuration**
   This is a hypothetical configuration for a system with improved airships capable of achieving airspeeds up to 25 m/s.

4. **Alternative distribution configurations**
   The optimised distribution configurations are alternative set-ups of airship number and positions. Three main types will be considered: a one airship-only system, a Randstad coverage distribution and finally a crime-rate optimised coverage.

5. **FSDS only system configurations**
   This configuration consists of a system capable of performing FSDS operations only. Both airship and CubeSat composed systems will be considered.

Table 9.1 shows how each of the configurations influence the system composition and cost.

Table 9.1: Financial matrix

	Coverage %	Temporal resolution (min)	Feasibility (1-5)	No. of airships	Cost (€ million)
Proposed configuration	99	1	5	15	271 ± 68
Manoeuvrable configuration	75 - 100	1 - 6	1	9	196 ± 49
Extended ITS FOV					
QD	99	1	2	15	245
PC	95	1	3	10	194 ± 48
Alternative distribution					
Single airship	8.7	1	5	1	58 ± 15
Randstad coverage	28	1	5	3	87 ± 22
Crime-rate based coverage	50	1	5	8	158 ± 40
FSDS only					
Airships	99	«30	5	3	55 ± 14
CubeSats	99	30	5	32 (CubeSats)	22 ± 6

The previous table provided with some interesting conclusions regarding the cost-efficiency of the NSS and its relation with coverage percentage and number of airships. The first thing the draws attention is how cheap the FSDS can be made if it is detached from the ITS. A NSS with only a FSDS can be operational using 3 airships only, all within the range of one ground station with the cost of €40.6M. When compared to the original proposed configuration of 15 airships it becomes clear just how much the ITS drives the overall design and its cost. For this same reason it can be shown that a CubeSat constellation designed for FSDS would only cost around €20M, €40M less than the same system when composed of airships although the airship solution could achieve a much smaller temporal resolution (in the order of minutes).

When including both the ITS and the FSDS in the NSS the price shoots up but there are still ways of reducing it when compared to the original. One of the options is to drop the requirement of total coverage and use specific airship distributions. These could be for example a crime-rate based system distribution, optimised for high-crime rate areas and composed of 8 airships and a with a total cost of around €131M. Another option would be to use a distribution covering the Randstad area (which effectively covers a major part of the population of the Netherlands). This set-up would be composed of 3 operational airships and would have an associated cost of €61M. The costs for a system composed of one airship only are also given in the table for comparison, however unlike the others this one does not include a maintenance bay. Following up from earlier in this chapter, a solution with airships with improved manoeuvrability, although hard to achieve technologically, could potentially be a system with 75% constant coverage and 95% coverage with a 5 minute response time. Such system would have a cost of €146M. Two other options presented, also for comparison, are configurations which use only one of the detection methods used by the ITS. A system using only the QD detection would look very similarly to the original configurations (since this detection method is the limiting factor of the design). A configuration using only the PC would be able to achieve a coverage of 95% using 10 airships and with an associated cost of €160M. Using the results presented in this report the ministry of VenJ should re-evaluate their requirements concerning the NSS. After that a path can be set out to continue this project towards realisation.

10 | Requirements

This chapter looks back to the requirements set in the baseline phase of the project and evaluates them using the final result of this project. Due to progressing insight, discussions with the stakeholders, and an updated project scope, some requirements have changed or are no longer relevant. After that, it is checked if the final system design complies with the requirements.

10.1. Requirement Changes

This section elaborates upon the changes made in the requirements set during the baseline phase of the project. The original requirements can be found in Appendix B of the baseline report [58]. In this section 3 tables will be presented.

Table 10.1 contains a list of all updated requirements. As they have been updated they also received a new identifier to distinguish them from the old ones. In requirement *NSS-SHR-1.04* the original minimum signal to noise ratio has been reduced from 100 to 80 to account for the fact that even with a lower SNR it is still possible to perform ITS and FSDS operations [24]. All other changes have to do with the fact that the requirements made explicit references to space elements which have now been replaced by stratospheric airships.

Table 10.1: Updated NSS requirements

Old Identifier	New Identifier	Requirement
NSS-SHR-1.04	NSS-SHR-1.11	The data provided by the ITS shall have a signal-to-noise ratio of at least 80.
NSS-SHR-1.07	NSS-SHR-1.12	The ITS shall be able to track individual objects for at least 1 year.
NSS-SHR-4.03	NSS-SHR-4.10	The NSS system shall be composed of a stratospheric airship in conjunction with a drone.
NSS-SHR-6.03	NSS-SHR-6.04	All NSS segments shall be recyclable.
NSS-SYS-1.01	NSS-SYS-1.11	The airship shall incorporate a camera to have 100 nm in the UV to NIR range (0.3 to 2 μm.
NSS-SYS-2.01	NSS-SYS-2.22	The airship payload shall have a pointing stability of at most 3.03 arcsec/s.
NSS-SYS-2.02	NSS-SYS-2.23	The airship payload shall have pointing accuracy of at most 5 arcsec.
NSS-SYS-2.03	NSS-SYS-2.24	The airship payload shall have a pointing knowledge of at most 5 arcsec.
NSS-SYS-2.04	NSS-SYS-2.25	The airship shall have a reliability of at least 75% after 10 years.
NSS-SYS-2.07	NSS-SYS-2.26	The airship shall have a communications bandwidth of 100 MHz.
NSS-SYS-2.08	NSS-SYS-2.27	The airship shall have a downlink margin of at least 3 dB.
NSS-SYS-2.09	NSS-SYS-2.28	The airship shall have a uplink margin of at least 3 dB
NSS-SYS-2.10	NSS-SYS-2.29	The airship payload shall have a power consumption of at most 5000 W.
NSS-SYS-2.11	NSS-SYS-2.30	The airship payload shall have a mass of at most 250 kg.
NSS-SYS-2.12	NSS-SYS-2.31	The airship shall be equipped with a autonomous safe mode.
NSS-SYS-2.15	NSS-SYS-2.32	The airship shall be able to communicate with the ground segment.
NSS-SYS-2.17	NSS-SYS-2.33	The airship shall be able to determine its own position.
NSS-SYS-2.18	NSS-SYS-2.34	The airship shall be able to maintain its prescribed position.
NSS-SYS-2.20	NSS-SYS-2.35	The airship payload shall be able to determine its own attitude.
NSS-SYS-2.21	NSS-SYS-2.36	The airship payload shall be able to control its own attitude.

A number of requirements have become obsolete as the project progressed. These have been listed in Table 10.2. The space segment requirements that have no meaning in the context of an airship system have been removed as well as the requirements relating to the launching of spacecraft. Early in the project it was decided that, rather than design new aerial segments (drones), they have to be of the shelf products. Thus, specific requirements relating to payload and com-

munications performance of the aerial segments were no longer considered relevant as they fall within the responsibility of the manufacturers. Finally, cost requirements have been scrapped, since VenJ indicated that they are more interested in what is possible from a technical point of view.

Table 10.2: Deleted NSS requirements

Identifier	**Requirement**
NSS-SHR-4.05	The space segment shall consist of CubeSats.
NSS-SHR-4.06	The space segment shall be of <TBD> U size.
NSS-SHR-6.01	The space segment shall have a <TBD> EOL decay orbit.
NSS-SHR-9.01	The life cycle cost shall be lower than or equal to 250,000 € per spacecraft.
NSS-SYS-1.08	The space observation system shall have an appropriate EOL decay orbit.
NSS-SYS-2.05	The space segment shall have an inclination of at least 53 degrees.
NSS-SYS-2.06	The space segment shall have an orbital altitude between 220 and 350 km.
NSS-SYS-2.13	The space segment shall be able to place itself in the required orbit when ejected from the launcher.
NSS-SYS-2.14	The space observation system shall be able to do Earth observations.
NSS-SYS-2.16	The space segment shall be able to operate in LEO environment.
NSS-SYS-3.01	The aerial segment shall have a pointing stability of at least <TBD> arcsec/sec.
NSS-SYS-3.02	The aerial segment shall have a pointing accuracy of at least <TBD> arcseconds.
NSS-SYS-3.03	The aerial segment shall have a pointing knowledge of at least <TBD> arcseconds.
NSS-SYS-3.04	The aerial segment shall have a communication bandwidth of <TBD> MHz.
NSS-SYS-3.05	The aerial segment shall have a total transmitting power of <TBD> W.
NSS-SYS-3.06	The aerial segment shall have a total communications receiving power of <TBD> W.
NSS-SYS-4.01	The launch element shall be able to bring the space segment to the required orbit height.
NSS-SYS-4.02	The launch element shall be able to facilitate the deployment of the space segment.
NSS-SYS-4.03	The launch element shall be able to bring the space segment to the required orbit inclination with a margin of at most <TBD> degrees.
NSS-SYS-7.03	The production phase shall last at most <TBD> weeks.
NSS-SYS-7.04	The launch campaign shall last at most <TBD> weeks.
NSS-SYS-7.05	The spacecraft life cycle cost shall be at most €<TBD>.
NSS-SYS-7.06	The launcher life cycle cost shall be at most €<TBD>.
NSS-SYS-7.07	The ground element life cycle costs shall be equal to or less than €<TBD>.
NSS-SYS-7.08	The program level life cycle costs shall be equal to or less than €<TBD>
NSS-SYS-7.09	The flight Support & Operations life cycle costs shall be equal to or less than €<TBD>.

Table 10.3 contains a list of new requirements that had to be included in the project to enable the selection of of-the-shelf drones.

Table 10.3: New NSS requirements

Identifier	Requirement
NSS-SYS-3.17	The FSDS Drone shall arrive at a location in under 10 minutes.
NSS-SYS-3.18	The FSDS Drone shall be able to operate beyond visual line of sight of the operator.
NSS-SYS-3.19	The FSDS Drone shall be able to measure concentrations of substances which lead to acute toxicity.
NSS-SYS-3.20	The FSDS Drone shall be able to measure the size of smoke and gas clouds with an accuracy of 20 m.
NSS-SYS-3.21	The FSDS Drone shall be able to determine the direction of movement of smoke and gas clouds.
NSS-SYS-3.22	The FSDS Drone shall be able to loiter in the affected area for at least 15 minutes.
NSS-SYS-3.23	The FSDS Drone shall be able to downlink location and observational data to the ground station of the drone.
NSS-SYS-3.24	The ITS Drone shall be able to reach its target within 10 minutes.
NSS-SYS-3.25	The ITS Drone shall be able to operate beyond visual line of sight of the operator.
NSS-SYS-3.26	The ITS Drone shall be able to loiter near its target for at least 30 minutes.
NSS-SYS-3.27	The ITS Drone shall be capable of imaging in the visible light spectrum.
NSS-SYS-3.28	The ITS Drone shall be capable of imaging in the TIR of the spectrum.
NSS-SYS-3.29	The ITS Drone shall be able to operate without the drone being detected by the target.
NSS-SYS-3.30	The ITS Drone shall be able to downlink location and observational data to the ground station of the drone.

10.2. REQUIREMENT COMPLIANCE

This section checks if the requirements are met. Each requirement table states the requirement identifier, followed by the requirement itself. Then it is indicated if the requirement is met; a check mark means the requirement is met, a cross means the system failed to meet the requirement, and an exclamation mark means the requirement still has to be verified for compliance because at the current stage of the project it is impossible to say this. If the requirement is not met, it will be discussed in the text after the requirement table why the requirement is not met and what value the system relating to the requirement has achieved. If the requirement was updated, the requirement from Section 10.1 is used instead from the one presented in the baseline report.

Identifier	Requirement	Check
NSS-SHR-1.02	The ITS shall have a spectral resolution of better than 100 nm within the UV to NIR spectrum.	✓
NSS-SHR-1.03	The ITS shall have a temporal resolution of at least 1 minute.	✓
NSS-SHR-1.05	The ITS shall be able to resolve an object of at least 2 × 2 meters.	✓
NSS-SHR-1.06	The ITS shall be able to track at least 1000 objects simultaneously.	✓
NSS-SHR-1.08	The ITS shall be able to determine the start/stop moments of tracked objects.	✓
NSS-SHR-1.09	The ITS shall be able to track objects without being detected.	✓
NSS-SHR-1.10	The ITS shall be able to track objects within the borders of the Netherlands.	✓
NSS-SHR-1.11	The data provided by the ITS shall have a signal-to-noise ratio of at least 80.	✓
NSS-SHR-1.12	The ITS shall be able to track individual objects for at least 6 months.	!

The result for requirement *NSS-SHR-1.12* is unknown. In the design the choice was made to track targets with both a panchromatic coating and quantum dots. The panchromatic coating is a nor-

mal car paint, so this will last longer than the six months requirement. However, there is currently no information on the durability of a QD paint. More research on QDs has to be performed to find out how long a target marked with QDs can be detected by the system. Although the marker might be still on the targets after the six month duration, the system can be instructed to not track these targets after the six months have passed. The data generated on these targets after the six months will not be saved.

Identifier	Requirement	Check
NSS-SHR-2.01	TThe FSDS shall have a Noise Equivalent Differential Temperature of 100 mK or lower in the Thermal Infrared wavelength region.	!
NSS-SHR-2.03	The FSDS shall have a signal-to-noise ratio of at least 100.	!
NSS-SHR-2.04	The FSDS shall have a spatial resolution of at least 100 meters.	✓
NSS-SHR-2.05	The FSDS shall have a temporal resolution of at least 30 minutes.	✓
NSS-SHR-2.06	The FSDS shall be able to detect the composition of smoke and gas clouds.	✓
NSS-SHR-2.07	The FSDS shall be able to detect the size of smoke and gas clouds.	✓
NSS-SHR-2.08	The FSDS shall be able to predict the spread of smoke and gas clouds.	✓
NSS-SHR-2.09	The FSDS shall be able to detect smoke and gas clouds in the Netherlands.	✓
NSS-SHR-2.10	The FSDS shall be able to detect smoke and gas clouds in day- and nighttime.	✓

For *NSS-SHR-2.01* and *NSS-SHR-2.03* the requirement status is unknown. To check these requirements, additional information on the FSDS payload camera is required which is unavailable.

Identifier	Requirement	Check
NSS-SHR-3.02	The NSS shall have at least one ground station.	✓
NSS-SHR-3.03	The NSS ground segment shall be able to communicate with all other NSS segments.	✓
NSS-SHR-3.04	The NSS ground segment shall be able to communicate with the system users.	✓

Identifier	Requirement	Check
NSS-SHR-4.02	The NSS platform systems shall be constantly upgradeable.	✓
NSS-SHR-4.07	All communications within the NSS shall be inaccessible to unauthorised third parties.	✓
NSS-SHR-4.08	The NSS shall make gathered data available to its users with a delay of at most 60 seconds.	✓
NSS-SHR-4.09	The NSS shall store all raw data for at least 1 day.	✓
NSS-SHR-4.10	The NSS system shall be composed of a stratospheric airship in conjunction with a drone.	✓

Identifier	Requirement	Check
NSS-SHR-5.01	The NSS shall have a reliability of 75 % over 10 years.	✓
NSS-SHR-5.02	The choice of proper launch and operation scenarios shall enable safe and reliable functionality of the system.	✓

Identifier	Requirement	Check
NSS-SHR-6.02	The NSS shall be composed of non-toxic materials.	✓
NSS-SHR-6.04	All NSS segments shall be recyclable	✓

Identifier	Requirement	Check
NSS-SHR-7.01	The imposed bottom-up versus top-down engineering budgets shall comply with the system end-to-end operability.	✓

Identifier	Requirement	Check
NSS-SHR-8.01	The mission development phase shall last no longer than 2 years.	×

Requirement *NSS-SHR-8.01* regarding mission development will not be met. The proposed airship, the Thales Stratobus, will be available in 2020, meaning that the mission development phase will last at least three more years. It should be possible to have the mission development phase last no longer than five years. In Chapter 12 more information can be found on Post DSE project logic and development.

Identifier	Requirement	Check
NSS-SYS-1.02	All parts of the system shall be able to transmit data to mission control.	✓
NSS-SYS-1.04	All parts of the system shall have a closed link budget.	✓
NSS-SYS-1.05	The camera chosen for the FSDS shall be able to measure 100 mK temperature differences.	!
NSS-SYS-1.06	All systems shall be upgradeable.	✓
NSS-SYS-1.09	All Systems shall incorporate green non-toxic materials.	✓
NSS-SYS-1.10	All system's bottom-up versus top-down engineering shall comply with the end-to-end operability.	✓
NSS-SYS-1.11	The system shall incorporate a camera to have 100 nm in the UV to NIR range (300 nm to 2 μm).	✓

Requirement *NSS-SYS-1.05* cannot be verified for the same reason as requirements *NSS-SHR-2.01* and *NSS-SHR-2.03*. More information on the FSDS payload camera is required to see if the selected camera meets the given requirement.

Identifier	Requirement	Check
NSS-SYS-2.22	The airship payload shall have a pointing stability of at least 3.015 arcsec/s .	✓
NSS-SYS-2.23	The airship payload shall have a pointing accuracy of at least 5 arcsec.	✓
NSS-SYS-2.24	The airship payload shall have a pointing knowledge of at least 5 arcsec.	✓
NSS-SYS-2.25	The airship shall have a reliability of at least 75 % after 10 years.	✓
NSS-SYS-2.26	The airship shall have a communication bandwidth of 100 MHz.	✓
NSS-SYS-2.27	The airship shall have a downlink margin of at least 3 dB.	✓
NSS-SYS-2.28	The airship shall have an uplink margin of at least 3 dB.	✓
NSS-SYS-2.29	The airship payload shall have a power consumption of at most 5000 W.	✓
NSS-SYS-2.30	The airship payload shall have a mass of at most 250 kg.	✓
NSS-SYS-2.31	The airship shall be equipped with an autonomous safe mode.	✓
NSS-SYS-2.32	The airship shall be able to communicate with the ground segment.	✓
NSS-SYS-2.33	The airship shall be able to determine its own position.	✓
NSS-SYS-2.34	The airship shall be able to maintain its prescribed position.	✓
NSS-SYS-2.35	The airship payload shall be able to determine its own attitude.	✓
NSS-SYS-2.36	The airship payload shall be able to control its own attitude.	✓

Identifier	Requirement	Check
NSS-SYS-3.09	The aerial segment shall have a reliability of 75% over 10 years.	✓
NSS-SYS-3.13	The aerial segment shall be able to operate in atmospheric environment.	✓
NSS-SYS-3.16	The aerial segment shall be able to communicate with the ground segment.	✓
NSS-SYS-3.17	The FSDS Drone shall arrive at a location in under 10 minutes.	✓
NSS-SYS-3.18	The FSDS Drone shall be able to operate beyond visual line of sight of the operator.	✓
NSS-SYS-3.19	The FSDS Drone shall be able to measure concentrations of substances which lead to acute toxicity.	✓
NSS-SYS-3.20	The FSDS Drone shall be able to measure the size of smoke and gas clouds with an accuracy of 20 m.	✓
NSS-SYS-3.21	The FSDS Drone shall be able to determine the direction of movement of smoke and gas clouds.	✓
NSS-SYS-3.22	The FSDS Drone shall be able to loiter in the affected area for at least 15 minutes.	✓
NSS-SYS-3.23	The FSDS Drone shall be able to downlink location and observation data to the ground station of the drone.	✓
NSS-SYS-3.24	The ITS Drone shall be able to reach its target within 10 minutes.	✓
NSS-SYS-3.25	The ITS Drone shall be able to operate beyond visual line of sight of the operator.	✓
NSS-SYS-3.26	The ITS Drone shall be able to loiter near its target for at least 30 minutes.	✓
NSS-SYS-3.27	The ITS Drone shall be capable of imaging in the visible light spectrum.	✓
NSS-SYS-3.28	The ITS Drone shall be capable of imaging in the TIR spectrum.	✓
NSS-SYS-3.29	The ITS Drone shall be able to operate without the drone being detected by the target.	✓
NSS-SYS-3.30	The ITS Drone shall be able to downlink location and observation data to the ground station of the drone.	✓

Identifier	Requirement	Check
NSS-SYS-5.02	The ground segment shall be able to process received data.	✓
NSS-SYS-5.03	The ground segment shall be able to communicate telemetry with the other segments.	✓
NSS-SYS-5.04	The ground segment shall be able to receive payload data from the other elements.	✓

Identifier	Requirement	Check
NSS-SYS-6.01	The mission control element shall enable a datalink between ground element and observation system.	✓

Identifier	Requirement	Check
NSS-SYS-7.01	The preliminary design phase shall last at most 3 weeks.	✓
NSS-SYS-7.02	The detailed design phase shall last at most 5 weeks.	✓

11 | Verification and Validation

In the design process of the NSS, a couple of tools have been used and it is necessary that those tools are verified and validated. Verification is checking whether the written program accurately represents the actual mathematical formulas and models it should represent. Validation is the process of determining whether the written model or program accurately represents the real world as seen from the intended use of the model [59]. This chapter verifies and validates the tools being used throughout the design process of the NSS.

11.1. Verification

Verification of a code is checking whether the code does not contain any errors. Bugs are errors, but they are errors due to the programming language so are related to the program language used. Those could be fixed by running the program and fixing the bugs by reading what is being said in the console from the program. Calculation errors also exist, and should be fixed as well. This could be done by inputting certain numbers into the program and knowing what should come out.

11.1.1. Link tool

This tool is used to determine the required antenna diameter, the necessary power and the gains for the antennas. The tool was made in Excel, as this is most convenient: by changing parameters, the SNR comes out, as well as the gains the antennas have. The tool was checked using another link tool that was used during the Mid term review. In the MTR, this other tool has already been verified and validated [2]. However, this tool was not used for the final review, because that tool mainly dealt with spacecraft (CubeSats) and link budgeting for spacecraft is slightly different from airships. Spacecraft have a limited time they are in contact with the ground station, whereas the airships are constantly in contact with the ground station. This enabled us to basically choose a certain data rate that fitted the amount of data that is being send; not every data will be send to the ground station. Though, still a lot of data will be send down, as in total, a lot of data is generated. The data rate was set at 200 Mbit/s.

Firstly, a couple of program characteristic checks were done, such as unit tests and order of magnitude tests. In calculating the SNR, a lot of use is made of calculating with dBs. The program is in excel; boxes in which dBs are calculated, the input of that box is increased by a factor of 10. The outcome of that box should be increased by 10, which was the case for all the boxes. If it were not the case, the equation for that box was rewritten. The program is also checked on boxes which have error messages in them, such as #DIV/0! or #VALUE!. The first error means that something is divided by zero, which is obviously not possible and should be fixed. The second error means that one of the input boxes does not have a value assigned to it, such that the output box does not do the calculation. It is then made sure that the input boxes have a value assigned to it at all times.

Using the tool used in the MTR, this current link tool was verified by plugging the same values into both tools. A receiver antenna of 0.05m, transmitter antenna of 0.5 m, a downlink frequency of 26.5 GHz were plugged in and a transmitter power of 20 W was plugged in. The tool from the MTR gave a value of 12.7 dB and the tool for the Final review gave a value of 11.7 dB. This is within the 10 % margin that was previously set. Even though the tool does not reproduce the same exact value, the SNR is at least underestimated, in that way the link will not be in danger of not closing at all. Also, the SNR meets the requirement for the modulation scheme used, with a certain margin. Therefore, it can be said that the tool is verified.

11.1.2. SENSOR AND OPTICS TOOL

The sensor and optics tool calculates the necessary diameter of the aperture, with the SNR as input. During the MTR, a comparable tool was being used. This tool underwent a couple of changes. The main change that was made is that now the SNR is the input, whereas in the other tool the SNR was the output, and the input values were changed such that the SNR came out as more than 100. However, this tool gave rather high values for the SNR although no error was detected. That is one of the reasons that the SNR is now taken as an input from which the aperture size is calculated.

First thing that is being checked is whether the program contains any errors. By running the program, no errors are present, at least no syntax errors or other program errors. Secondly, it is checked whether the calculations that were put in the program were entered correctly. Every individual line of calculation will be checked on this. No mistakes were found in the calculation part.

Now that unit test have been executed, as well as checks on the calculations, it is necessary to do a check where the input values are changed. The other parameters will also be looked at, by how much they have changed, when changing that input value. It is first done with the SNR, which is changed from 80 to 160, i.e. doubling it. Doubling SNR leads to a 4 times as large signal strength, which leads to a four times as large area of the aperture, because it is linearly proportional. A 4 times larger area means a twice as large diameter, because the aperture diameter is quadratically related to the area. The pixel size is also quite important, and this increases linearly with focal length, which has increased twice as well, due to keeping the focal number constant. So the pixel size will increase by a factor of two as well. Another change of input is done (by leaving the SNR at 160): the shutter time is increased by a factor of 10. This results in the aperture area to increase to increase by a factor of 10, the diameter will increase by a factor of $\sqrt{10}$, and so will the focal length and pixel size. In Table 11.1 a table can be found with these changes due to the change of input variables. Units are intentionally left out since it is about the ratio between the value before and after the unit change.

Table 11.1: Changes of different parameters after changing different input values

	Before	After	Ratio
SNR	80	160	2
S	$6.40 \cdot 10^2$	$25.6 \cdot 10^2$	4
A	0.128	0.512	4
D	0.404	0.808	2
f	0.808	1.62	2
d	20.2	40.4	2

(a) Changing SNR from 80 to 160

	Before	After	Ratio
S	$25.6 \cdot 10^2$	$25.6 \cdot 10^2$	1
A	0.512	5.12	10
D	0.808	2.55	3.16
f	1.62	5.11	3.15
d	40.4	128	3.17
t_i	0,001	0,0001	0.01

(b) Changing t_i from 10^{-3} to 10^{-4} at SNR = 160

From the two tables the conclusion can be drawn that the optics tool is verified, since the calculated values using the program differ by the factor they should be differing from the value before and after the unit change. In the second column, Table 11.1b, the ratio between the 'before' and 'after' values for the aperture, focal length and pixel size is approximately equal to $\sqrt{10} \approx 3.16$.

11.2. VALIDATION

Validation is executed after the verification process has been executed. Validation is performed using experiments. During the DSE project, it is not really possible to do experiments on the things that are being researched, therefore validation for every tool is not possible. However, the model is considered validated if the error in the numerical model and real life do not differ more than 10 %.

11.2.1. LINK TOOL

The link tool was validated using an example in SMAD [45], page 480. The inputs were plugged into the tool. A couple of different steps in between had to be added to calculate other parameters, which were in turn inputs for other parameters. The inputs were given in the tool, and it was found that the received SNR for this spacecraft is 5 dB, which is 0.1 dB lower than the one given in the book. This is before adding modem implentation loss and considering uplink. Afterwards, it gets to a margin of 3.1 dB, where the book gets a margin of 3.0 dB. Therefore, it can be concluded that the tool is validated as well.

11.2.2. SENSOR AND OPTICS TOOL

The optics tool should be validated as well. In Chapter 4.2, some kind of validation is already present, because the outcome of the optics tool is compared to a real life example of an existing camera. The reference camera was chosen in such a way that both sensors were approximately the same size. Table 4.11 is a table which consists of data of the colour imager that is being used for the ITS system. The table also consists of data on the DSC-RX10M3 camera. The data on the colour imager is determined using the program and taking a specific sensor for the colour imager. The other camera is taken as a reference, to actually check whether the calculated values make sense (validating the outcome of the tool). From this table, it is concluded that the data that is generated using the tool is quite accurate: the diffraction limit is within 0.03 m, the focal length is the same and the GSD is in the same order of magnitude as well. The mass of the colour imager was estimated as well, using a density of 1 kg/dm^3, which is the same density as water. This is quite a large density for a camera, considering the fact that a lot of air/empty space is inside a camera. The large density was taken for contingency, to at least overestimate the mass instead of underestimate it. This way, the total payload of mass will not be overestimated, such that the airship is always able to take the calculated amount of weight for the payload on board. However, for these two cameras the weight matched quite well. The mass for the IRIS was estimated at 4 kg with an error of 1 kg, and the DSC-RX10M3 is 1.1 kg, but also has volume that is 3 times smaller. The tool should not be validated on the mass estimation though, since that is not the purpose of the tool.

Another validation was done with the IRIS camera, which is compared with the FLIR Rs8300 camera in Table 4.14. In this table it can be seen that the IRIS camera has a GSD of 0.45 m, which is within the range of the GSD the FLIR RS8300 camera could take. Also, the diffraction limit is approximately the same as well, with a deviation of 0.06 m. Focal length for the IRIS was calculated to be 66 cm and the aperture was half of this (since the focal number was taken to be 2), for the other camera these values were between 12-120 cm for the focal length and the aperture is 29 cm. So these values are matching quite well as well. The only thing that does not quite match is the estimated weight. The mass of the IRIS is estimated to be 50 kg, whereas the FLIR is 35 kg even having a larger volume. The density of the IRIS was approximated at 1 kg/dm^3 as well, which is quite large and done on purpose, as mentioned before. However, the mass calculation was not the purpose of this tool and since the other parameters match quite well with the reference cameras, it can be said that the tool is successfully validated.

12 | Post DSE Project Logic

In this chapter the Post DSE project logic is discussed for NSS since the project is supposed to be continued after DSE. The flow chart and Gantt chart presented give an estimate how long it will take before the product can actually be used. Firstly, the flowchart is presented and lastly the Gantt chart will be discussed of the post DSE process.

12.1. Flow Chart Post DSE

As can be seen in Figure 12.1 the post dse process is divided into 5 phases: DSE, preliminary, detailed, production and operational phase. After presenting the results to the ministry of Security and Justice, the first phase has been completed.

From there, the preliminary phase of the project starts where payload is further designed and Thales also enters the picture. Next to this, the coatings are further studied and a start is made with the schedule of the operations of the airship and drone. Also the software development for both image processing and operations is started. Lastly, the ground element (maintenance base and antennas) is designed in detail for it must be ready during the production phase. Finishing this phase results in the start of phase three.

Phase three is the detailed design phase in which the total payload, coating process and the airship is designed into detail and it is tested. Concurrently, the production process is set up and the building is started on the maintenance base. Testing on the drones and installation of them is started too. The last element in the detailed design phase is finishing upon all software running the system. If all goes well a permit to fly and operate the system will be given.

Since all systems have been tested and designed into detail, production (phase 4) can be started. Thales beliefs that the Stratobus will be flying in 2020 and the sixteen airships can be produced in 2 years.[1] Therefore, part of the system can already be operable during part of the production phase. Not the whole of the Netherlands is covered though, however high risk areas can be covered first by the first airships.

12.2. Gantt Chart Post DSE

The Gannt Chart for the post DSE project logic can be founding Figure 12.2. The different phases found in flow chart now have a time estimate given to them. The preliminary phase is estimated to last twelve months. The first step will be having an intense meeting with Thales discussing the possibilities of the system and the specifications. From there, the design is started. Phase three, the detailed design phase, will take up to 24 months. The payload is designed and tested and after that a fully fledged prototype will fly. When the detailed design phase is finished, the two year production of the system will start. As can be seen in the Gantt Chart and mentioned before the system will be operable when in production phase.

[1] http://www.janes.com/article/68513/stratobus-demonstrator-set-for-2018-launch

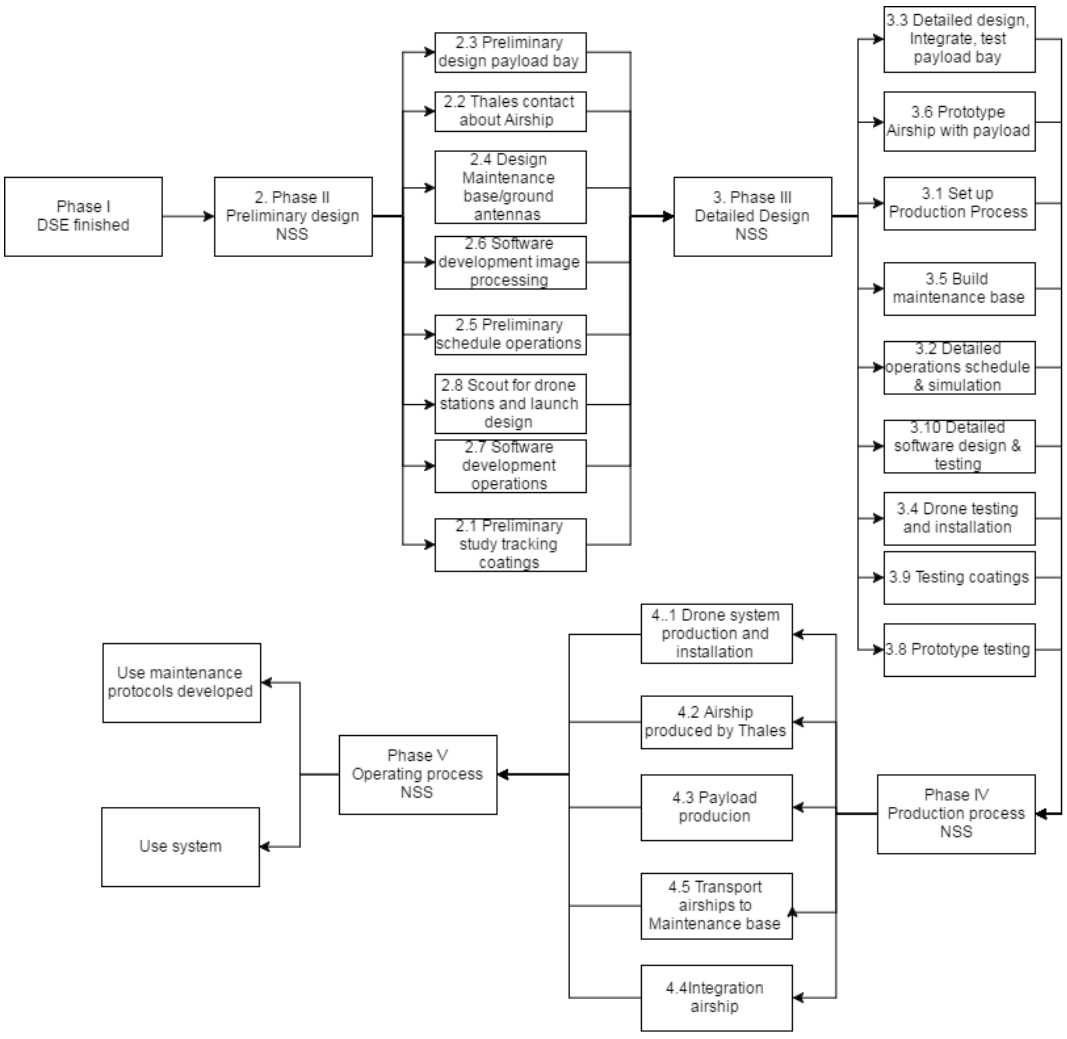

Figure 12.1: Flowchart post DSE

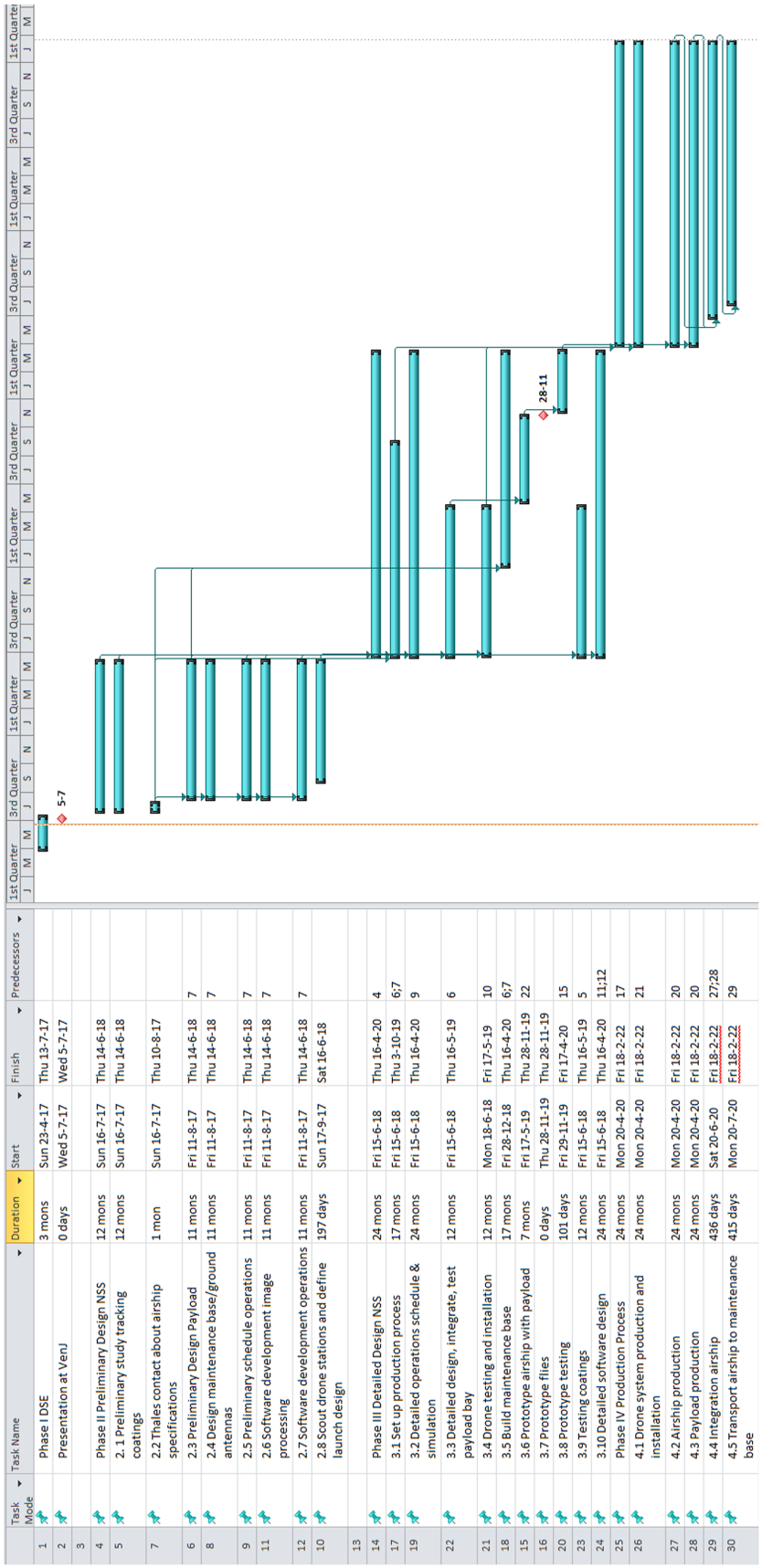

	Task Mode	Task Name	Duration	Start	Finish	Predecessors
1		Phase I DSE	3 mons	Sun 23-4-17	Thu 13-7-17	
2		Presentation at VenJ	0 days	Wed 5-7-17	Wed 5-7-17	
3						
4		Phase II Preliminary Design NSS	12 mons	Sun 16-7-17	Thu 14-6-18	
5		2. 1 Preliminary study tracking coatings	12 mons	Sun 16-7-17	Thu 14-6-18	
7		2.2 Thales contact about airship specifications	1 mon	Sun 16-7-17	Thu 10-8-17	
6		2.3 Preliminary Design Payload	11 mons	Fri 11-8-17	Thu 14-6-18	7
8		2.4 Design maintenance base/ground antennas	11 mons	Fri 11-8-17	Thu 14-6-18	7
9		2.5 Preliminary schedule operations	11 mons	Fri 11-8-17	Thu 14-6-18	7
11		2.6 Software development image processing	11 mons	Fri 11-8-17	Thu 14-6-18	7
12		2.7 Software development operations	11 mons	Fri 11-8-17	Thu 14-6-18	7
10		2.8 Scout drone stations and define launch design	197 days	Sun 17-9-17	Sat 16-6-18	
13						
14		Phase III Detailed Design NSS	24 mons	Fri 15-6-18	Thu 16-4-20	4
17		3.1 Set up production process	17 mons	Fri 15-6-18	Thu 3-10-19	6;7
19		3.2 Detailed operations schedule & simulation	24 mons	Fri 15-6-18	Thu 16-4-20	9
22		3.3 Detailed design, integrate, test payload bay	12 mons	Fri 15-6-18	Thu 16-5-19	6
21		3.4 Drone testing and installation	12 mons	Mon 18-6-18	Fri 17-5-19	10
18		3.5 Build maintenance base	17 mons	Fri 28-12-18	Thu 16-4-20	6;7
15		3.6 Prototype airship with payload	7 mons	Fri 17-5-19	Thu 28-11-19	22
16		3.7 Prototype flies	0 days	Thu 28-11-19	Thu 28-11-19	
20		3.8 Prototype testing	101 days	Fri 29-11-19	Fri 17-4-20	15
23		3.9 Testing coatings	12 mons	Fri 15-6-18	Thu 16-5-19	5
24		3.10 Detailed software design	24 mons	Fri 15-6-18	Thu 16-4-20	11;12
25		Phase IV Production Process	24 mons	Mon 20-4-20	Fri 18-2-22	17
26		4.1 Drone system production and installation	24 mons	Mon 20-4-20	Fri 18-2-22	21
27		4.2 Airship production	24 mons	Mon 20-4-20	Fri 18-2-22	20
28		4.3 Payload production	24 mons	Mon 20-4-20	Fri 18-2-22	20
29		4.4 Integration airship	436 days	Sat 20-6-20	Fri 18-2-22	27;28
30		4.5 Transport airship to maintenance base	415 days	Mon 20-7-20	Fri 18-2-22	29

Figure 12.2: Gantt chart post DSE

13 | Conclusions & Recommendations

The Ministry of Security and Justice is currently investigating whether innovative satellite applications can assist them in their task to keep the Netherlands safe. This project determines the feasibility of using satellites or pseudo-satellites in order to assist the fire department in its effort to detect fires and monitor the movement of harmful smoke and gas clouds, and to assist law enforcement agencies when remotely track objects of interest. The feasibility study was performed by designing a modular National Safety System in compliance with the requirements set by VenJ and by keeping track of issues arising from either those requirements or from the involved physics. Thus a system had to be designed that is capable of detecting fires, detecting clouds of smoke and gas, monitoring the spread of those clouds, analysing the composition of those clouds, and tracking marked objects.

During the midterm phase of the project it was concluded that a satellite system could not reasonably meet the time and spatial resolution requirements set by the ministry to track targets. Therefore, the primary payload platform became a network of stratospheric airships. A trade-off indicated the Thales Stratobus to be the platform of choice.

The project had the added challenge that a new target marker had to be found which made it possible to identify targets from a distance without individuals easily discovering the marker. For that purpose, two complementary marking techniques were selected and investigated. The design in this report makes use of target marking by either a transparent quantum dot paint or by a panchromatic coating. The first method relies on dissolved quantum dots which allow the paint to absorb incoming visible light and re-emit that as a peak in the infrared part of the electromagnetic spectrum. A hyper-spectral imager is capable of detecting those peaks and thus, by extension, the target. However, as it is theoretically possible to detect the marker using specialised shortwave infrared cameras, this cannot be the sole method of marking an object. As a result, the panchromatic paint was added as a marking strategy. This method relies on the fact that two objects can have the same colour that each stem from a different electromagnetic reflection spectrum. Again a hyper-spectral imager would be capable of detecting the unique fingerprints in the spectrum to identify the target. This method also has limitations as there are a limited amount of possible different markers and these coatings, when compared to the quantum dot paint, are difficult to apply as they require the application of a seamless top coating. NASA's Hyperion Imaging Spectrometer forms the basis of the target tracking payload and is capable of detecting both the quantum dot paint and the panchromatic coating. However, due to Hyperion's limited instantaneous field of view it is impossible for the imager to scan the entire coverage area of a single airship within the required 1 minute time-frame. Due to its mass it is also impossible to add multiple such cameras to the payload bay. Therefore, four specialised Colour Imagers were added to the design which are capable of scanning the entire coverage area for potential targets by looking at shape and colour. These cameras have a large field of view despite their small ground sampling distance and are meant to identify potential targets after which Hyperion searches for the marker to confirm the target. Finally an infrared camera, called IRIS, was designed and added to allow an operator to observe during night-time when Hyperion and the four Colour Imagers do not work. The combination of all the tracking cameras, in conjunction with intelligent software, allows the system to both autonomously track targets during the day, and allow operators to evaluate situations on the ground during day- as well as nighttime operations.

Fire and smoke detection and tracking is, on the other hand, relatively simple as this has been implemented countless times before. It relies on imaging the environment in a limited number of wavelengths, in separate bands ranging from the visible light to the thermal infrared, and requires, unlike object tracking, neither a high spatial or spectral resolution. The AMS Wildfire scanner, designed and created by NASA, was selected as the best available existing system to perform those tasks. It comes in a fully integrated system, including a stabilisation system. For the chemical analysis of smoke and gas clouds, which the ministry sees as useful but secondary task, a

hyper-spectral imager is necessary. The Hyperion, which is part of the tracking payload, is exactly that and is thus also capable of determining the chemical composition of clouds of smoke and gas.

In order to fulfil these tasks and cover the entirety of the Netherlands, all these instruments will be fitted on a network of 15 permanently operational stratospheric airships and 1 additional airship for redundancy. Unfortunately, the identification, tracking, cloud tracking, and chemical analysis systems only work during the daytime and clear skies. Fire detection can be performed during clear night and an operator can manually track targets using IRIS as well. During the midterm phase of this project it was decided that, because of the aforementioned reasons, drones have to complement the airship network to maintain functionality of the system during the night and overcast situations which compose at least 50% of the time. Using the set requirements on drone performance it was decided that the system needs 18 GasFinder2 drones to perform the chemical analysis and smoke tracking when the airship network is unable to and a total 74 Aeryon Skyranger drones to be able to perform the target tracking in night and overcast situations. The selection of the drones was weighed in their favour by the fact that both already contain the payload necessary to perform their respective mission.

To maintain the airship and drone network, an extensive ground support segment is necessary to allow for constant communication, mission control, and maintenance. For this purpose two ground stations are necessary as well as a large maintenance base and a mission control centre. The airships can continuously scan the entire Netherlands as long as atmospheric and lighting conditions allow them. If the airships are no longer capable of performing their tasks, a fleet of drones stands ready to take over their functions for as long as it is cloudy or night-time. The network nature of the system allows it to also respond fast and adequately to unforeseen changes such as an unexpected loss of an airship. As can be seen, in order to fulfil all the requirements set by VenJ a large system is required and this naturally comes at a cost.

Developing, constructing, and installing the National Safety System has an estimated cost of 245 million euros and will take a minimum of 5 years to complete. Maintaining the system would require an additional annual cost of 14 million euros. All costs are estimated for a period of 5 years after which the system needs a complete overhaul. And this lays bare one of the biggest problems with the expectations of the ministry.

During the design of this system, it was discovered that every major design choice was driven by the identification and tracking system. The stringent requirements of being able to keep track of at least one thousand targets throughout the Netherlands, with an interval of at most one minute, drove the design away from a satellite solution. During this project the fire and smoke detection system was not considered separate from the identification and tracking system. The midterm phase of this project however, suggested that when only performing the fire and smoke detection, satellites suddenly become a feasible option.

To ensure the success of this project it is necessary to further investigate several avenues of interest.

- A quantum dot paint that can radiate in the infrared has to be developed. Such research can be conducted by organisations such as TNO or a university/institution such as Steele Lab.
- More research is required in the field of panchromatic coating techniques and can be performed by a company such as Akzo Nobel. A detailed analysis must show the further potential of this technique while experiments must prove their potential as a target marker that can be imaged from a distance.
- The payload of the system has to be developed. For the development of the spectral imagers contact should be made with TNO. The optics also have to be developed for which companies such as Cosine should be contacted.
- In discussion with Thales, the stratospheric airships can perhaps be developed further. It might be possible to improve the propulsion system of the airship giving them increased manoeuvrability which opens up the possibility of using less airships at the cost of only minimal coverage reduction.

- More research in optimised airship placement patterns could drastically reduce the amount of needed airships as it might only be necessary to continuously monitor certain areas.
- The ministry should reconsider their wish to perform identification and tracking within the context of the satellite innovation programme. A study could be conducted to investigate the idea of just performing fire detection and smoke monitoring using satellites.
- For a fire detection system, the ministry could also consider working together with the German space agency (DLR) on their satellite fire detection system called FireBIRD, or buying data from other satellite networks such as NASA's FireSat network.

The Ministry of Security and Justice can use the recommendations and conclusions presented in this report to further develop the National Safety System and ensure the continued safety of the citizens of the Netherlands.

Bibliography

[1] P. Lindstrand, P. Groepper, and I. Schäfer. High altitude long endurance aerostatic platforms: the european approach. slides, 2015.

[2] F.M. Knyszewski, J.J. Lubberding, A. Malkaoui, R.J. Meesen, C.M. Niemeijer, B.G. van Noort, M. Rozemeijer, R. Sprenkels, and J.M. de Zoete. A national safety system for the netherlands design synthesis exercise - ae3200, mid term review, abridged. Technical report, Delft University of Technology, May 2017.

[3] A. Abuelgasim and R. Fraser. Day and night-time active fire detection over north america using noaa-16 avhrr data. In *IEEE International Geoscience and Remote Sensing Symposium*, volume 3, pages 1489–1491 vol.3, 2002.

[4] Tom X.-P. Zhao, Steve Ackerman, and Wei Guo. Dust and smoke detection for multi-channel imagers. *Remote Sensing*, 2(10):2347–2368, 2010.

[5] *Is microwave radiation useful for fire detection?*, volume 965, 2001.

[6] *New scanning infrared gas imaging system (SIGIS 2) for emergency response forces*, volume 5995, 2005.

[7] C. Clerbaux, J. Hadji-Lazaro, S. Turquety, G. Mégie, and P.-F. Coheur. Trace gas measurements from infrared satellite for chemistry and climate applications. *Atmospheric Chemistry and Physics*, 3(5):1495–1508, 2003.

[8] BRUKER Optics BOPT. Sigis2 scanning infrared gas imaging system specifications. Specifications Sheet, 2011.

[9] J. Burns. Applications of lidar in wildfire management. Graduation Essay, 2012.

[10] T. Engel and P. Reid. *Physical Chemistry*. Pearson Education, inc., Upper Saddle River, NJ, USA, 2006.

[11] X. Zhang, C. Hagglund, and E.M.J. Johansson. Highly efficient, transparent and stable semi-transparent colloidal quantum dot solar cells: a combined numerical modeling and experimental approach. *Energy Environ. Sci.*, 10:216–224, 2017.

[12] M.P. Genovese, I.V. Lightcap, and P.V. Kamat. Sun-believable solar paint. a transformative one-step approach for designing nanocrystalline solar cells. *ACS Nano*, 6(1):865–872, 2012. PMID: 22147684.

[13] *Polarization in remote sensing*, volume 1747, 1992.

[14] Thales Group. Gmti/sar radar. slides, 2016.

[15] A. Stockman, Donald I.A., N. MacLeod, and E. Johnson. Spectral sensitivites of the human cones. *Journal of the Optical Society of America A*, (2):2491–2521, December 1993.

[16] S. Kim, S.-H. Gong, J.-H. Cho, and Y.-H. Cho. Unidirectional emission of a site-controlled single quantum dot from a pyramidal structure. *Nano Letters*, 16(10):6117–6123, 2016. PMID: 27624194.

[17] M. Val Martin, J.A. Logan, R.A. Kahn, F.-Y. Leung, D.L. Nelson, and D.J. Diner. Smoke injection heights from fires in north america: analysis of 5 years of satellite observations. *Atmospheric Chemistry and Physics*, 10(4):1491–1510, 2010.

[18] S.H. Westin, H. Li, and K.E. Torrance. A comparison of brdf models. *Eurograpics Symposium on Rendering*, pages 1–10, 2004.

[19] M.D. King, W.P. Menzel, P.S. Grant, J.S. Myers, G.T. Arnold, S.E. Platnick, L.E. Gumley, S.-C. Tsay, C.C. Moeller, M. Fitzgerald, K.S. Brown, and F.G. Osterwisch. Airborne scanning spectrometer for remote sensing of cloud, aerosol, water vapor, and surface properties. *Journal of Atmospheric and Oceanic Technology*, 13(4):777–794, 1996.

[20] J. Myers. Nasa airbone infrared remote sensing systems. Slides, 2009.

[21] J. Myers and E. Hildum. The nasa uas ams ocean color imager. Slides, 2009.

[22] P.W. Merlin. Ikhana - unmanned aircraft system western states fire missions, August 2009.

[23] CMOSIS. Cmv50000 area sensor. Product Sheet, 2017.

[24] J.M. Kuiper. Personal Correspondence, 2017.

[25] J. Pearlman, C. Segal, P. Clancy, N. Nelson, P. Jarecke, M. Ono, D. Beiso, L. Liao, K. Yokoyama, and S. Carman. The eo-1 hyperion imaging spectrometer. Slides.

[26] *EO-1/Hyperion hyperspectral imager design, development, characterization, and calibration*, volume 4151, 2001.

[27] J. Pearlman, C. Segal, L. Liao, M. Carman, M. Folkman, B. Browne, L. Ong, and S. Ungar. Development and operations of the eo-1 hyperion imaging spectrometer. Slides, 2004.

[28] M. Carman. Hyperion grating imaging spectrometer, technology workshop slides. Slides, 2001.

[29] *TROPOLITE, on the path of atmospheric chemistry made simple*, volume 9241, 2014.

[30] *A new design approach to innovative spectrometers. Case study: TROPOLITE*, volume 9131, 2014.

[31] Jupiter mw very high resolution ir detectors for mid wave infrared imaging. Technical specifications, Sofradir - EC, SOFRADIR EC INC. 373 US Hwy 46W, Fairfield, NJ 07004 USA, 2011.

[32] Flir rs8300. Technical specifications, FLIR, FLIR Systems Inc. 27700 SW Parkway Ave. Wilsonville, OR 97070 USA.

[33] Thomas Myers George D. Modica, Thomas Nehrkorn. An investigation of stratospheric winds in support of the high altitude airships. Technical report, Atmospheric and Environmental Research, Inc., Lexington, Massachusetts, Systems Technology, Inc., Hawthorne, California, 2007.

[34] George D. Modica, Thomas Nehrkorn, and Thomas Myers. An investigation of stratospheric winds in support of the high altitude airship p2.5.

[35] Flavio Araripe d'Oliveira, Francisco Cristovão Lourenço de Melo, and Tessaleno Campos Devezas. High-Altitude Platforms - Present Situation and Technology Trends. *Journal of Aerospace Technology and Management*, 8:249 – 262, 09 2016.

[36] Two axes high speed gimbal led platform series iipsc - hsg. Technical specifications, IMAR Navigation and Control, St. Ingbert, Germany, 2016.

[37] ilpsc-msg-60 and ilpsc-msg-130 - two axes gyro stabilized gimballed platform. Technical specifications, IMAR Navigation and Control, St. Ingbert, Germany, 2016.

[38] N. Ricciardi. Personal Correspondence, 2017.

[39] Airins - georeferencing and orientation system for air applications. Technical specifications, IXBlue, 2015.

[40] Galina Ilieva, José C. Páscoa, Antonio Dumas, and Michele Trancossi. A critical review of propulsion concepts for modern airships. *Central European Journal of Engineering*, 2(2):189–200, 2012.

[41] S. Cote and A.R.L. Tatnall. The hopfield neural network as a tool for feature tracking and recognition from satellite sensor images. *International Journal of Remote Sensing*, 18(4):871–885, 1997.

[42] A.J. Tatem, H.G. Lewis, P.M. Atkinson, and M.S. Nixon. Super-resolution target identification from remotely sensed images using a hopfield neural network. *IEEE Transactions on Geoscience and Remote Sensing*, 39(4):781–796, Apr 2001.

[43] R. Li, W. Wang, and H.Z. Tseng. Detection and location of objects from mobile mapping image sequences by hopfield neural networks. *Photogrammetric Engineering & Remote Sensing*, 65(10), 1999.

[44] L.M. Duan, M.D. Lukin, J.I. Cirac, and P. Zoller. Long-distance quantum communication with atomic ensembles and linear optics. *Nature*, 414:413–418, 2001.

[45] J.R. Wertz, D.F. Everett, and J.J. Puschell. *Space Mission Engineering: The New SMAD*. Microcosm Press, Hawthorne, CA, USA, 1 edition, 2011.

[46] D. Kuiawa. Safety in confined spaces: Some things you need to know. *EHS Today*, pages 51–52, 2012.

[47] R. Snook. Laser techniques for chemical analysis. *Chem. Soc. Rev.*, 26:319–326, 1997.

[48] Peter W., Franz S., Karl M., Robert K., Robert M., and Bernd J. Near- and mid-infrared laser-optical sensors for gas analysis. *Optics and Lasers in Engineering*, 37(2):101 – 114, 2002. Optical Methods in Earth Sciences.

[49] M. Santarelli. Mj2411 renewable energy technology module: Electrochemical systems for energy notes on hydrogen technologies. Notes.

[50] Steven J. Davis, Ken Caldeira, and H. Damon Matthews. Future co2 emissions and climate change from existing energy infrastructure. *Science*, 329(5997):1330–1333, 2010.

[51] C.B. Murray, C.R. Kagan, and M.G. Bawendi. Synthesis and characterization of monodisperse nanocrystals and close-packed nanocrystal assemblies. *Annual Review of Materials Science*, (30):545–610, August 2000.

[52] J.T. Cullen and M.T. Maldonado. *Biogeochemistry of Cadmium and Its Release to the Environment*. Springer Netherlands, Dordrecht, 2013.

[53] The National Hydrogen Association. Hydrogen safety fact sheet. Safety Fact Sheet.

[54] High altitude platforms (haps) market by type (airships, tethered aerostat systems, unmanned aerial vehicles (uavs)), by payload (communication systems, surveillance systems, navigation systems), by application (government & defense, commercial) - growth, share, opportunities & competitive analysis, 2015 - 2022. Technical Report 57720-03-16, Credence Research, Mar 2016.

[55] G.G. Bennett. The calculation of astronomical refraction in marine navigation. 1982.

[56] R.P.H. Berton. Variational calculation of three-dimensional atmospheric refraction: part i. description and validation of the method. *JOURNAL OF OPTICS A: PURE AND APPLIED OPTICS*, (8):817–830, August 2006.

[57] Ministerie van Economische Zaken. Nota ruimtevaartbeleid 2016. Kamerbrief, 2016.

[58] F.M. Knyszewski, J.J. Lubberding, A. Malkaoui, R.J. Meesen, C.M. Niemeijer, B.G. van Noort, M. Rozemeijer, R. Sprenkels, and J.M. de Zoete. A national safety system for the netherlands design synthesis exercise - ae3200 baseline report. Technical report, Delft University of Technology, May 2017.

[59] Z. Papp E. Mooij and W. van der Wal. *Simulation, Verification and Validation Lecture Notes*. TU-Delft, Delft, The Netherlands, 2017.